

<sup>12</sup>  
I 29A  
# 343  
cy. 3  
CIVIL ENGINEERING STUDIES

STRUCTURAL RESEARCH SERIES NO. 343

Private Communication  
Not for Publication



Metz Reference Room  
Civil Engineering Department  
2206 C.E. Building  
University of Illinois  
Urbana, Illinois 61801

# DISTRIBUTION OF STRESSES AND PARTITION OF LOADS IN GUSSETED CONNECTIONS

By

P. C. Birkemoe,  
R. A. Eubanks,  
and  
W. H. Munse

DEPARTMENT OF CIVIL ENGINEERING  
UNIVERSITY OF ILLINOIS  
URBANA, ILLINOIS  
MARCH, 1969

DISTRIBUTION OF STRESSES AND PARTITION  
OF LOADS IN GUSSETED CONNECTIONS

by

P. C. Birkemoe

R. A. Eubanks

and

W. H. Munse

Department of Civil Engineering  
University of Illinois  
Urbana, Illinois

March, 1969

DISTRIBUTION OF STRESSES AND  
PARTITION OF LOADS IN GUSSETED CONNECTIONS

Peter Christian Birkemoe, Ph.D.  
Department of Civil Engineering  
University of Illinois, 1966

ABSTRACT

Load partition and stress distribution in riveted and bolted structural joints are two associated behavioral phenomena which have received continued attention from structural researchers and designers in an attempt to understand better the behavior of multiply fastened joints and to design them adequately. This study presents a basic analysis of various physical parameters and their effects on load partition and stress distribution in gusseted connections. The gusseted connection under investigation is a particular type of riveted or bolted connection which has additional variables associated with the shape and size of the gusset plate. Analytical and experimental studies were conducted concurrently to justify the conclusions as well as study the assumptions made in arriving at the analytical models.

Analytically, two elastic joint problems were studied: (1) the attachment of a tension member by a single row of fasteners to a semi-infinite plate, (2) the similar attachment to a symmetrical tapered gusset plate. The parameters studied include the number of fasteners, the fastener pitch, the edge distance of fasteners, the fastener and tension member flexibilities, and thickness and geometry of the plate. The member to plate connections were evaluated in terms of the load partition among the fasteners as well as the stress distribution at various locations

in the plate. It was found that, individually, many of the joint parameters did not appreciably affect the load partition in the connection; however, cumulatively they could have detrimental effects. One parameter, the edge distance of the first fastener, did not affect the load partition but caused severe stress conditions at the edge of the plate on the line of loading.

The finite geometry plate, studied experimentally, was fabricated and tested with variable geometry or taper of the gusset plate; the plate was loaded by lap plates connected by tight fitting pins. The elastic stress distribution was studied using brittle lacquer techniques and electrical resistance strain gages at specific locations on the gusset. Individual fastener loading was measured using a special technique involving the placement of strain gages on the gusset near the loaded pins. The load partition of the pinned joint was examined for five geometries and variable numbers of fasteners. Geometry did not appreciably affect the load partition until extreme geometries, which resulted in a change of the gusset net cross-sectional area, were reached.

## ACKNOWLEDGMENT

This investigation was conducted as a doctoral research study in the Department of Civil Engineering and was sponsored in part by the Research Council on Riveted and Bolted Structural Joints, the Illinois Division of Highways, and the Bureau of Public Roads -- Department of Commerce.

The author wishes to express his sincere appreciation to Professor W. H. Munse and Professor R. A. Eubanks of the Department of Civil Engineering for their interest and guidance during the development and completion of this investigation. Encouragement and technical advice on the experimental phase of the study by Professor E. Chesson, Jr., University of Delaware (formerly of the University of Illinois) is also gratefully acknowledged. Gratitude is expressed to the laboratory technicians under the direction of D. F. Lange and later O. H. Ray for the careful preparation and instrumentation of test specimens. Special acknowledgment is expressed to the consulting staff of the Computer Science Department whose help proved invaluable in the efficient use of the computer facilities.

The author expresses his gratitude for the sponsorship of this research by the Research Council and for the suggestions made by Council Members during the development of the study.

## TABLE OF CONTENTS

	<u>Page</u>
LIST OF FIGURES. . . . .	vi
I. INTRODUCTION . . . . .	1
1.1 Historical Review . . . . .	1
1.2 Present Design Criteria . . . . .	7
II. OBJECT AND SCOPE OF THIS INVESTIGATION . . . . .	8
III. ANALYTICAL INVESTIGATIONS. . . . .	10
3.1 Introduction. . . . .	10
3.2 Semi-infinite Plate Solution; General Considerations. . . . .	11
3.3 Finite Plate Solution . . . . .	17
3.4 Analytical Results. . . . .	19
3.4.1 General. . . . .	19
3.4.2 Load Partition, Semi-infinite Plate. . . . .	21
3.4.3 Stress Distribution, Semi-infinite Plate . . . . .	25
3.4.4 Load Partition and Stress Distribution, Finite Plate . . . . .	27
IV. EXPERIMENTAL INVESTIGATION . . . . .	33
4.1 Introduction. . . . .	33
4.2 Design of Specimen. . . . .	33
4.3 Fabrication . . . . .	35
4.4 Instrumentation . . . . .	35
4.5 Test Procedure. . . . .	38
4.6 Results . . . . .	40
4.6.1 Load Partition . . . . .	40
4.6.2 Strain Distribution. . . . .	42
V. COMPARISON OF ANALYTICAL AND EXPERIMENTAL RESULTS. . . . .	45
5.1 Load Partitioning . . . . .	45
5.2 Strain Distribution . . . . .	46
VI. SUMMARY AND CONCLUSIONS. . . . .	48
6.1 Conclusions . . . . .	48
6.2 Areas for Future Study. . . . .	50
LIST OF REFERENCES . . . . .	51
FIGURES. . . . .	54

## TABLE OF CONTENTS (Continued)

	<u>Page</u>
APPENDIX A: NOMENCLATURE . . . . .	91
A.1 General Nomenclature . . . . .	91
APPENDIX B: LOADED RIGID CIRCULAR INCLUSION IN A SEMI-FINITE SHEET . . . . .	93
APPENDIX C: LOADED RIGID CIRCULAR INCLUSION IN A FINITE SHEET . . . . .	99
APPENDIX D: FASTENER FLEXIBILITY AND LOCAL BEARING DEFORMATION . . . . .	109

## LIST OF FIGURES

<u>Figure</u>		<u>Page</u>
3.1	Analytical Models. . . . .	54
3.2	Compatibility of Deformations. . . . .	55
3.3	Load Partition for Variable Number of Fasteners. . . . .	56
3.4	Variation in Fastener Load with Number of Fasteners. . . . .	57
3.5	Load Partition for Variable Fastener Pitch . . . . .	58
3.6	Fastener Load Variation for Variable Fastener Pitch. . . . .	59
3.7	Load Partition for Variable Edge Distance of First Fastener. . . . .	60
3.8	Fastener Load Variation for Variable Edge Distance of First Fastener . . . . .	61
3.9	Fastener Load Variation for Variable Plate Thickness . . . . .	62
3.10	Variation of Fastener Load with Lap Plate Area . . . . .	63
3.11	Load Partition for Variable Fastener Flexibility . . . . .	64
3.12	Variation of Fastener Load with Fastener Flexibility . . . . .	65
3.13	Load Partition and Stress Distribution for a Rectangular Section of a Semi-infinite Plate . . . . .	66
3.14	Contribution of a Single Fastener Loading to the Transverse Edge Stress . . . . .	67
3.15	Transverse Edge Stress for Variable Number of Fasteners and Edge Distance. . . . .	68
3.16	Specifications for Finite Plate Problem. . . . .	69
3.17	Load Partition and Stress Trajectories for Finite Plate. . . . .	70
3.18	Gross Section Stresses for Finite Plate. . . . .	71
3.19	Net Section Stresses for Finite Plate. . . . .	72

## LIST OF FIGURES (Continued)

<u>Figure</u>		<u>Page</u>
4.1	Gusset Plate Detail. . . . .	73
4.2	Schematic Diagram of Experimental Apparatus. . . . .	74
4.3	Fastener Load Sensing Information. . . . .	75
4.4	Strain Gage Locations. . . . .	76
4.5	Gusset Plate and Fixtures in Test Configuration. . . . .	77
4.6	Sample of Calibration Data . . . . .	78
4.7	Sample of Fastener Load Data . . . . .	79
4.8	Gusset Plate Specimen at Different Test Stages . . . . .	80
4.9	Variation of Fastener Load with Plate Geometry Changes . . . . .	81
4.10	Load Partition for Variable Number of Fasteners. . . . .	82
4.11	Variation of Fastener Load with Total Number of Fasteners. . . . .	83
4.12	Axial Strain At Gross Section of Plate For Variable Geometry . . . . .	84
4.13	Axial Strain at Net Section of Plate For Variable Geometry . . . . .	85
4.14	Transverse Edge Strain for Variable Geometry and Joint Load . . . . .	86
4.15	Brittle Lacquer Stress Trajectories for Variable Plate Geometry . . . . .	87
5.1	Comparison of Analytical and Experimental Load Partition . . . . .	88
5.2	Comparison of Analytical and Experimental Axial Strains (Gross Section). . . . .	89
5.3	Comparison of Analytical and Experimental Axial Strains (Net Section). . . . .	90
B.1	Semi-infinite Plate Problem. . . . .	102
C.1	Finite Plate Residual Problem. . . . .	112
D.1	Total Fastener Flexibility . . . . .	117

## I. INTRODUCTION

### 1.1 Historical Review

The analysis of gusset plates as an integral part of gusseted connections has long been recognized as one of the weak links in the design of structural frameworks. Researchers have looked at various aspects of this problem during the past century and have conducted studies and analyses of a number of the problems associated with gusseted connections. A chronological review of some of the principal experimental and analytical contributions to the study of the problem follows. Many of the works to be cited deal with subjects more general than the behavior of gusset plate connections. Until recently the literature has dealt with stress distribution in plates loaded by individual rivets and bolts, the development of techniques to analyze the load partition of riveted and bolted joints, and the techniques and results of the experimental testing of numerous individual gusseted connections. This literature is cited, however, because it contains the basis for the development of our present knowledge on riveted and bolted connections. A gusseted connection is one particular variation under the general classification of riveted and bolted joints.

The problems associated with the non-uniform distribution of load in gusseted as well as other types of riveted connections were recognized many years ago, but all of the major work on gusset plate analysis has been done since the start of the twentieth century.

In 1913 the problem of stress distribution near a rivet hole was studied analytically in Japan by Yokota<sup>(1)</sup>, while in England the

problem was studied experimentally with much success by Coker and Scoble<sup>(2)</sup>.

Batho<sup>(3)</sup>, in 1916, made one of the first and what remains a classical analytical approach to the partition of load in riveted joints. Work of a similar nature was being carried out in Germany during the same period by numerous investigators and the results of much of their work is cited in a design text authored by Bleich<sup>(4)</sup> in 1924.

The first major experimental work on gusset plates was that of Wyss<sup>(5)</sup> in 1923. This work remains as the most comprehensive work to date with respect to the behavior of gusseted bridge connections. He used relatively large specimens and performed a detailed analysis of the test data for many loads and gusset plate configurations. His tests included secondary effects since the plates were part of an actual truss. His results are somewhat limited for current evaluation since the detailing practices used in Germany at that time were much different than those used today.

Again from Germany in 1929, Hertwig and Peterman<sup>(6)</sup> presented their work on the experimental determination of the load partitioning in riveted joints. Particularly significant was their technique of load measurement; the load was correlated with the rotation of the rivet heads.

Hrenikoff<sup>(7)</sup>, in 1934, reasserted and refined to some extent the work of Batho<sup>(3)</sup> and other early research on the subject. His work was criticized for not being original, but it does provide a good summary of the "state of the art" up to that time.

In 1937, one of the few recorded gusset plate failures occurred and was attributed to poor detailing practices.<sup>(8)</sup> Fatigue failures have

been found in gusset plates and in the components of gusseted connections; however, documentation of these failures is quite limited.

Rust<sup>(9)</sup>, in 1939, completed some photoelastic work on the transfer of stress in gusset plates and published a report regarding gusset specifications and design. No quantitative answers were obtained, but general qualitative answers provided some feel for the behavior of a gusseted connection. In this photoelastic study the load transmission was not by rivets, pins, or bolts so these variables remained in question.

Many of the specific studies cited thus far appear in a literature review on riveted joints published by DeJonge<sup>(10)</sup> in 1945. Abstracts of all important work done on riveted joints until 1940 are contained in this review; the author has found this review invaluable in his literature research.

In 1941 Hrennikoff<sup>(11)</sup> presented one of the first simplified elasticity solutions having direct application to the gusset plate problem. The method, very similar to a finite difference approach neglected the manner in which the load was applied and was concerned only with the stresses far from the point of load application.

Late in the 1940's, the aviation industry published numerous articles concerned with partition of load in riveted and bolted joints. Of particular interest is the work of Vogt<sup>(12)</sup> and the work of Tate and Rosenfeld<sup>(13)</sup> because they have correlated experimental and analytical studies and have assembled the work of earlier researchers to make rational approximations for fastener deformations and local plate deformations.

Also in the late 1940's Grinter<sup>(14)</sup> suggested a method by which designers could approximate the stresses in gusset plates using their knowledge of structural frameworks. The partition of load was neglected in this study as in Hrennikoff's<sup>(11)</sup> and generally the method was quite cumbersome.

In the 1950's a considerable amount of experimental work was done on riveted and bolted joints. At the Universities of Tennessee<sup>(15)</sup> and Kentucky<sup>(16, 17)</sup> several aluminum models of gusset plates were fabricated and tested; they were modeled after gusset plates found in the lower chords of Pratt and Warren type trusses. Attempts were made to devise empirical methods for the design of these types of gusset plates.

At the University of Michigan, Sheridan<sup>(18)</sup> attempted for the first time, as far as this author has been able to determine, to vary the geometry of a gusset plate and to study the effect on the stress or strain distribution in the plate. In this investigation no emphasis is placed on the load partition among the fasteners; the validity of various simple analyses to determine the stress distribution in simple connections was studied.

At Purdue University<sup>(19)</sup> a gusseted structural joint was tested to compare the structural behavior of rivets and high strength bolts. A sharp increase in the use of bolts (high strength) as opposed to the use of rivets initiated many studies of this type. At Purdue, Carter<sup>(20)</sup> studied, photoelastically, the effect of the local stress concentrations in plates loaded by structural fasteners and related them to the fatigue behavior of single fastener joints. This work provides an insight into the local behavior of riveted and bolted joints in the elastic range. At

the University of Illinois Chesson and Munse<sup>(21, 22)</sup> tested a number of large truss-type connections and found ultimate strengths lower than expected in a number of cases. Various types of failures were exhibited in these tests, thus further accentuating the complexity of gusseted connection behavior.

Francis<sup>(22)</sup>, for the Aluminium Development Association, made one of the first significant attempts to analyze the load partition of riveted joints above the elastic limits of the fastener and the plate materials; his development of a graphical technique for determining load partition is quite unique. In 1960 Rumpf<sup>(24)</sup> extended the work of Francis to the analysis of the ultimate strength of bolted steel connections. Fisher<sup>(25, 26)</sup> adapted Rumpf's graphical analysis for computer computation and with extensive experimental testing refined an analysis for long bolted plate splices using certain materials and fasteners.

The most recent analysis of a gusseted connection was done by Lehman<sup>(27)</sup> in 1960. He performed an analysis of a "Y" type connection composed of three tension members joined by a rectangular plate. He used a finite-difference technique and assumed the loading to be parabolic line loads. This is apparently the first attempt in gusset plate analysis to apply the load in a realistic manner. The difficulties encountered in this analysis stemmed from the large number of finite difference equations necessary for an adequate solution.

The adaptation of a classical closed form elasticity solution to the problem of plate connections using rivets and bolts was investigated by Budiansky and Wu<sup>(28)</sup> and was later used by Bloom<sup>(29)</sup>. This method of assuming a loaded fastener to act as a loaded rigid inclusion

in the plate, allows considerable flexibility in its use and provides a more realistic approach to the problem of plate connections.

The preceding review of analytical and experimental research related to gusseted connections should provide a brief sketch of the development of knowledge in the area of riveted and bolted connections and a guide to the development of the present study. A look at the present design criteria follows to illustrate a designer's freedom in proportioning a gusseted connection.

### 1.2 Present Design Criteria

A structural designer may specify the size, shape, and thickness of a gusset plate when designing a gusset connection. According to most structural design codes, gusset plate thickness is determined by fastener bearing stress requirements; the size and shape are usually chosen so that minimum edge distance requirements for the fasteners in the connected members are satisfied. The size and shape criterion may, of course, be arbitrarily overridden for economic or aesthetic reasons. An inspection of truss bridges will illustrate a wide range of gusset plate sizes and shapes; gusset plates vary from simple polygonal to very irregular shapes.

The AISC Specifications<sup>(30)</sup> for the design of structural steel for buildings is an example of a well known and widely used building code which makes no mention of minimum requirements on gusset plate thickness. The only requirements on size are determined by the required minimum edge distances. Several bridge specifications specify a minimum thickness and also that the plate be able to resist shear, direct stress, and flexure acting on a weak or critical section. Not only is it difficult to determine the critical section, but the ordinary beam formulas often

used to analyze such a section to check the stress requirements have been shown to be of questionable value<sup>(15)</sup>.

Present design criteria seem to have been developed without adequate consideration of the behavior of gusseted connections and the numerous parameters which affect this behavior.

## II. OBJECT AND SCOPE OF THIS INVESTIGATION

The behavior of gusseted connections is so complex that few generalizations can be made about the effect of the numerous parameters which are involved. This section indicates the manner in which the gusset plate study is conducted and the extent to which it is investigated.

The study includes analytical and experimental investigations of a very basic type of gusseted connection. Many of the experimental investigations, previously mentioned in Section 1.1, indicate a need for a more detailed study of the parameters which affect the behavior of simple riveted or bolted joints of the variety used for truss-type bridge hanger connections. It is believed that this type of connection is sufficiently basic to indicate how the behavior of more complicated connections might be affected by the same parameters.

The intention of the analytical study is to develop a mathematical model which relates fastener loads to deformations throughout the gusset plate, to combine this relationship with rational assumptions for the load deformation behavior of the connected member, and finally to use this combination as an analytical model in which individual parameters can be studied. This has been done for two types of gusset plates, (1) a semi-infinite plate, and (2) a symmetrical finite plate. The load partition among the fasteners of the connection is studied as joint parameters, e.g. pitch, gusset thickness, fastener flexibility, etc., are varied. The stress distribution in the gusset plate which results from the calculated load partition is then investigated. The method used to obtain the approximate elasticity solution of the finite plate is growing in popularity and has been used

to obtain good approximate solutions to a number of special boundary value problems. Its application to a problem of this type may be of separate interest; details of the elasticity solutions are included as appendices. All computations for the analytical study were programmed for computer solution; a complete program including a brief description of its relation to the analytical development is also included as an appendix.

The experimental study consists of a series of idealized model tests of a symmetric gusset plate connection in which the geometry of the gusset and the total number of fasteners in the joint are varied. The major purpose of the study was to justify the assumptions of the analytical model. The resulting load partition and strains at certain specified points in the plate are presented. Finally, the results of the analytical and experimental models are compared, evaluated, and summarized. Conclusions are presented and recommendations are made for future study.

### III. ANALYTICAL INVESTIGATIONS

#### 3.1 Introduction

An analytical investigation of the elastic behavior of a gusset plate connection requires the development of a simple analytical model with which desired parameters can be varied and their effects on the behavior studied. The development of such a model requires a judicious selection of analytical methods and assumptions which will, within reasonable limits, portray the behavior of the gusseted connection.

The two major objectives of this study are to determine the gusset plate contribution to the non-uniform load partitioning among the fasteners of the gusseted connection and the stress distribution resulting from the fastener loading.

As mentioned previously, Section 1.1, several analytical methods have been applied to the gusset problem to determine the stress distribution for a particular assumed load condition. Also, several techniques have been devised to determine, based on compatibility, the load partition in simple lap joints. These compatibility relationships were founded on basic assumptions regarding the load-displacement characteristics of the individual components of the joint. There was no direct association with the loads and the stress-strain properties of the plates.

It is believed that a combination of the two analytical approaches with some refinement in the treatment of the gusset plate is required to provide a link between individual fastener loads and the stress-strain distribution in the plate. Such a combination should provide the mathematical model necessary for the study of the gusseted

connection behavior. The load-deformation or stress-strain relationships for the gusset plates are derived from the plane theory of elasticity for small deformation in a homogeneous, isotropic, elastic material.

The mathematical model for the semi-infinite plate connection is presented and discussed in Section 3.2. A similar approach is developed in Section 3.3 for a symmetric finite plate joint. Following these formal derivations of the two problems being studied, the results of a number of parameter variations are presented and briefly discussed in Section 3.4.

### 3.2 Semi-infinite Plate Solution; General Considerations

The choice of an analytical model for the study of plate connections using a finite number of point fasteners (i.e. rivets, bolts, pins) leads one immediately to the question of the size and shape of the plates being connected. Since primary emphasis in this study is being placed on the plate contribution to the behavior of a joint, an adequate solution of the plate problem is required. A semi-infinite plate provides, perhaps, the most basic as well as practical geometry to begin the study of the problem of gusset connections. In such a plate, the choice of mathematical model to represent the application of load by a fastener is difficult. This difficulty exists since there are three structural fasteners, each of which differs from the others in the mechanics of load transfer.

A structural rivet usually fills the hole in the connected parts after being driven and the load in a riveted connection is

transmitted by means of friction developed between the connected parts and by bearing of the rivet on the connected plates. However, the magnitude of the frictional resistance is uncertain and as a result the proportion of the load transmitted by these mechanisms is uncertain and will in fact vary with the magnitude of the loading.

The high strength structural bolt, on the other hand, is usually installed with an oversized hole in the connected parts and tightened to maintain a clamping force sufficient for a transfer of load predominantly by the friction developed between the connected parts. The third fastener, the interference body bolt combines in some fashion the described rivet and bolt mechanisms since its knurled shank is driven into the hole in the parts being connected, thus putting the fastener into bearing at a finite number of points. Subsequently the bolt is tightened to a high clamping force which develops frictional resistance between the connected parts. When using a bearing type fastener (rivet), at least a part of the load is applied to one side of the hole in the connected parts, while in a friction type fastener (high strength bolt) the force is distributed over an area on the surface of the plate near the edge of the hole.

Plane-elasticity solutions of a highly complicated nature<sup>(1)</sup> have been developed for representation of the bearing type of load transfer and extremely simple solutions are available for a force at a point in an elastic sheet. The author felt that the approximation of bearing type of load transfer would not be practical in light of its complexity and other assumptions which will have to be made. Although quite simple in form, point force solutions also present complications, in that displacements

are poorly defined in the neighborhood of the load. A method used by Budiansky and Wu<sup>(28)</sup>, that of considering the fastener to be a loaded rigid inclusion, yields a relatively simple method for representing the load transfer mechanism.

The infinite plate with a loaded rigid inclusion has a closed-form solution in plane elasticity which satisfies exactly the boundary condition imposed by the inclusion. A good approximate solution to a semi-infinite plate loaded by a rigid inclusion was used by Bloom<sup>(29)</sup> in his study of infinitely long stringers connected to a plate, and is presented in detail in Appendix B. This solution yields stresses and displacements throughout the semi-infinite plate for a unit load acting on a rigid inclusion; this is the basic solution used in the study of the semi-infinite joint in Fig. 3.1(a). It should be emphasized that displacements are available from this solution. Other analyses<sup>(14, 27)</sup> of the stress condition in plates which use the finite difference approximation, avoid the question of displacements. The importance of displacements will be pointed out in the following derivation of joint compatibility.

The development of the remaining relationships from the analytic model involves making some simplifying assumptions about the deformations of the connecting member and fasteners. In the elastic range fastener and local deformations are approximately linear, as pointed out by a number of researchers<sup>(4, 12, 13)</sup>; the fasteners are considered, therefore, to behave as simple springs. Again following the assumptions of previous research on simple riveted lap joints by Batho<sup>(3)</sup>, the member connected to the plate was considered to deform as though it was in uniform tension (deformation =  $\frac{PL}{AE}$ ) where  $P/A$  is the

uniform stress,  $L$  is the length over which deformation is considered, and  $E$  is the modulus of elasticity. This assumption does not account for local bearing deformations in the lap plates. These deformations are quite local and were assumed to be part of the total fastener flexibility; this matter is discussed in Appendix D where an approximate value for total fastener flexibility,  $C_t$ , is developed.

As far as the mathematical model is concerned, the manner in which the connecting member is attached to the plate, i.e., single or double shear, is arbitrary if the connection is assumed not to bend due to the dissymmetry of single shear loading. The fastener in double shear is allowed less freedom of movement, resulting in a more critical load partitioning. The effect of fastener flexibility as presented in Section 3.4 will make this fact more apparent. Throughout this study, as pointed out in Appendix D, the connecting members load the gusset in double shear. For this reason the "connecting members" are also referred to as "lap plates".

For an elastic joint which deforms in the manner suggested one may write the compatibility equations for displacements of the fasteners and the connected parts. From the elasticity solution of the loaded semi-infinite plate (Appendix B) we obtain the displacement along the  $x$  axis,  $u_{ij}$ , for  $n$  fastener positions and for each of  $n$  fastener load positions;  $u_{ij}$  is the displacement at the  $i$ th fastener due to a unit load at the  $j$ th fastener (fasteners are numbered in order beginning at the one closest to the edge of the plate). This is an approximation to a problem of  $n$  rigid inclusions; here, only the loaded inclusion has been approximated as rigid. The remaining inclusions are replaced by

plate material. The displacement at fastener locations other than the loaded inclusion is calculated at the point corresponding to the center of the fastener. The deformation of the  $i$ th interval of the plate due to a load at the  $j$ th fastener is then given by

$$\epsilon_{ij} = u_{ij} - u_{i+1,j} \quad (3.1)$$

where,  $1 \leq i \leq n - 1$ , and  $1 \leq j \leq n$

As assumed, the deformation of the connecting member in the  $i$ th interval will be  $\frac{Q_i p}{A_s E}$ , where  $Q_i$  is the total load transmitted by the lap plates in the  $i$ th interval,  $p$  is pitch of the fasteners and  $A_s$  is the effective cross-sectional area of the lap plates. The total local and fastener deformation is then approximated by

$$\delta_i = C_t f_i$$

where  $f_i$  is the  $i$ th fastener load. Using Fig. 3.2 as an illustration we may write the compatibility relationship for the  $i$ th interval

$$p + \Delta_i^G + \delta_i = p + \Delta_i^L + \delta_{i+1} \quad (3.2)$$

where  $\Delta_i^G$  is the deformation of the  $i$ th interval of the gusset plate and  $\Delta_i^L$  is the deformation of the  $i$ th interval of the lap plates. In terms of physical properties and loads  $\Delta_i^G$  and  $\Delta_i^L$  become

$$\Delta_i^G = \sum_{k=1}^n \epsilon_{ik} f_k \quad (3.3)$$

$$\Delta_i^L = \frac{p}{A_s E} \sum_{k=i+1}^n f_k$$

Substituting into Eq. 3.2 and simplifying we obtain the general compatibility equation for the  $i$ th interval in terms of the load.

$$\sum_{k=1}^n \epsilon_{ik} f_k - \frac{p}{A_s E} \sum_{k=i+1}^n f_k + C_t (f_i - f_{i+1}) = 0 \quad (3.4)$$

Since there are  $n-1$  intervals, only  $n-1$  independent equations exist, which is one less equation than the number of unknown fastener loads. The solution is achieved by specifying the total load on the joint or assuming a value for one of the fastener loads. The latter method is the one used by the author in the computer solution of the problem.

The development of the general compatibility equation (Eq. 3.4) has introduced numerous variables related to the elastic properties of the various components of the connection. Beginning with the determination of the plate influence coefficients  $\epsilon_{ij}$  we may vary:

1. modulus of elasticity
2. Poisson's ratio
3. diameter of inclusion
4. edge distance of the first inclusion
5. pitch of the inclusions
6. thickness of the plate

Independent of these choices other variables are

1. cross-sectional area of connecting member
2. modulus of elasticity of the connecting member
3. total fastener flexibility

Discretion must be used in the choice of variables, so that the conditions resulting from various assumptions made during the derivation are not violated. Variations of a number of the joint parameters are presented and discussed in Section 3.4.

Now, having developed the major hypothesis for the semi-infinite plate connection one proceeds in a similar manner to the more tedious analytical problem of the finite plate.

### 3.3 Finite Plate Solution

The natural continuation of the study of plate behavior in a gusseted connection is to approach a more complicated plate geometry than that of the semi-infinite plate. A symmetrical plate connection (Fig. 3.1) was chosen for investigation, based on the ease of obtaining an elasticity solution for such a plate and on the results of Sheridan's<sup>(18)</sup> work with eccentric connections; he found "the greatest divergence from plane on specimens with no eccentricity of loading". A common use of this shape of plate is the lower chord hanger connection in many trussed bridges. The elasticity solution of the gusset plate used to obtain the influence coefficients is the only respect in which the semi-infinite and finite plates vary from one another in formulation; consequently only the additional geometric variables will now be discussed.

The elasticity solution approximating the symmetrical plate problem is presented in detail as Appendix C. As with the semi-infinite plate, the solution for a loaded rigid inclusion in an infinite plate is used as a base and functions are added which cause the infinite plate stresses to vanish on the chosen finite plate boundaries. The solutions, performing this function, are truncated power series of the complex displacement potentials  $\phi$  and  $\psi$  discussed in considerable detail in Appendix C.

To define adequately the finite plate problem several additional properties, pertaining to the plate shape and solution desired, must be added to the six variables mentioned for the semi-infinite solution in Section 3.2.

The size and shape of the plate will be described by the boundary point coordinates which are specified for the 'point matching' scheme discussed in Appendix C. Depending on the desired accuracy of the solution and on the loading, a number of points on the boundary of the plate are chosen. Also related to the accuracy of the solution, are the number of terms to be evaluated in each of truncated power series  $\phi$  and  $\psi$ . Actual choices of these additional parameters will be discussed in the following major section on results (Section 3.4).

Obviously then for the complete solution of the finite plate joint of  $n$  fasteners,  $n$  sets of series coefficients are required; one set for each fastener load position. Then, using the infinite plate solution and the series solution for the residual problem, the displacement  $u_{ij}$  and their adjustments, caused by the stress release, may be computed. From here, as in the semi-infinite plate joint we proceed to calculate

the fastener load partition for variable fastener and lap plate flexibilities.

The stresses at any point in the finite plate may be computed for a particular load partition and total load by superimposing the stresses at that point caused by each fastener load; each stress computation for a fastener load involves the superposition of the infinite plate and boundary adjustment stresses. The stresses at the point for each fastener load may then be superimposed. The results of the analytic investigations, including the load partition and stress distribution for the finite plate joint, just discussed, are presented in the following section

### 3.4 Analytical Results

#### 3.4.1 General

The elastic solutions of the two gusset-type joints shown in Fig. 3.1, commensurate with the assumptions and approximations presented in Sections 3.2 and 3.3, will be illustrated in Section 3.4 by varying a number of the joint parameters and studying the resulting effects on the fastener load partition and on the stress distribution in the plate. All calculations for the two problems were programmed and performed using the University of Illinois IBM 7094 digital computer. The computer programming is not presented in this report but is available in the original thesis at the University of Illinois Library.

Primary emphasis in this study has been on structural connections, i.e. those used in bridges, buildings, etc. Approximate values of the

modulus of elasticity and Poisson's ratio for steel ( $E = 30,000$  ksi and  $\nu = 1/3$ ) were used throughout. Hybrid connections are conceivable in, for example, aircraft structures where aluminum plates may be joined by steel rivets or bolts. However, this particular aspect of the problem is left for future study.

The closed form of the semi-infinite plate solution suggests that it be used as the primary model for the initial variation of parameters. The finite plate solution can then be used to illustrate the geometric parameter effect.

The following subsections are presented along this line of thought. First, the plate and connecting member parameters are varied using the semi-infinite joint and then a finite plate is solved to show the finite plate geometry effects.

Parameters to be varied are:

1. total number of fasteners
2. edge distance of first fastener
3. fastener pitch
4. thickness of gusset
5. area of lap plates
6. fastener flexibility
7. geometry of plate

It should be mentioned here that a gusseted connection may have any number of complexities introduced by the type and number of members connected as well as the manner in which these members are loaded. The complications introduced by these variables are avoided

in this study since it was felt that these added variables would confuse the already complicated analytical problem.

#### 3.4.2 Load Partition, Semi-Infinite Plate

The variables for the semi-infinite plate joint, with the exception of the material constants  $E$  and  $\nu$  are as follows:

$$d, h_e, p, t, n, A_s, C_t$$

As discussed in the scope of the investigation an experimental study was conducted concurrently with the analytical study. A set of dimensions of similar magnitudes to the experimental dimensions will be taken as a base from which individual parameter variations may be studied. Some of the values for dimensions of length may be immediately expressed as multiples of other dimensions since only their relative magnitudes have an effect on the solution.

Further non-dimensional reduction was not attempted because of the number of approximations involved in determining the quantity  $C_t$ . Generally, each parameter was varied over a wide range of values approaching, in some cases, unrealistic behavior. The reasonable range over which parameters might vary in structural steel connections, using a variety of fastening devices, will be discussed as each parameter is cited.

The load partition has been presented in a number of ways in past research, the most usual being in terms the percentage of the total load. Present design procedures are based on the assumption of equal load distributed to each fastener. Therefore, the author felt that a normalized load partition would be a more meaningful way of illustrating

the behavior of the joint with respect to the assumed idealistic behavior; the fastener load partition is based on an average load of unity per fastener. Then, a fastener load of 1.50 indicates that the fastener load is 50% above the average load per fastener on that particular joint.

The following dimensions were used as base values of comparison.

$$d = .375 \text{ inches}$$

$$h_e = 3d = 1.125 \text{ inches}$$

$$p = 3d = 1.125 \text{ inches}$$

$$t = .25 \text{ inches}$$

$$A_s = 2.0 \text{ inches}$$

$$C_t = .25 \times 10^{-3} \text{ inches/kip}$$

$$n = 7$$

These dimensions are similar to those of the experimental model but have been, for convenience, arbitrarily rounded to whole or rational numbers. The value for  $C_t$  which is based on  $d$ ,  $t$ , and an assumed thickness for the lap plates is discussed in Appendix D.

A generally accepted fact is that load partition becomes more severe with an increase in the number of fasteners in a joint. Figure 3.3 illustrates the effect on the load partition of varying the number of fasteners from 3 through 10. In each case, of course, the total load increases as well as the number of fasteners. Figure 3.4 illustrates the net effects more vividly. Here the loads in the first and last fasteners and the minimum load at any interior fastener are plotted with

respect to the total number of fasteners in the joint. It is apparent that the load in the first fastener is most effected by the change in the total number of fasteners. The variation in the total number of fasteners can be considered as a variation in joint length since the pitch has been held constant.

A designer may vary pitch over a considerable range, however normally he seeks to keep it at a minimum (usually  $3d$ ). In Fig. 3.5, returning to the seven fastener joint, the pitch is varied from the minimum value of  $3d$  to twice this value or  $6d$  and the resulting load partition is plotted. Figure 3.6 illustrates that again the first fastener is most effected by the change. For a realistic range of values of pitch, perhaps  $3d$  to  $4d$ , the effect in itself is hardly significant.

Another parameter, which, within certain restrictions, is the choice of the designer, is the edge distance of the first fastener. Figure 3.7 shows the load partition for a seven fastener joint at three different edge distances. The edge distance of infinity is not a realistic edge distance but does show the limiting affect of the stress free edge on the joint load partition. The joint having an infinite edge distance would be equivalent to an infinite plate joint. The first, last, and minimum loads for intermediate edge distances are shown in Fig. 3.8. There is little change in load except as the edge distance becomes infinite. The first fastener load tends to decrease with decreasing edge distance as would be expected. Values of edge distance smaller than  $3d$  were not considered in light of the assumptions made in the

elasticity solution of the semi-infinite plate (Appendix B). One would expect the load in the first fastener to drop rather quickly as the edge distance approaches zero.

The remaining plate variable, that of thickness, is difficult to vary independently since it is associated with value of  $C_t$ . Keeping this in mind one may investigate the independent variation of  $t$  in Fig. 3.9. The first fastener load increases with the thickness at about the same rate as the last fastener load decreases, the minimum remaining fairly constant. As will be pointed out later in the section, this is similar to the effect of the variation of lap plate area. The two variables remaining are the total area of the lap plates and total fastener flexibility.

The lap plate area is representative of the stiffness of the members which might be joined by a gusset plate. Figure 3.10 illustrates the variation in fastener load for all possible values of  $A_s$ . The limiting values exhibit the expected behavior, i.e. as the area of lap plates in the fastener intervals approaches zero, all of the load goes to the first fastener and, as the area becomes infinite, a load partition for a joint with a rigid connecting member, allowing only local deformations, exists. For this particular joint parameter only a small range of areas is realistic, perhaps from  $A_s = 1.0$  to  $A_s = 4.0$ . The last parameter to be varied for the semi-infinite plate is the fastener flexibility,  $C_t$ . This parameter is undoubtedly the most indeterminate of all of the joint parameters. It accounts for all of the deformations local to the fastener, except the ones accounted for in the elasticity

solution of the gusset plate. The assumption of  $\delta_i = C_t f_i$  indicates basically that the deformation is linear and unaffected by other fastener loads. A value of zero for  $C_t$  would be a reasonable approximation for a bolted joint before slip occurs, although even in this case some local deformation would occur. A value of infinity for  $C_t$  would lead one to the idealistic behavior with uniform loading of all fasteners. This case, of course, is not physically possible. Therefore, a realistic value of  $C_t$ , lies somewhere between in 0 and  $\infty$ , depending upon the thickness of the plates and the fastener used. In Appendix D a reasonable value has been obtained for  $C_t$  relating it to the other base parameters of the plate. The effect of variations in  $C_t$  above and below this value ( $C_t = .25 \times 10^{-3}$  in/kip) on the load partition is illustrated in Fig. 3.11. Here it is interesting to note the manner in which the variable  $C_t$  affects the partitioning of load. The minimum loads are affected quite drastically, as are the end loads. This is shown again in Fig. 3.12. It is estimated that for this joint, depending on the fastener used,  $C_t$  could vary realistically between 0 and  $.4 \times 10^{-3}$  in/kip.

#### 3.4.3 Stress Distribution, Semi-infinite Plate

The stress distribution in the gusset plate was one of the prime considerations of this investigation. Early in the development of the analytical work the stress distribution throughout a rectangular section of the semi-infinite plate was studied using a set of parameters, which were similar to those of the experimental model, the purpose being to check equilibrium of the system as well as to investigate the load

transfer. The total load based on 3 kips per fastener is equal to the loading on the experimental model. Some of the results of this investigation are shown in Fig. 3.13. The tractive stresses are plotted along the boundaries of the rectangular section chosen for investigation. On the boundary of this section which is perpendicular to the line of load the stress,  $\sigma_x$ , acts to resist the external loading, while on the boundary of the section which is parallel to the line of loading the shear stress,  $\tau_{xy}$ , acts to resist the external loading. At this particular section the total load applied to the semi-infinite plate is resisted by the direct tension on one boundary and by shear on the other two; for this section approximately half of the load is transferred by shear and half by direct stress. Figure 3.13 has been presented here to illustrate the load transfer in the semi-infinite plate and will be used later in comparison with the load transfer in the finite plate.

While studying the stress in the plate of Fig. 3.13 a very high transverse stress ( $\sigma_y$ ) was discovered along the stress-free edge at the line of loading. This high tensile stress tends to split the plate apart along the load line. The high transverse stress diminished rapidly away from the stress-free edge.

To study the splitting stress more closely the effect of an individual fastener at a variable edge distance was investigated (Fig. 3.14). Using this figure one may, for a given load, edge distance, fastener diameter, and plate thickness, calculate the transverse edge stress; the quantity  $P/dt$  is commonly used to denote the average bearing stress of a rivet or bolt and is used in the dimensionless ratio,  $\frac{\sigma}{P/dt}$ ,

in Fig. 3.14 for convenience in relating the five quantities mentioned. Stresses for  $h_e < 3d$  were not plotted since, as explained in Appendix B, the approximation of the elasticity solution of the semi-infinite plate is not valid for small edge distances.

Figure 3.14 illustrates that the splitting stress diminishes quite rapidly as edge distance increases. However, the stress does not approach zero so rapidly as to allow one to neglect the effect of fasteners far from the edge.

The edge stress for a variable number of fasteners and for an edge distance of the first fastener is illustrated in Fig. 3.15. In addition to the variables used in Section 3.4.2 a total average load of three kips per fastener is maintained for all cases. This illustration is not completely realistic since  $t$ ,  $A_s$ , and  $C_t$  would normally vary with the design load, but it does show that the edge distance of the first fastener and the total number of fasteners in the joint affect this edge stress considerably.

For the semi-infinite plate, the most critical stress seems to be the splitting stress just discussed. This stress will be discussed again in the next section in connection with the finite plate and later in the experimental study.

#### 3.4.4 Load Partition and Stress Distribution, Finite Plate

The complete solution for the load partition and the stress distribution of a particular finite plate joint is presented here to illustrate the solution technique and the effect of the geometric variables. Extensive variation of parameters has not been attempted for the finite

plate since it is believed that the results of the parameter variation on the semi-infinite plate adequately describe the effects of a similar variation on the finite plate. More detailed variation of geometric parameters has been left for future study.

The solution of the finite plate problem differs from the solution of the semi-infinite plate problem only in the manner in which the elasticity solution for the plate is obtained. The finite plate solution requires several more input parameters to describe the shape and size of the plate and to indicate the extent of the precision to be carried out in computations. The details of the theory on the solution of the finite plate problem are presented in Appendix C and discussed further in Section 3.3. The problem is discussed here in terms of the actual manipulations performed and results obtained.

In addition to the plate variables listed in Section 3.2 for the semi-infinite plate the coordinates of a number of points on the boundary of the plate are specified. Generally, the more points defining the boundary the better the solution to the problem. It was found during development of the computer solution that the distribution of the points on the boundary also affected the precision of the solution.

The coordinates of the boundary points are most conveniently expressed in realistic dimensions of length. However, the power series expansions used in the solution necessitate a scaling of these dimensions to avoid the generation of very large or very small numbers which are not within the range of operation of the IBM 7094 digital computer.

In connection with the truncated power series generated for the solution, the number of terms to be expanded in the series must be

defined. Generally, as with the boundary points, the larger number of terms used in the series the better the solution.

In summary, the additional variables required for the finite plate solution are the following:

1. Boundary points,  $z_i$  (a finite number of points at a selected distribution)
2. A scale factor for the plate dimensions
3. The number of terms in the  $\phi_1$  and  $\psi_1$  series

Figure 3.16 illustrates the selection of a set of points,  $z_i$ , for a particular shape of finite plate. The plate chosen has a taper of 1:2. It is 10 inches wide and 12 inches long measured from the origin to the boundary perpendicular to the line of load. There are 33 boundary points shown intuitively distributed to improve the approximation to the solution in the region where the loads are close to the edge of the plate and where the boundary changes direction sharply. One inclusion is shown solid in Fig. 3.16 to emphasize that the problem is solved independently for each load location. The 33 points on the boundary generate 64 separate conditions to be met by the series solution. The "least squares" approach explained in Appendix C allows one to choose fewer terms in the series than are required to satisfy exactly the boundary conditions specified at each point. For the problem of Fig. 3.16, sixteen terms in each series proved to be quite sufficient to generate an adequate solution. An optimization of the number and distribution of the points as well as the number of terms in the series may be possible; however, the author has found that an adequate choice of variables can be made quite easily after a trial solution. For the

plate specifications in Fig. 3.16 a solution was obtained and the load partition with the resulting stress trajectories are presented in Fig. 3.17. The state of stress was evaluated at a number of points on the gross and net sections shown in Fig. 3.17. These results are plotted and presented as Fig. 3.18 and Fig. 3.19 for gross and net sections respectively.

An integration of the  $\sigma_x$  stress over the gross section satisfies equilibrium of the system. The only apparent discrepancy lies in  $\sigma_y$  and  $\tau_{xy}$  not vanishing on the boundary. Little error is indicated however.

The net section stresses show some discrepancy on the boundary. This is largely due to the fact that the net section happens to pass through a corner of the plate where the solution is not well defined.

An immediate check on the elasticity solution of the entire stress distribution is to evaluate the combined stress along the boundary due to all fastener loads to see how well the stress free boundary conditions are met. The stress condition for each point as numbered on Fig. 3.16 is tabulated in the table on the next page. The solution could have been presented in a more non-dimensional form, but it was felt that in connection with the entire study the dimensional form is more easily understood. Also presented is a list of the variables associated with this solution. If the stress free condition was satisfied perfectly  $\sigma_2$  column would be zero and the principal orientations would be the same as the orientation of the boundary at every point (either  $0^\circ$  or  $26.5^\circ$ ).

## FINITE PLATE STRESSES AT BOUNDARY

$$\begin{aligned}
 t &= .25 \text{ in.} & A_s &= 1.5 \text{ sq. in.} \\
 d &= .375 \text{ in.} & C_t &= .000250 \text{ inches/kip} \\
 h_e &= 1.25 \text{ in.} & n &= 7 \\
 p &= 1.125 \text{ in.} & f_i (\text{ave.}) &= 3 \text{ kips}
 \end{aligned}$$

Point Number	Coordinates x inches    y inches		$\sigma_x$ psi	$\sigma_y$ psi	$\tau_{xy}$ psi	$\sigma_1$ psi	$\sigma_2$ psi	Principal Orientation degrees
1	12.0	0.00	9	5110	0	5110	9	.0
2	12.0	0.10	9	5023	-30	5023	9	-.3
3	12.0	0.20	7	4767	-54	4768	7	-.7
4	12.0	0.30	3	4360	-66	4361	2	-.9
5	12.0	0.50	-23	3189	-42	3190	-23	-.7
6	12.0	0.70	-39	1755	48	1757	-41	1.5
7	12.0	0.80	-12	1019	115	1032	-25	6.3
8	12.0	0.90	69	307	195	417	-41	29.3
9	11.9	1.05	473	-52	-202	542	-121	18.8
10	11.8	1.10	792	190	-529	1100	-118	30.2
11	11.7	1.15	1161	365	-755	1616	-91	31.1
12	11.6	1.20	1554	482	-921	2083	-47	29.9
13	11.4	1.30	2321	609	-1170	2915	16	26.9
14	11.2	1.40	2965	690	-1396	3628	27	25.4
15	11.0	1.50	3452	784	-1630	4225	12	25.4
16	10.8	1.60	3812	898	-1862	4720	-9	26.0
17	10.6	1.70	4098	1016	-2065	5134	-20	26.6
18	10.3	1.85	4470	1171	-2292	5645	-4	27.1
19	10.0	2.00	4833	1279	-2449	6082	30	27.0
20	9.5	2.25	5410	1356	-2677	6742	25	26.4
21	8.5	2.75	6057	1466	-3057	7584	-61	26.5
22	7.5	3.25	6100	1559	-3005	7596	63	26.5
23	6.5	3.75	5443	1381	-2704	6794	30	26.5
24	5.5	4.25	3933	986	-2088	5015	-97	27.4
25	5.0	4.50	3123	741	-1617	3941	-76	26.8
26	4.5	4.75	2483	503	-1058	2942	45	23.4
27	4.0	5.00	2132	302	-441	2233	202	12.9
28	3.5	5.00	2817	55	-199	2832	41	4.1
29	3.0	5.00	3528	-57	-59	3529	-58	.9
30	2.0	5.00	4839	-60	51	4839	-61	-.6
31	1.0	5.00	5765	20	49	5766	20	-.5
32	0.5	5.00	6015	49	27	6015	49	-.3
33	0.0	5.00	6100	59	-0	6100	59	.0

The residual normal stress  $\sigma_2$  oscillates about zero along the boundary showing maximum deviation at or near the corners. This is to be expected because the truncated power series approximation cannot represent the sharp discontinuity at the corners. These deviations are very small compared to the magnitudes of stress throughout the plate; the average gross section stress is 8400 psi. The maximum deviation of 202 psi is only about 4% of this value. All of the other  $\sigma_2$  deviations are considerably less. Some deviation is introduced through the discrete character of the method which is being used; no attempt has been made to satisfy the boundary conditions on more than a finite number of points. Part of the deviation undoubtedly is caused by the round off error accumulated in the computer calculations.

A major advantage of this method is that the field equations (equilibrium and compatibility) are satisfied exactly on the interior of the plate. Since the external equilibrium has been verified and the boundary condition has been approximated to the degree observed above, it is felt that this method adequately solves the plane elasticity problem for the finite plate.

## IV. EXPERIMENTAL INVESTIGATION

### 4.1 Introduction

The experimental investigation presented in this section was conducted to study under controlled conditions the behavior of a very basic type of gusset plate connection. The experimental phase was developed and performed simultaneously with the analytical study previously presented. The dimensions and physical properties of the specimen and material were similar to those assumed in the analysis. A new technique was developed to indicate the partition of load among the fasteners of the connection. The gusset was instrumented to measure the strain distribution at certain selected points.

All testing was performed within the elastic range of the connection materials. Several parameters were varied using only one specimen; these included gusset plate geometry and total number of fasteners.

In the following sections the design fabrication and instrumentation of the specimen are described. The test procedure and a summary and discussion of the experimental results are then presented.

### 4.2 Design of Specimen

The word "design" may be somewhat ambiguous in light of the comments of Section 1.2 concerning the present status of gusseted connection design; however, a simple symmetrical gusseted hanger-type connection was proportioned using common design requirements for the tension: shear: bearing ratio.

A seven fastener joint was chosen, based largely on having a sufficient number of fasteners in a line to cause a relatively severe load partitioning and to provide a sufficient variation in the number of fasteners by removal of fasteners, i.e. the total number of fasteners could be made equal to 2, 3, 4, 5, 6, or 7.

The double symmetry which occurs when a symmetric gusset plate is loaded in double shear was found to be advantageous from the standpoint of the ease of making test measurements.

Since all testing was to be done in the elastic range of the gusset plate material, an ASTM A514 steel having a 90 ksi minimum yield stress, was chosen for the plate material. The fastening device was chosen to be a tight fitting pin for reason of easy assembly and removal as well as its basic nature of transferring load entirely through the fastener, i.e. providing no friction between the connected parts. The material used for the pins was "drill rod." In pilot tests it was found that the yield strength of the "drill rod" was such that the pin would remain undeformed after loadings equal to those of its intended application.

The gusset specimen detail is shown in Fig. 4.1. Generally, the overall size of the specimen was determined from instrumentation criterion and the ease in handling of the test apparatus. The net section area of the lap plates is approximately 1.3 sq. inches which yields a T:S:B ratio of 1.0:0.84:1.5. The critical bearing is, of course, in the gusset plate and was made lower than allowable to avoid permanent bearing deformations.

Also shown in Fig. 4.1 are five arbitrarily selected plate geometries beginning with a rectangle numbered "1". The geometries will be referred to by number as they are shown in Fig. 4.1.

#### 4.3 Fabrication

The gusset plate specimen and lap plates were painstakingly fabricated to assure good alignment and ease of assembly as well as to remove any undesired variables such as eccentricity. The gusset plate was cut from a slightly oversize piece of 1/4 inch steel plate and finished on both surfaces with a hand sander to remove mill scale and to reduce the thickness to within  $0.250'' \pm 0.002''$ . Warpage in the plate was checked and the plate straightened insofar as possible.

The lap plates were cut and machined from the same type steel as the gusset plate. Both of the lap plates and the gusset plate were then carefully aligned and clamped as a unit to the bed of a horizontal milling machine. The pin holes were then drilled and reamed to assure matching as well as accurate spacing and alignment. The pins were cut to size and marked to assure being placed in the same hole and in the same orientation upon each subsequent reassembly. The pins were then polished so that they could be inserted and removed with ease.

The fabrication and assembly of the test specimen was carefully controlled since the deformations at full load are very small and slight inaccuracies in fabrication would produce a behavior far from the idealized behavior sought in this study.

#### 4.4 Instrumentation

The instrumentation as discussed in this section includes a description of the loading fixtures and the load measuring devices. Special emphasis is placed on the method devised to measure the individual loads transmitted by the fasteners of the pinned joint. The placement of

strain gages at selected locations on the gusset plate and the application of a brittle lacquer coating to the connection will also be described.

The gusset plate specimen was attached to loading fixtures and mounted in a large universal testing machine as shown schematically in Fig. 4.2. The loading fixtures were designed to resist more than adequately the maximum load applied to the specimen and were attached to the specimen with high strength bolts for easy removal and reuse. A pinned joint at one end of the loading apparatus and a ball seat at the other end were provided to avoid any secondary effects from eccentric loading. The entire load rig was placed in a large universal testing machine which acted as a loading frame. To provide more accurate control and greater convenience, the load application and measurement were accomplished using a 20 ton hydraulic jack operated by a hand pump. A calibrated weighbar which utilized output from electric resistance strain gages was used for a load indication; the loading capabilities of the universal testing machine were not used.

A number of researchers have devised methods for the measurement of the load transmitted by the fasteners in riveted and bolted joints. These methods range from the measurement of the rotation of the ends of the fasteners during loading to the placement of numerous resistance strain gages on the lap plates to measurement of the load transmitted by the lap plates so that load in the individual fasteners can be calculated. This latter method requires a large number of strain gages to obtain good calculated loads and may be desirable when the fastener pitch is large enough to provide convenient instrumentation of the lap plates as well as a more uniform lap plate loading.

From observation of the photoelastic studies of Carter<sup>(20)</sup> and Coker<sup>(2)</sup>, it was felt that placement of miniature strain gages on the surface of the loaded plate at or near the compression side of the fastener would allow, after calibration, a sensitive means of measuring the individual fastener loads. Placement of the gages on the compression side of the holes near the edge of the hole reduced the effect other fasteners might have on the load indication. A schematic presentation of this action is presented in Fig. 4.3. To check the effect a three pin double shear lap joint was tested using 5/16 inch pins and 1/4 inch square foil-type resistance strain gages mounted on only one surface of the center plate. Results were erratic and showed a non-linear behavior. The holes in the pilot specimen were reamed to 3/8 inch diameter and 1/8 inch square gages were mounted on both surfaces of the plate; the gages were wired to cancel any bending effect caused by unequal loading in the lap plates. A consistent, sensitive and predominantly linear response was obtained from this arrangement.

Based on the pilot studies, the fastener load sensing instrumentation was used as shown in Fig. 4.3. One-eighth inch square gages were placed about 3/32 of an inch from the edge of the 3/8 inch hole on the load line. The response from the gages was approximately 1200 micro inches for the 5 kip maximum load applied to each fastener during calibration. The maximum effect from a load in an adjacent fastener was between 50 and 100 micro inches for the 5 kip load, a relatively small effect.

For convenience and efficiency in the recording of data the total load and individual fastener loads were used as input to the two axis of an x-y recorder. A multiple contact switch was used for selection of the fastener load to be measured, and each fastener load sensing device was

provided with a means for individual zero adjustment. With this arrangement, the X-Y recorder, after adjustment and calibration, was used to plot total load versus fastener load response for each fastener; this was done for each fastener when it was loaded individually and when loaded as part of a composite joint using 2 through 7 fasteners. Additional discussion on load measurement will be presented in the next section on test procedure.

For an experimental determination of the stress or strain distribution in the gusset plate, foil-type resistance strain gages were used at the net and gross sections as shown in Fig. 4.4. Gages were mounted on only one half of one side because of the double symmetry of the connection; three gages on the net section were rosettes. Two additional gages were placed symmetrically opposite to the gages shown with an asterisk in Fig. 4.4 to check for eccentricity of loading. After testing had begun, an additional gage was placed on the edge of the plate on the load line to check the high splitting stresses indicated in the analytical solutions and mentioned earlier in Section 3.4.3.

One surface of the plate was left relatively free of external gages and was polished to provide a surface for application of brittle lacquer for the study of strain trajectories.

In summary, the gusset plate was instrumented for measurement of total load and individual fastener load; the plate was also instrumented with strain gages at a number of points and sprayed with brittle lacquer to indicate the distribution and flow of strain throughout the plate.

#### 4.5 Test Procedure

The gusset plate specimen (Fig. 4.1) was tested for the five geometries indicated; the procedure used for a typical test is described here.

Initially the gusset plate specimen and load fixtures were fitted up and while hanging, supported only at the top, the high strength bolts in the top and bottom load fixture connections were snug tightened to ensure proper alignment of all components. These bolts were then tightened to a high tension. The lower load fixture remained assembled during all tests and specimen alterations.

The photograph in Fig. 4.5 shows the specimen in place and viewed from the side used for the brittle lacquer study. With the specimen in place it was wired, as shown in Fig. 4.2, to the X-Y recorder; the recorder could then be balanced and calibrated. All pins except one were removed and a load calibration was made using the X-Y recorder to record total load on one axis and load response from the fastener on the other. A portion of this record for the number 4 fastener is shown in Fig. 4.6. The influence of the number 4 fastener load on three other load indicating gages is shown by the two curves having negative slope. The opposite slope is, of course, due to a tensile strain which is opposite in sign to the compressive strain recorded for the fastener load. Each of the remaining six gages were calibrated in the same manner, recording the effects of each pin on the gages at the unloaded holes.

After calibration a number of fastener combinations were tested. An example of the load data for a five fastener joint is shown in Fig. 4.7. The non-linearity of response for total load less than 2 kips is caused by a lack of uniformity in pickup of load in the 5 fasteners; despite the care in fabrication and assembly this behavior was unavoidable. The various fastener combinations were loaded to a average load of 3 kips per fastener above an initial load of 3 kips making sure that the most critically loaded fasteners were not overloaded.

For a number of fastener combinations the individual strain readings were taken from the surface gages at the net and gross sections of the gusset plate for the same total load ranges which were used for the load partition measurements.

With seven fasteners in place the specimen was sprayed with brittle lacquer to indicate the strain trajectories for that particular gusset plate geometry. The strains in the gusset were slightly below the threshold strain required to crack the brittle lacquer at room temperature; therefore, the specimen was cooled slightly with compressed carbon dioxide to induce cracking. Crack patterns which were then quite visible were outlined. These lines are visible in the photograph shown in Fig. 4.8(a); the horizontal member shown in Fig. 4.8a was used only to make sure that the lap plates did not separate from the main plate during load application.

After the brittle lacquer crack patterns were recorded, the specimen was removed from the testing machine, the upper load fixture and lap plates were removed, and the gusset plate geometry was altered for the next test. Shown in Fig. 4.8(b) is one of the geometric alterations of the gusset plate connection viewed from the gaged side of the specimen. In the following section the data from the tests on various geometries and fastener combinations are presented.

## 4.6 Results

### 4.6.1 Load Partition

The parameters varied in the experimental study of load partition are the plate geometry and the total number of fasteners.

The experimental load partition was obtained from the reduction of data of the type shown in the calibration curves of Fig. 4.6 and the composite load data of Fig. 4.7. Compensation was made for the effect of each fastener load on the load sensing gages of the other fasteners. As a check on the accuracy of the measurements and the method, the total load obtained from summing the individual fastener loads was compared with the measured total load. Errors were less than 5%; the sum of the individual fastener loads was consistently less than the measured total load. The variation in geometry is described in terms of the angle between the tapered edge of the gusset plate and a perpendicular to the load line as shown in Fig. 4.9; the fastener loads are presented as in the analytic study in terms of an average load of unity per fastener.

In Fig. 4.9 the first, last, and minimum fastener loadings are shown in terms of the geometry of the plate. Although the five tests did show some scatter, the expected trend occurred as indicated in the analytical work, i.e., the reduction of load in the first fastener with the simultaneous increase of load in the last fastener. No noticeable change occurs until after the gusset has been altered to such a severe angle that the net cross-sectional area of the gusset is reduced.

For the second geometry the variation in load partition is shown in Fig. 4.10 for a variation in the total number of fasteners. As in the analytical study the first fastener load becomes more severe with increased total number of fasteners, while the last fastener loading and the minimum fastener loading change much less severely. This variation of fastener load is indicated in another manner in Fig. 4.11 for the third geometry. The first, last, and minimum fastener loadings are plotted in terms of the total

number of fasteners and indicate the type of behavior indicated in Fig. 4.10. The load partition results for the first three geometries are basically the same except for some scatter, which is quite small considering that the joint was reassembled for each test and that much of the data reduction was made by visual graphical interpretation. It should be mentioned that the experimental load partitioning presented here is the partition which would have occurred if all of the fasteners began to take load at the same time. As indicated earlier in Fig. 4.7 the fasteners did not all pick up load simultaneously. The smooth load partitions presented here are nothing more than the load taken by the fasteners after initial preload (total load = 3 kips). This is justified by the linear elastic behavior of the pins during calibration.

One factor which was not accounted for in the measurement of the individual fastener loads is the effect of change in shape of the hole on the response of the individual load indicating gages. Calibration was made on a lightly loaded plate; however, the individual loads in a load partitioning were measured when the plate was loaded by as many as six other fasteners. It is believed that the effect of this factor was small, based on the good agreement between the total measured load and the sum of individual loads.

#### 4.6.2 Strain Distribution

The measurement of strains in the gusset plate using electrical resistance strain gages is a relatively straightforward operation. Gross and net section axial strains are presented for the five geometries of gusset plate. Transverse edge or splitting strains are also presented in terms of variable geometry. Finally, sketches of the brittle lacquer

patterns are shown to illustrate, for the first three geometries the variation of stress or strain distribution with geometry.

Axial strain distribution at the gross section of the gusset plate, which is shown for each geometry in Fig. 4.12, is non-uniform, as would be expected, but does not vary appreciably with changes in geometry. The strain distributions for the first three geometries are so close that the plotted points are shown joined by one curve. A similar presentation of the net section strains is shown in Fig. 4.13. Again, the most significant change in strain occurs when the cross-sectional area is reduced by the geometry alterations. The net section strains could not be measured very close to the center of the gusset because of the position of the lap plates. As with the load partition, the strains shown are based on the increase above an initial strain caused by a pre-load on the joint of 3 kips.

The experimental transverse edge strain is shown in Fig. 4.14 in terms of geometry of the gusset plate. The measured strain is shown for 3 load levels which average 1, 2, and 3 kips per fastener. Since results were not available for the first geometry, an analytical result from the semi-infinite plate study is shown for  $\theta = 0^\circ$ . There appears to be good agreement. The improvement, i.e. the reduction in the value of the transverse edge strain, is quite favorable for increased taper of the gusset; however, for usual shapes of gusset plates the magnitude of strain is still quite significant.

A qualitative picture of the variation of stress trajectories for a variation in plate geometry is shown in Fig. 4.15. What can be noted quite readily is that much of the corner material in the first geometry is very

lightly stressed and as a result is not used effectively. Thus, the earlier results which indicated little change in load partition for the first three geometries are very feasible since much of the material which was removed did not add significantly to the structural integrity of the joint.

Results from the experimental study will now be discussed in the following section in terms of the analytical results previously presented and their significance in explaining the behavior of a gusseted connection.

## V. COMPARISON OF ANALYTICAL AND EXPERIMENTAL RESULTS

### 5.1 Load Partitioning

The load partitioning phenomena in a gusseted connection are dependent on a large number of variables, as is illustrated by the parameter variation of Section 3.4.1. Partitioning is difficult to reproduce analytically; consequently an evaluation of the various assumptions made in the development of the analytical relationships is very important in the final evaluation of the results.

Referring to Fig. 3.4 and Fig. 4.10 one sees that the prevalent trends for the variation in fastener loading with the change in the number of fasteners for the analytical semi-infinite plate joint and the experimental finite plate joint are generally the same. This comparison and agreement helps to substantiate and justify the soundness of the choice of the semi-infinite plate model for the extensive study of the variation of parameters in Section 3.4.1.

A direct comparison of the load partitioning obtained from the two analytical models and the experimental model is indicated in Fig. 5.1. The analytical solution for the semi-infinite plate is almost identical to the load partition of the second gusset geometry; the results from this geometry are representative of the results from the first four experimental geometries. The semi-infinite plate load partitioning is the same as that shown in Fig. 3.13 and the variables listed in that figure are similar to those for the experimental case. The variables for the analytical finite plate were not exactly the same as those for the experimental case; the areas of the lap plates were smaller than those of the experimental plates.

The reason for this inconsistency is that only one complete finite gusset problem was computed; the change in dimensioning was necessary for technical reasons associated with the distance between last fastener and the origin Fig. 3.16; these reasons are discussed in Appendix C.

Recomputation was not considered desirable because of the small difference in dimensions. When compared with the semi-infinite results, the analytical finite plate load partition results show the type of variation which would be expected. The analytic finite plate should, however, compare more favorably in magnitude with the experimental load partition shown in Fig. 5.1.

The failure of the analytical result to check more closely is probably due to some of the analytical assumptions, i.e., a value of  $C_t$  could, of course, be chosen to yield better agreement. Experimentally an effect was indicated in the latter geometries which was not taken into consideration analytically. Namely, the load started to drop in the last fastener, indicating, perhaps, that for more flexible gusset plates the elongation of the holes in regions of high strain may be contributing significantly to the load partitioning. This factor was not considered in the analytical assumptions, but at this point it is difficult to determine how significant this effect is with respect to the numerous assumptions made.

## 5.2 Strain Distribution

To make a comparison between the stress or strain distribution obtained from the analytical and experimental studies, the analytical stresses were converted to strains assuming  $E = 30,000$  ksi and  $\nu = 1/3$ .

Noting again that there were slight variations in the dimensions of the analytical and experimental models, the author chose for comparison the strains at the gross and net sections of plate geometry No. 4; as shown earlier, the axial strains did not vary to any great extent for the first 4 geometries. The comparisons are shown in Fig. 5.2 and Fig. 5.3. As would be expected the analytical strains are higher at the center line, due to the smaller fastener pitch; the closer spacing of the fasteners gives the effect of a more concentrated loading. The analytical load partition was somewhat different, as noted in the previous section. The experimentally determined load partition was, therefore, used in conjunction with the plate elasticity solution to compute the strain distribution for the same gross and net sections. These results indicate better agreement as is shown in Fig. 5.2 and Fig. 5.3.

A qualitative comparison can be made through visual inspection of the experimental stress trajectories of Fig. 4.15 and the analytical trajectories of Fig. 3.17. Very similar behaviors are indicated.

In Fig. 4.14 the analytical strain plotted for  $\theta = 0^\circ$  shows a continuation of the experimentally established trend. This strain was obtained directly from the semi-infinite plate solution.

The analytical and experimental strain distribution results show good agreement when one considers that the assumed modulus of elasticity could be in error from 5 to 10 percent and that certain of the plate dimensions were not identical.

## VI. SUMMARY AND CONCLUSIONS

### 6.1 Conclusions

In the first two sections the more important previous gusset plate research in the field of riveted and bolted connections is reviewed briefly, and the course of the present study is outlined. In the present study an investigation of basic type of gusseted connection was undertaken in considerable detail, both analytically and experimentally to ascertain the effect of a number of variables on load partition among the fasteners and stress distribution in the gusset plate.

Several conclusions can be drawn from the analytical variation of parameters in the particular case studied. The variables of fastener pitch and edge distance of the first fastener show only slight effects on the load partitioning for a reasonable range of values. The variables of gusset thickness and of lap plate area indicated similar effects on the load partitioning, but no generalizations can be made with respect to quantitative effects.

The increase in the number of fasteners of a joint, with all other variables remaining constant, causes a variation in load partitioning and a rapid increase of load in the first fastener.

The total fastener flexibility, as described in Appendix D, is an important factor since it changes with the size and type of fastener used. Very severe changes in the load partitioning are produced in the end fasteners of a joint by a decrease in the fastener flexibility. The fastener flexibility has been found to be an important factor and should be studied experimentally in more detail in the future.

Several conclusions may be drawn from the analytical study of stress distribution in the semi-infinite and in the symmetrical finite plate. It has been shown that a large transverse stress develops on the edge of a gusset plate at the load line. This stress tends to split the plate along the line of fasteners and increases with the proximity of the fasteners to the edge of the plate. Analytical relations have been developed to allow easy calculation of this stress for assumed load partitioning in the semi-infinite plate.

The experimental gusseted connections exhibit a behavior similar to the analytical models with few exceptions (See Section 5). From the study of the variation in plate geometry one may conclude that the load partition is only affected by extreme variations in gusset plate geometry. The measurement of the transverse edge strain confirmed the discovering of the splitting condition in the analytical results. The data also showed that the strain is somewhat relieved by increasing the taper of the gusset.

The elastic analysis of the gusset plate cannot be used to establish the ultimate strength or mode of failure for static loads. However, the stress distributions show that gusset plates can be expected to yield or perhaps rupture at either of two places, along the load line or at the last fastener. Failures of both types occurred in the static tests of truss-type connections reported by Chesson and Munse<sup>(21)</sup>. Thus, the present study helps greatly in explaining the unusual failures observed in these previous studies.

## 6.2 Areas for Future Study

The foregoing investigation has only provided a part of the answer to a very complex problem. Numerous variables involved with fabrication, installation, eccentric loading, etc. have been avoided and need to be considered in the future. The study has been limited to elastic behavior in the connection material. Fatigue failures have been a problem in riveted and bolted connections; some study is therefore necessary to correlate the fastener loading with the fatigue failures that have been reported.

The analytical model for the finite plate joint which was developed in this study has much potential but has not been used to full advantage. Further refinement as suggested in Section 5.1 is recommended for the future use of the analytical model.

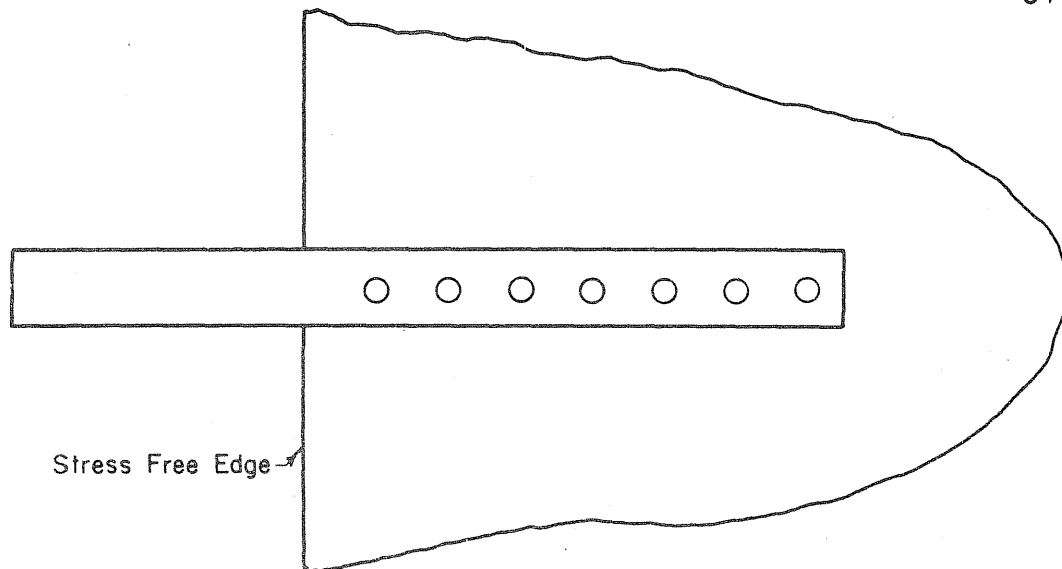
A study of the ultimate strength characteristics should be the next major step to be taken towards a better understanding of the problem associated with the design of gusseted connections. Sound and effective design recommendations of gusset plates would then be possible.

## LIST OF REFERENCES

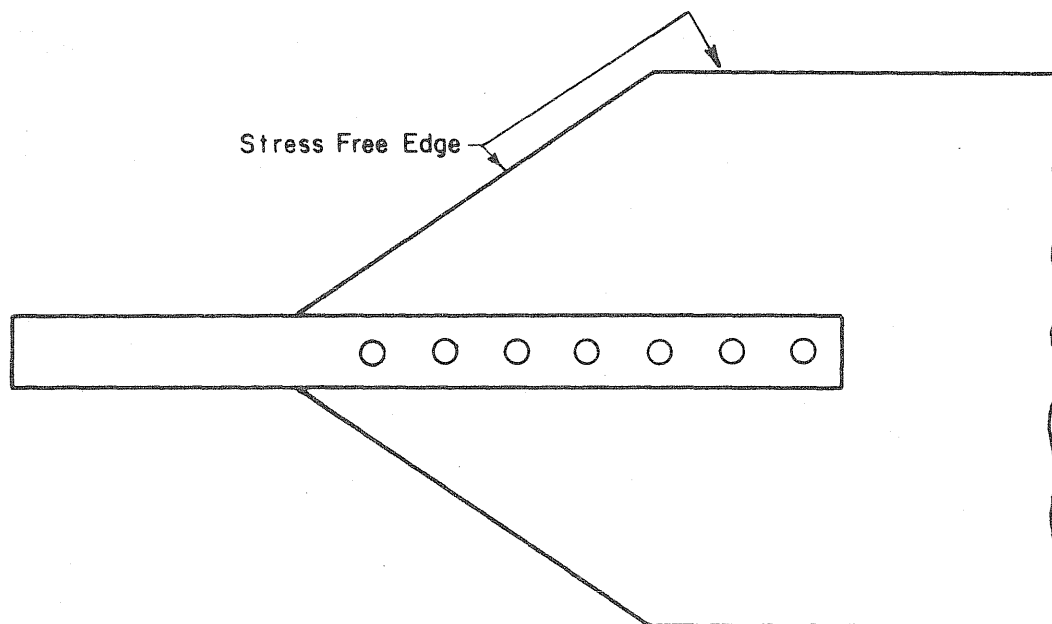
1. Yokota, S., "Stress Distribution in Riveted Plates under Forces Transmitted through Rivets", Society of Mechanical Engineers Journal, Vol. 14, No. 3, Tokyo, April 29, 1913.
2. Coker, E. G. and Scoble, W. A., "Distribution of Stress Due to a Rivet in a Plate", Engineering, March 28, 1913.
3. Batno, C., "Partition of Load in Riveted Joints", Journal of the Franklin Institute, Vol. 182, November, 1916.
4. Bleich, F., Theory and Design of Iron Bridges, Chapter on "Theory of Riveted Connections", J. Springer, Berlin, 1924.
5. Wyss, Th., von Dr.-Ing., "The Stress Fields of Gusset Plates of Steel Structures", (In German), Zeitschrift Des Vereines Deutscher Ingenieure, Vol. 67, Pt. 1, January-June, 1923, (Major work published in Forschungsheft 262).
6. Hertwig, A., Peterman, H., "Über die Verteilung einer Kraft auf Einzelnen Niete einer Nietereihe", Der Stahlbau (Die Bautechnik), December 13, 1929.
7. Hrenikoff, A., "Work of Rivets in Riveted Joints", ASCE Transactions, Vol. 49, 1934.
8. Hinkley, W. O., "Truss Failure Results from Using Gusset Plate as Chord Splice", Engineering News Record, May 27, 1937.
9. Rust, T. H., "Specification and Design of Steel Gusset Plates", ASCE Transactions, Paper 2058, Vol. 105, 1940.
10. DeJonge, A. E. R., Riveted Joints: A Critical Review of Literature Concerning their Development, American Society of Mechanical Engineers, New York, 1945.
11. Hrennikoff, A., "Solutions of Problems of Elasticity by the Framework Method", ASME Journal, A169, 1941.
12. Vogt, F., "Load Distribution in Bolted or Riveted Structural Joints in Light Alloy Structures", Technical Note No. 1135, National Advisory Committee for Aeronautics, Washington, D. C., 1947.
13. Tate, M. B. and Rosenfeld, S. J., "Preliminary Investigation of the Loads Carried by the Individual Bolts in Bolted Joints", Technical Note No. 1051, National Advisory Committee for Aeronautics, Washington, D. C., 1946.

14. Grinter, L. E., "Stresses in Gusset Plates by Use of an Analogous Grid", International Association for Bridge and Structural Engineers, September, 1948.
15. Whitmore, R. E., "Experimental Investigation of Stresses in Gusset Plates", University of Tennessee Engineering Experiment Station Bulletin, No. 16, May, 1952.
16. Irvan, W. G., Jr., "Experimental Study of Primary Stresses in Gusset Plates of a Double Plane Pratt Truss", University of Kentucky Engineering Experiment Station Bulletin, No. 46, December, 1957.
17. Hardin, B. O., "Experimental Investigation of the Primary Stress Distribution in the Gusset-Plates of a Double Plane Pratt Truss-Joint with Chord Splice at the Joint", University of Kentucky Engineering Experimental Station Bulletin, No. 49, September, 1958.
18. Sheridan, M. L., "An Experimental Study of the Stress and Strain Distribution in Steel Gusset Plates", University of Michigan, 1953.
19. Carter, J. W., McCalley, J. C., and Wily, L. T., "Comparative Test of a Structural Joint Connected with High Strength Bolts and a Structural Joint Connected with Rivets and High Strength Bolts", AREA Proceedings, Vol. 56, 1955.
20. Carter, J. W., "Stress Concentration in Built-Up-Structural Members and its Effect on their Endurance Limit", Doctoral Thesis Purdue University, 1951.
21. Chesson, E. and Munse, W. H., "Behavior of Riveted Connections in Truss-Type Members", ASCE Transactions, Paper 2955, Vol. 123, 1958.
22. Chesson, E. and Munse, W. H., "Riveted and Bolted Joints: Truss-Type Tensile Connections", ASCE Proceedings, Vol. 89, No. ST1, February, 1963.
23. Francis, A. J., "The Behavior of Aluminum Alloy Riveted Joints", Research Report No. 15, Aluminium Development Association, March, 1953.
24. Rumpf, J. L., "Ultimate Strength of Bolted Connections", Doctoral Thesis Lehigh University, 1960.
25. Fisher, J. W., "The Analysis of Bolted Plate Splices", Fritz Engineering Laboratory Report, No. 288.10, February, 1964.
26. Fisher, J. W., "Behavior of Fasteners and Plates with Holes", ASCE Journal, Vol. 91, No. ST6, December, 1965.

27. Lehman, Frederick G., "Stress Analysis of Gusset Plates", Doctoral Thesis Massachusetts Institute of Technology, June, 1960.
28. Budiansky, B. and Wu, T. T., "Transfer of Load to a Sheet from a Rivet Attached Stiffener", Technical Report No. 11, Division of Engineering and Applied Physics, Harvard University, February, 1961.
29. Bloom, J. M., "The Effect of a Riveted Stringer on the Stress in a Sheet with a Crack or a Cutout", Technical Report No. 20, Division of Engineering and Applied Physics, Harvard University, June, 1964.
30. Manual of Steel Construction Sixth Edition, American Institute of Steel Construction, 1963.
31. Muskhelishvili, N. I., Some Basic Problems of the Mathematical Theory of Elasticity, 3rd Revised and Augmented Edition Moscow, 1949, Translated from Russian by Radok, J. R. M., P. Noordhoff Ltd., 1953.
32. Sokolnikoff, I. S., Mathematical Theory of Elasticity, 2nd Edition, McGraw Hill Book Company, Inc., New York, 1956.
33. Conway, H. D., "The Approximate Analysis of Certain Boundary Value Problems", ASME Transactions, 27E (Journal of Applied Mechanics), 1960.
34. Hulbert, E. H., "The Numerical Solution of Two-Dimensional Problems of the Theory of Elasticity", Engineering Experiment Station Bulletin 198, Ohio State University, 1964.



(a) Semi-infinite Plate Connection



(b) Finite Gusset Plate Connection

FIG. 3.1 ANALYTICAL MODELS

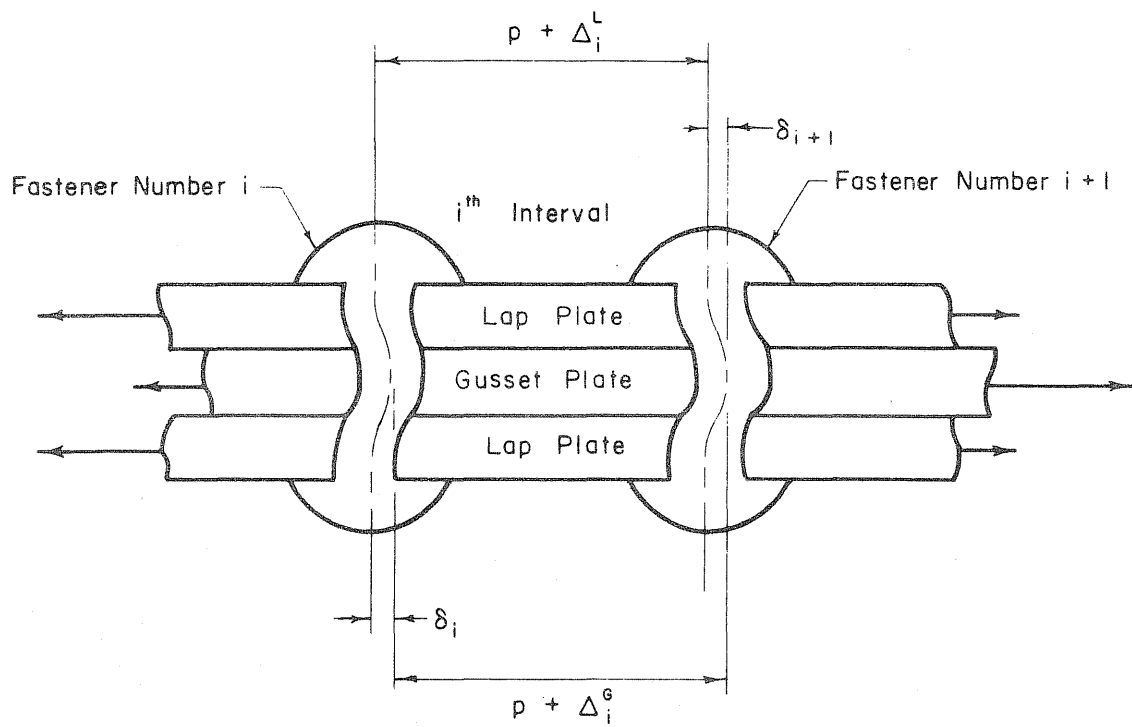


FIG. 3.2 COMPATIBILITY OF DEFORMATIONS.

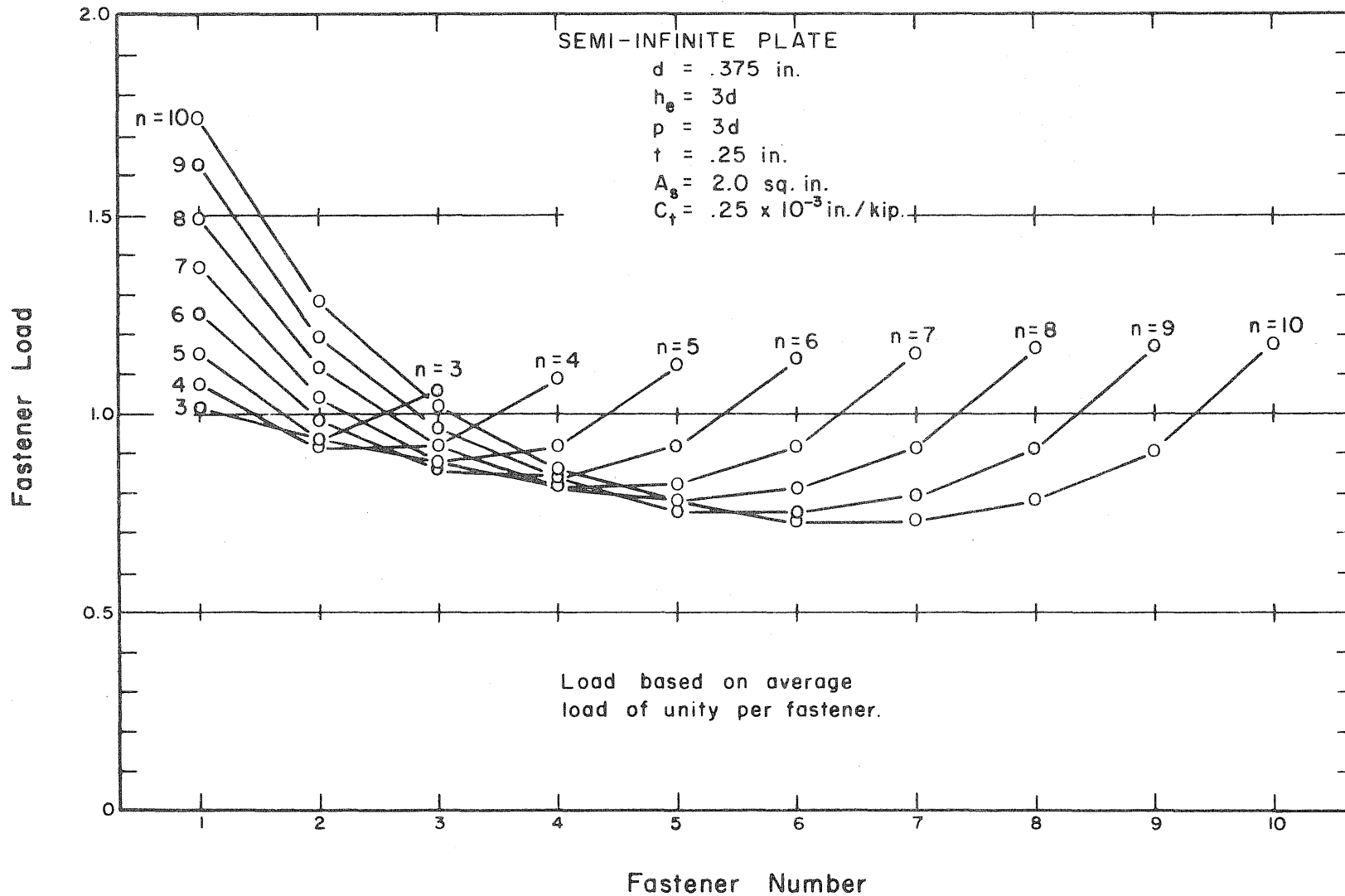


FIG. 3.3 LOAD PARTITION FOR VARIABLE NUMBER OF FASTENERS.

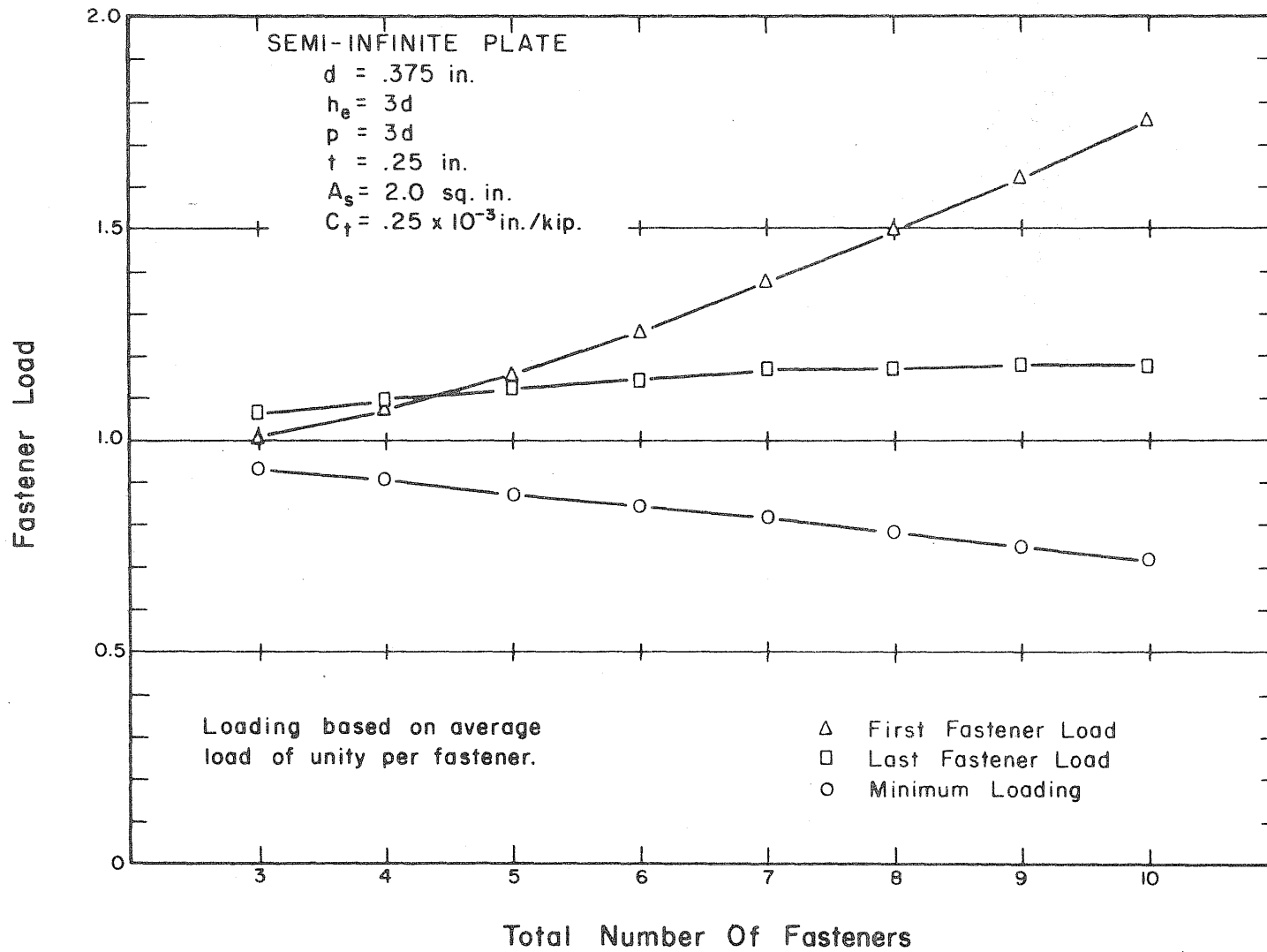


FIG. 3.4 VARIATION IN FASTENER LOAD WITH NUMBER OF FASTENERS.

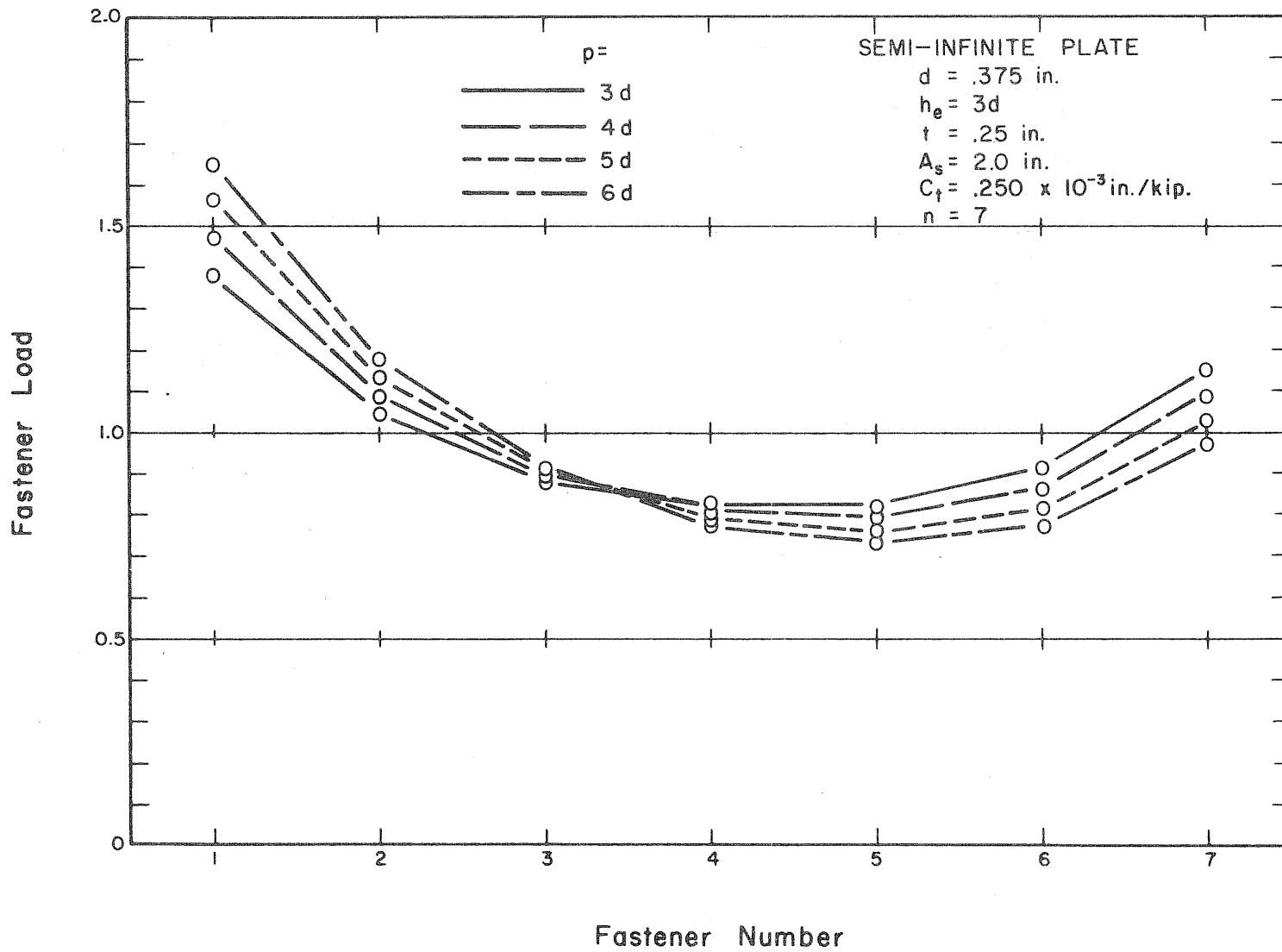


FIG. 3.5 LOAD PARTITION FOR VARIABLE FASTENER PITCH.

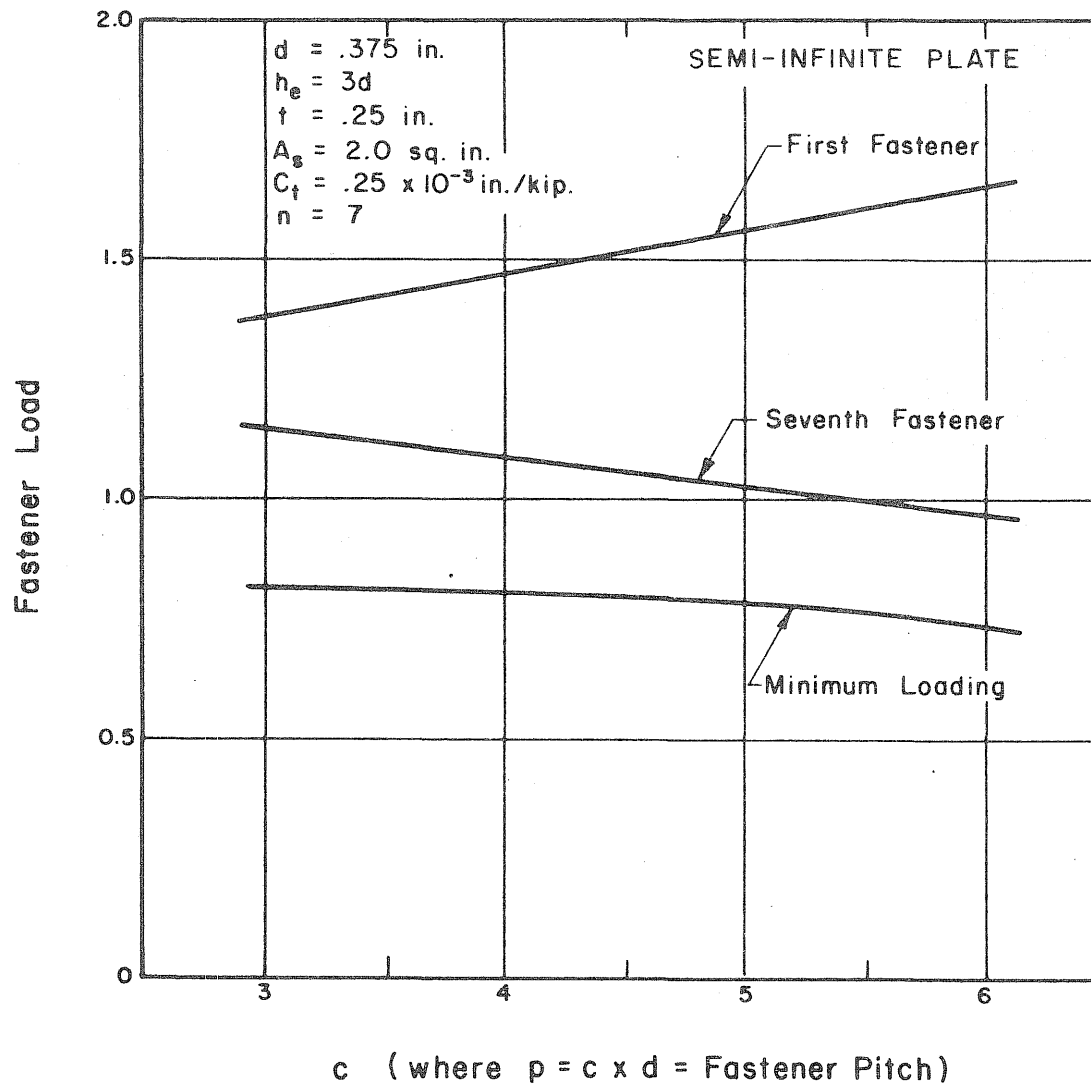


FIG. 3.6 FASTENER LOAD VARIATION FOR VARIABLE FASTENER PITCH.

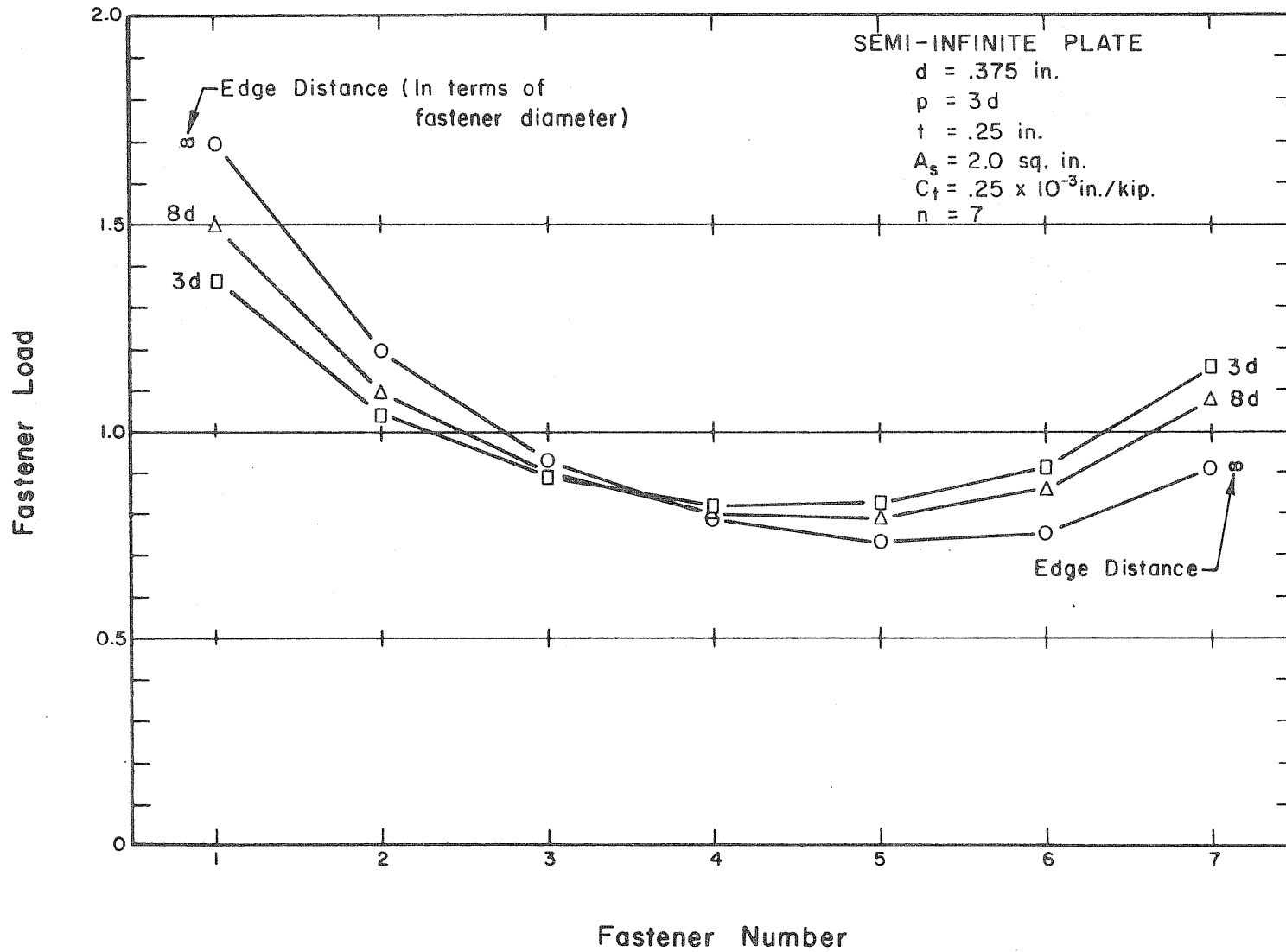


FIG. 3.7 LOAD PARTITION FOR VARIABLE EDGE DISTANCE OF FIRST FASTENER.

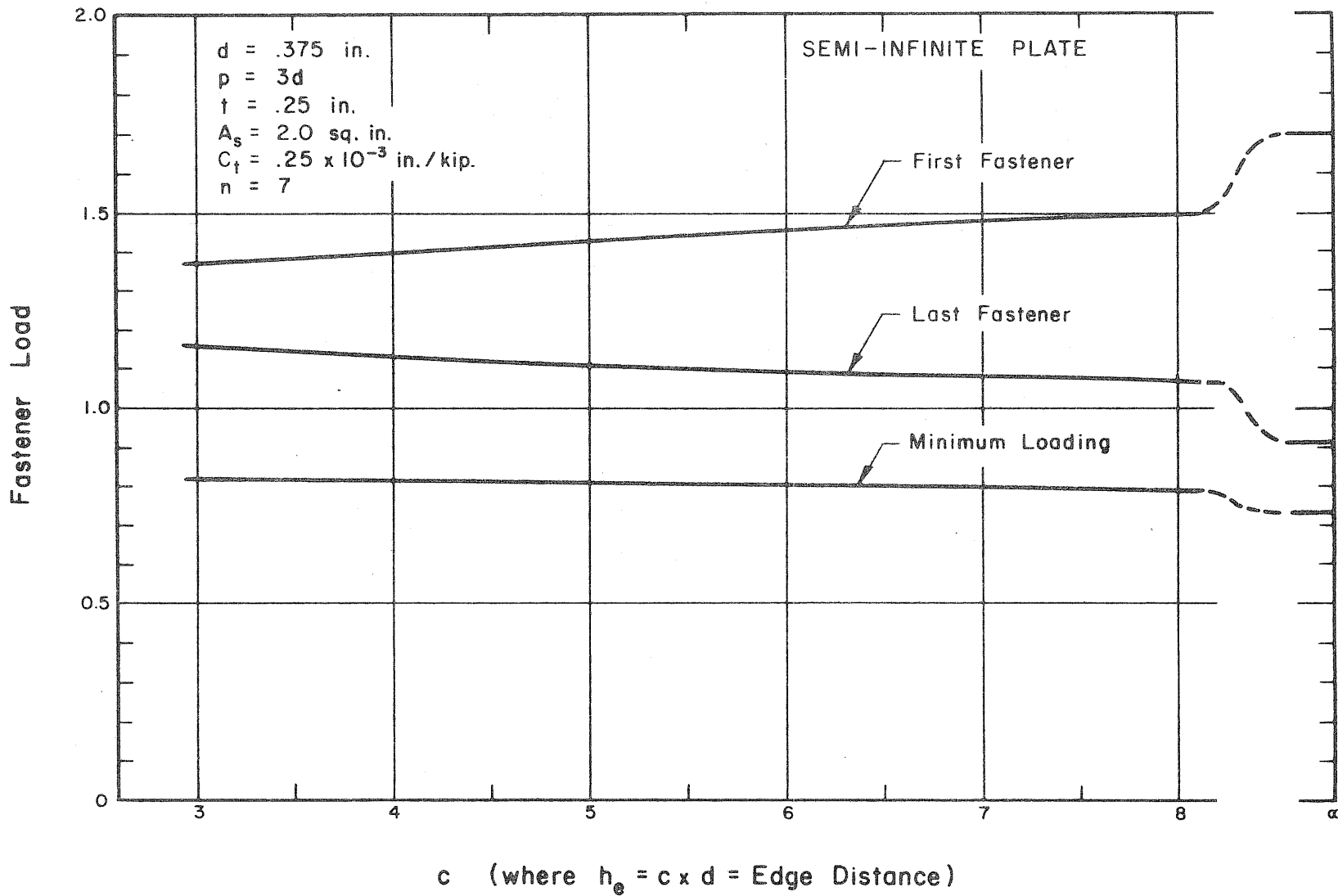


FIG. 3.8 FASTENER LOAD VARIATION FOR VARIABLE EDGE DISTANCE OF FIRST FASTENER.

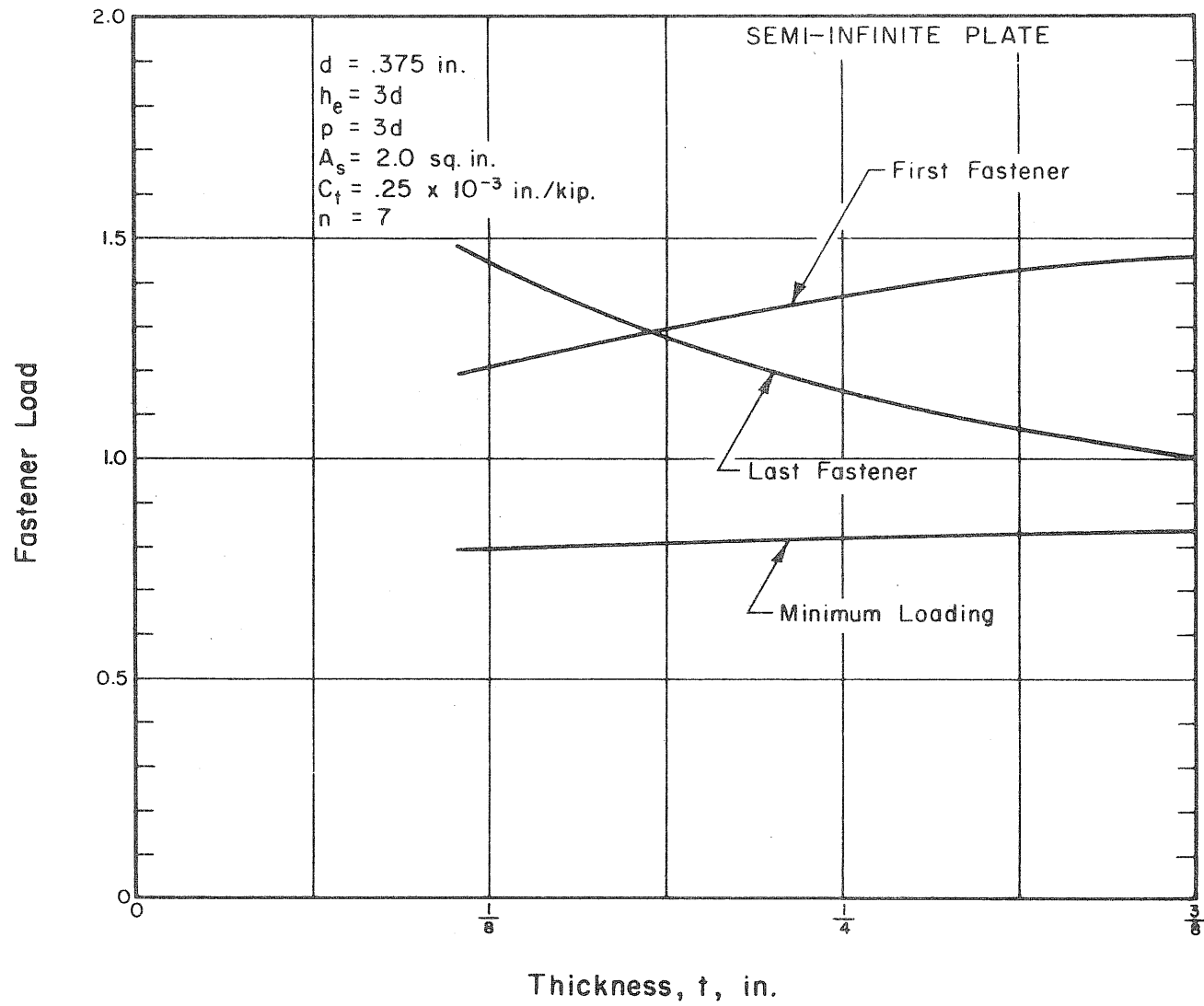


FIG. 3.9 FASTENER LOAD VARIATION FOR VARIABLE PLATE THICKNESS.

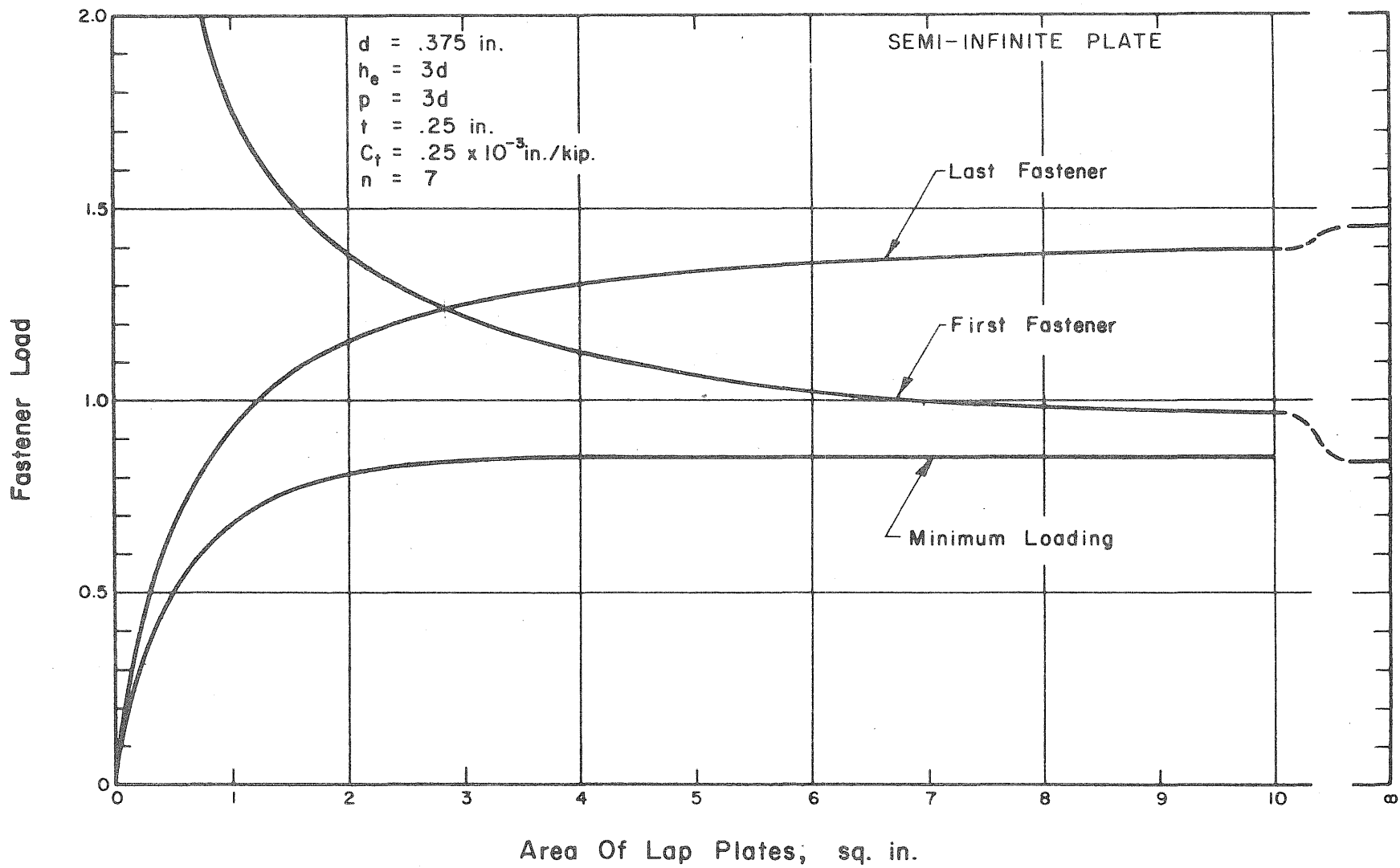


FIG. 3.10 VARIATION OF FASTENER LOAD WITH LAP PLATE AREA.

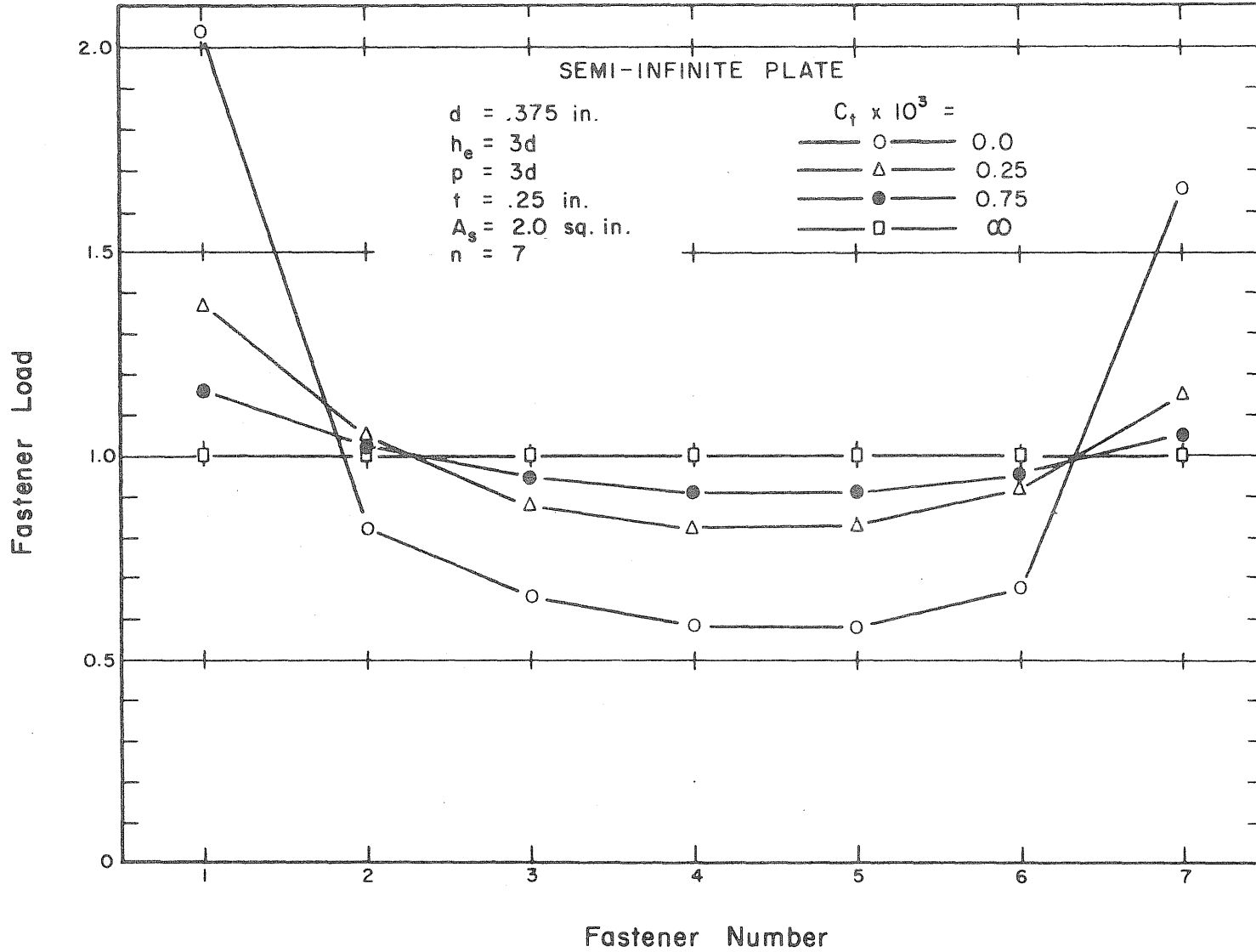


FIG. 3.11 LOAD PARTITION FOR VARIABLE FASTENER FLEXIBILITY.

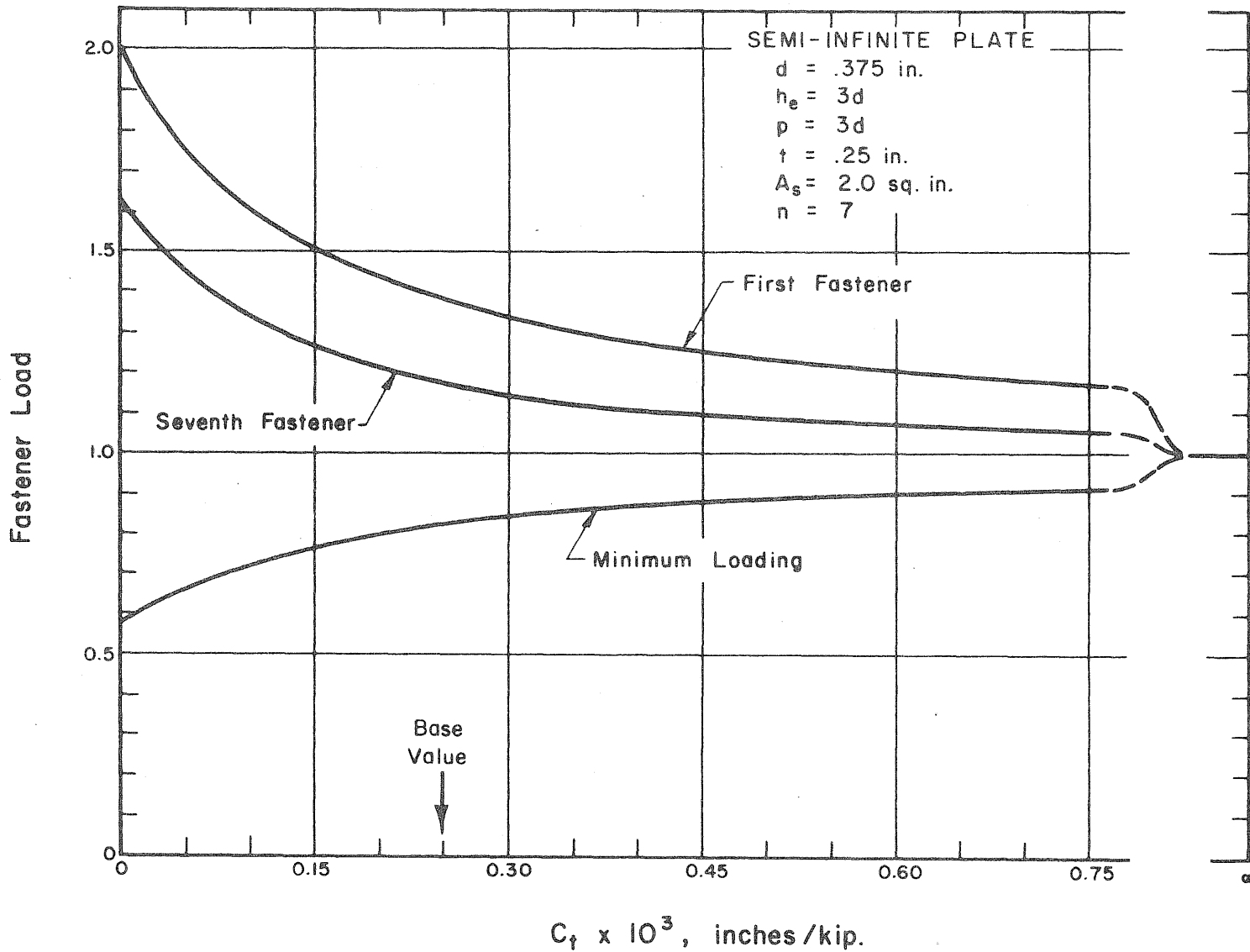


FIG.3.12 VARIATION OF FASTENER LOAD WITH FASTENER FLEXIBILITY.

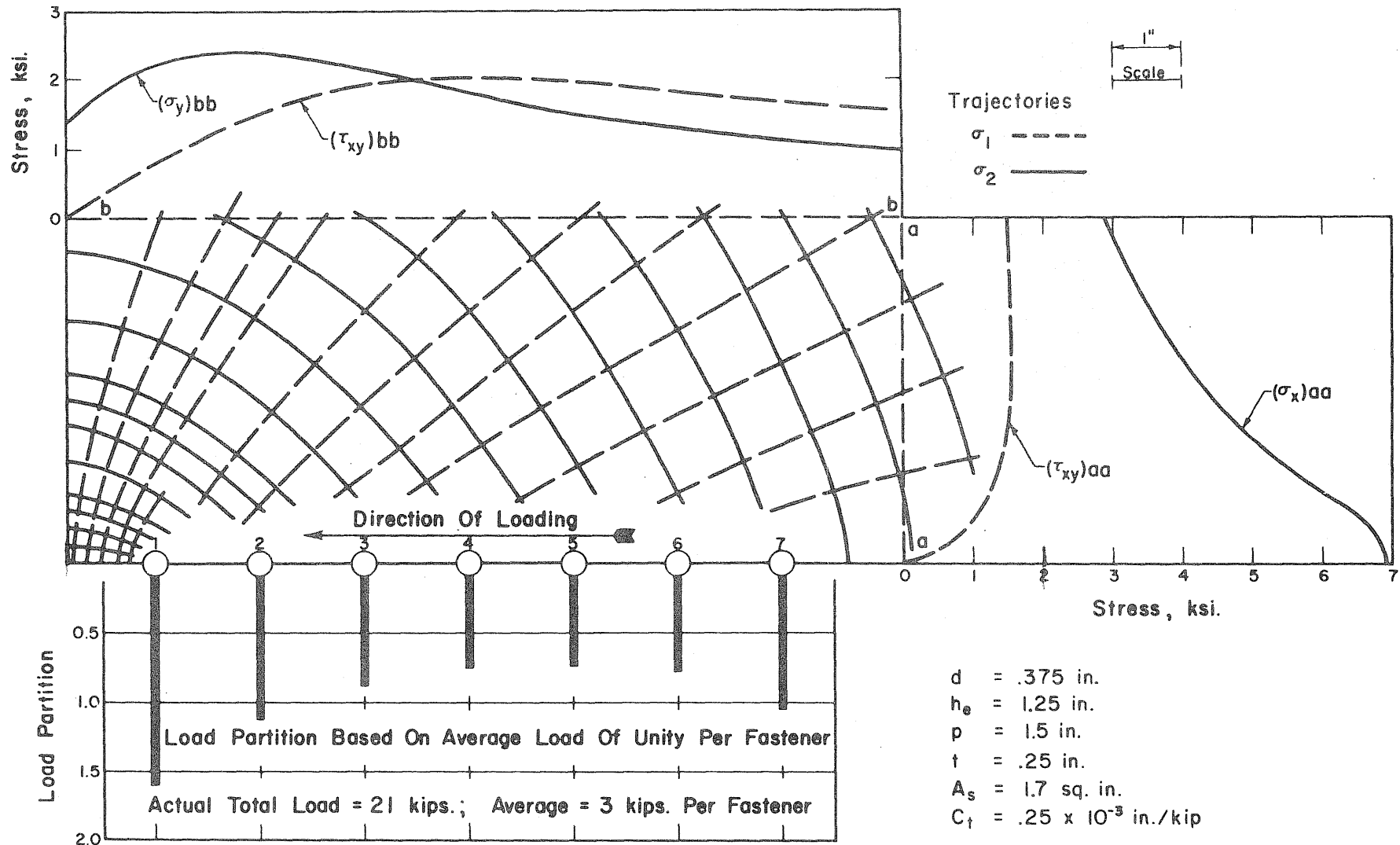


FIG. 3.13 LOAD PARTITION AND STRESS DISTRIBUTION FOR A RECTANGULAR SECTION OF A SEMI-INFINITE PLATE.

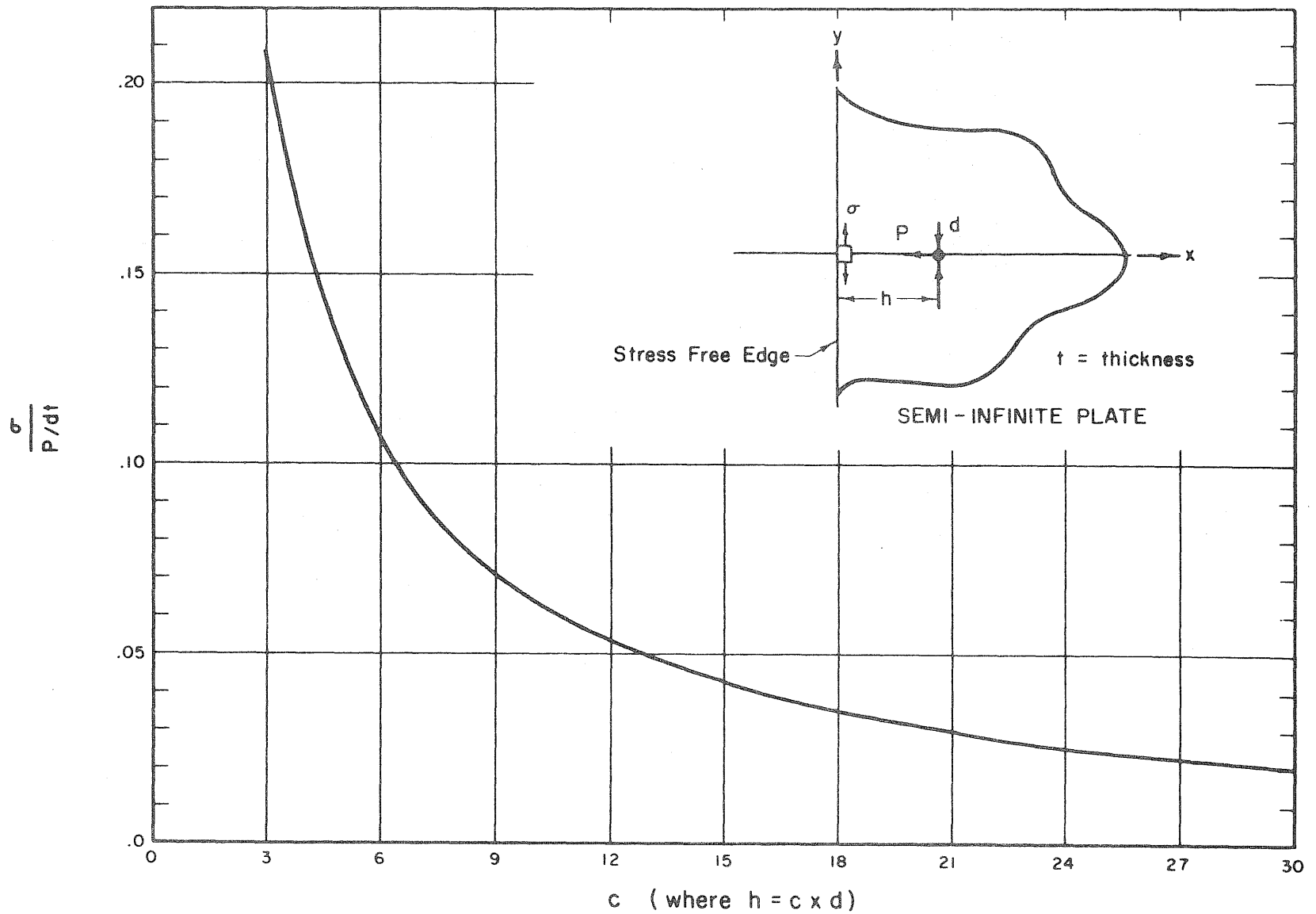


FIG. 3.14 CONTRIBUTION OF A SINGLE FASTENER LOADING TO THE TRANSVERSE EDGE STRESS.

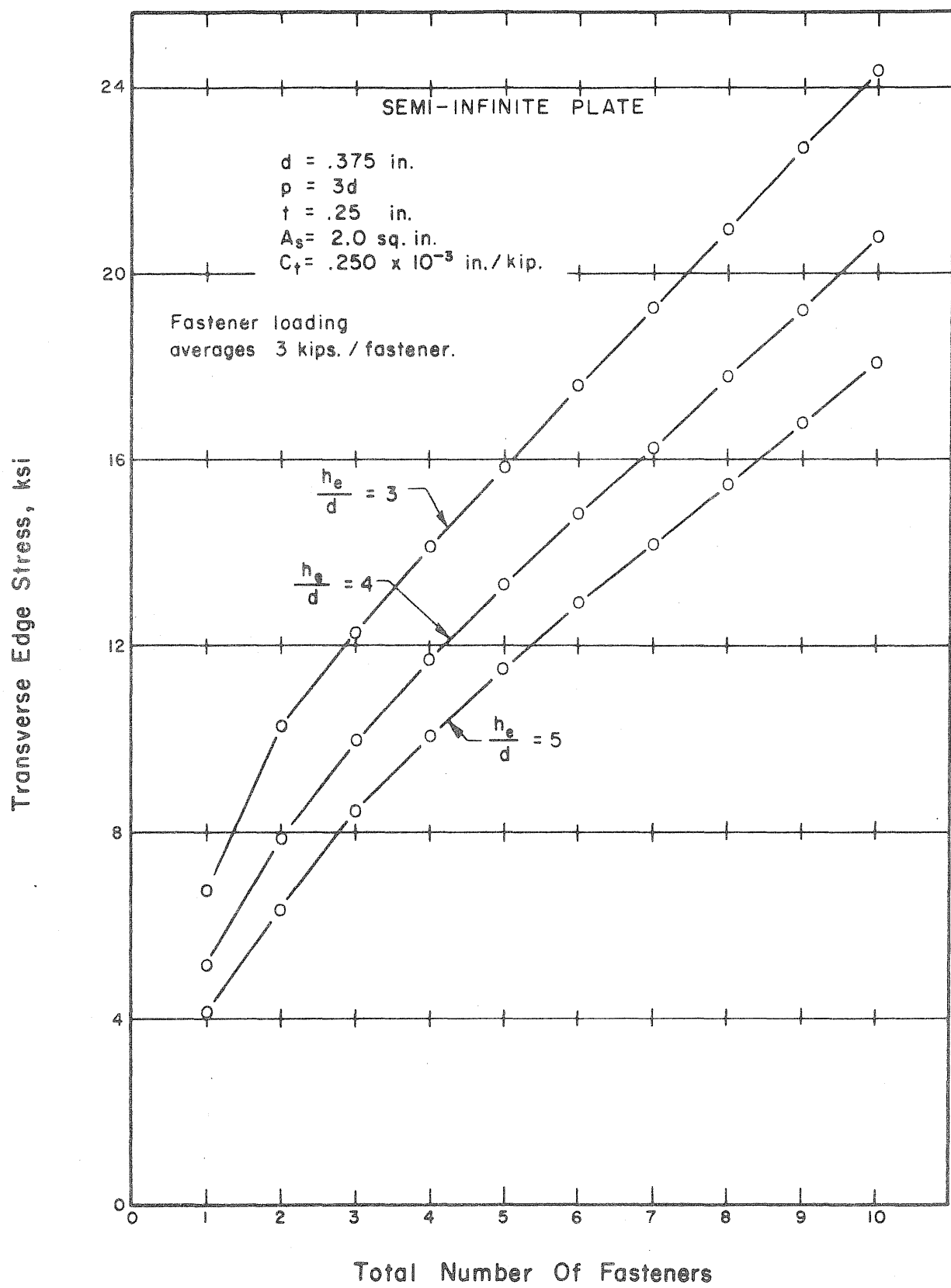


FIG. 3.15 TRANSVERSE EDGE STRESS FOR VARIABLE NUMBER OF FASTENERS AND EDGE DISTANCE.

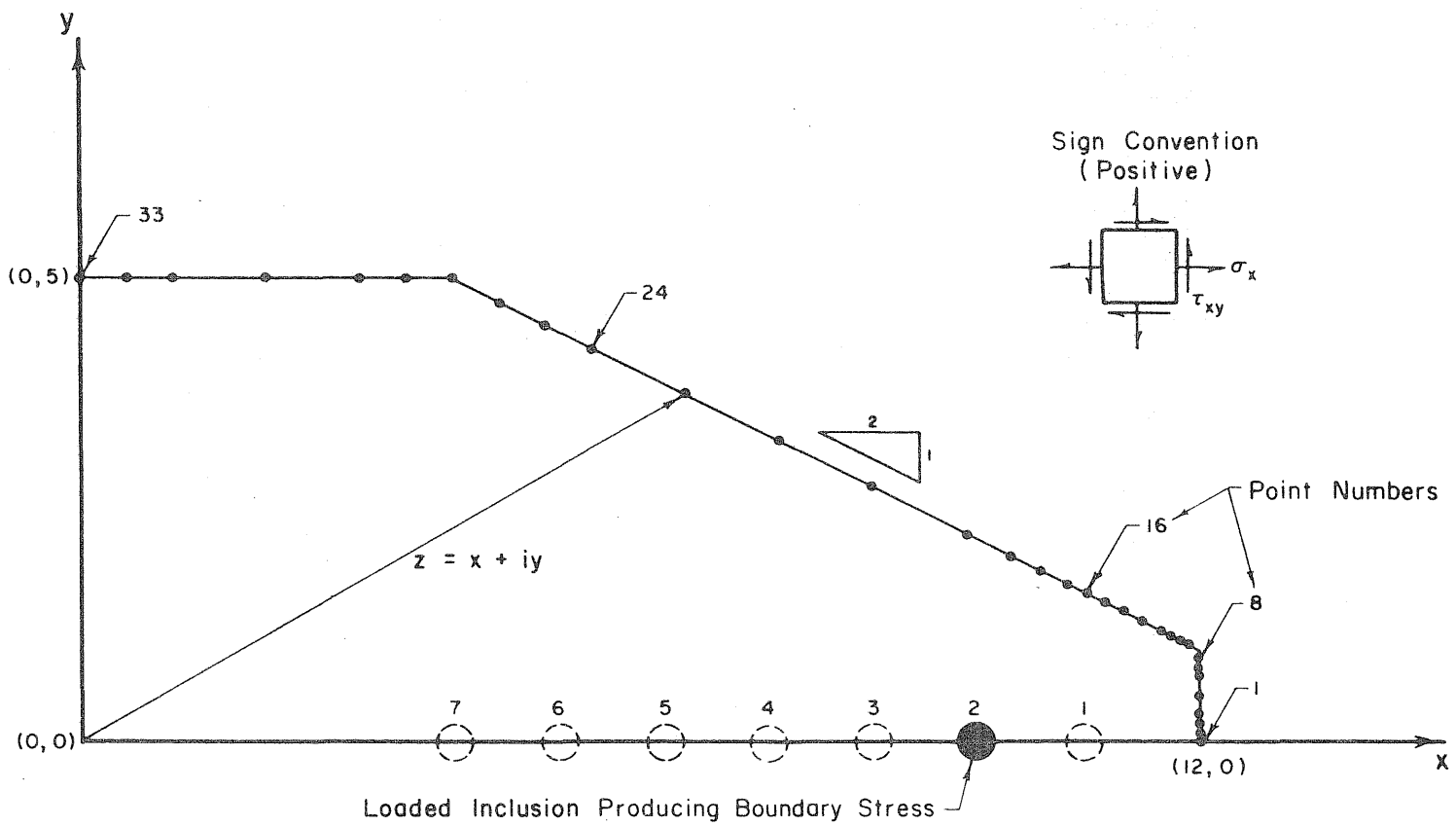


FIG. 3.16 SPECIFICATIONS FOR FINITE PLATE PROBLEM

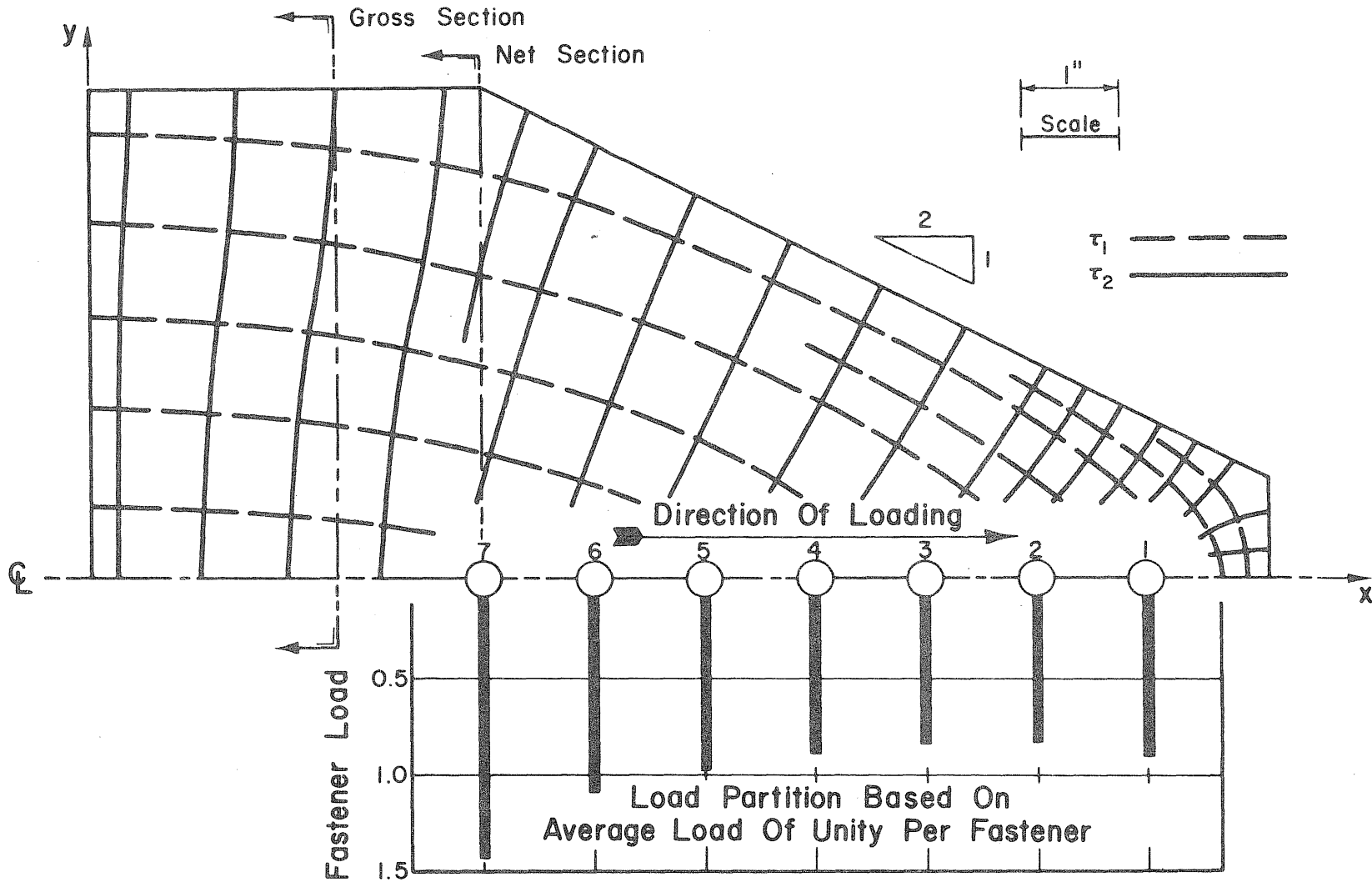


FIG. 3.17 LOAD PARTITION AND STRESS TRAJECTORIES FOR FINITE PLATE

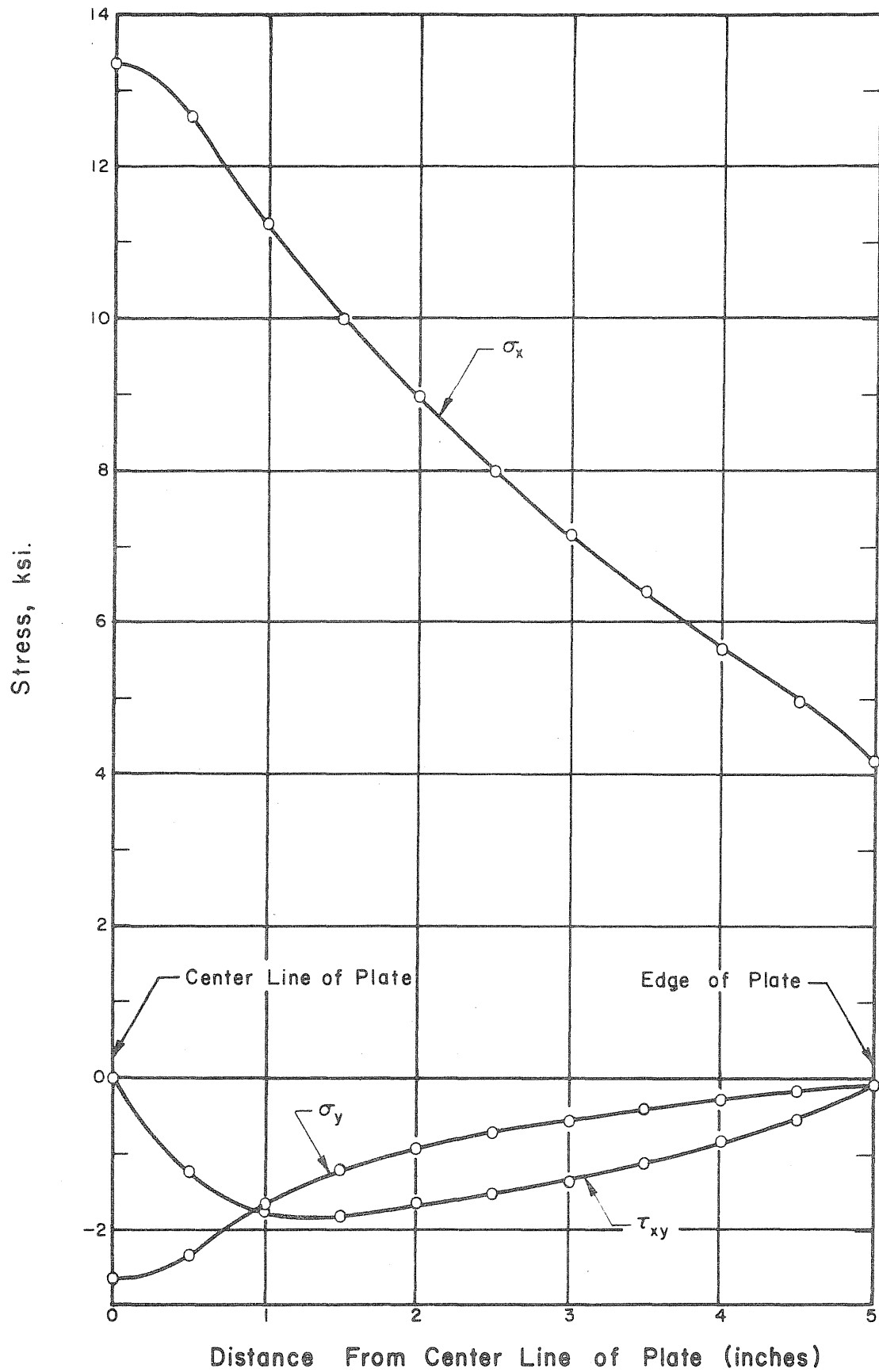


FIG. 3.18 GROSS SECTION STRESSES FOR FINITE PLATE.

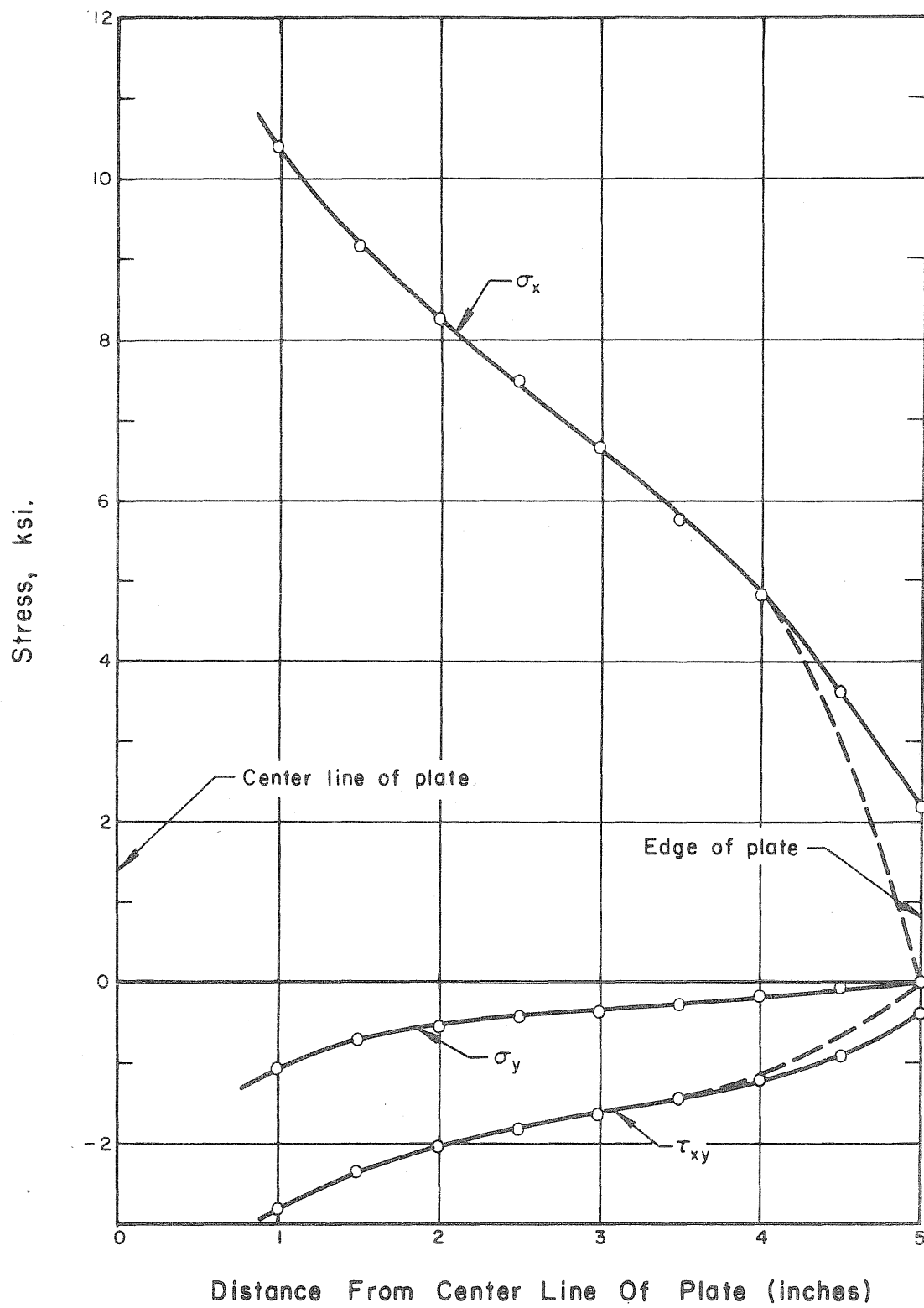


FIG. 3.19 NET SECTION STRESSES FOR FINITE PLATE.

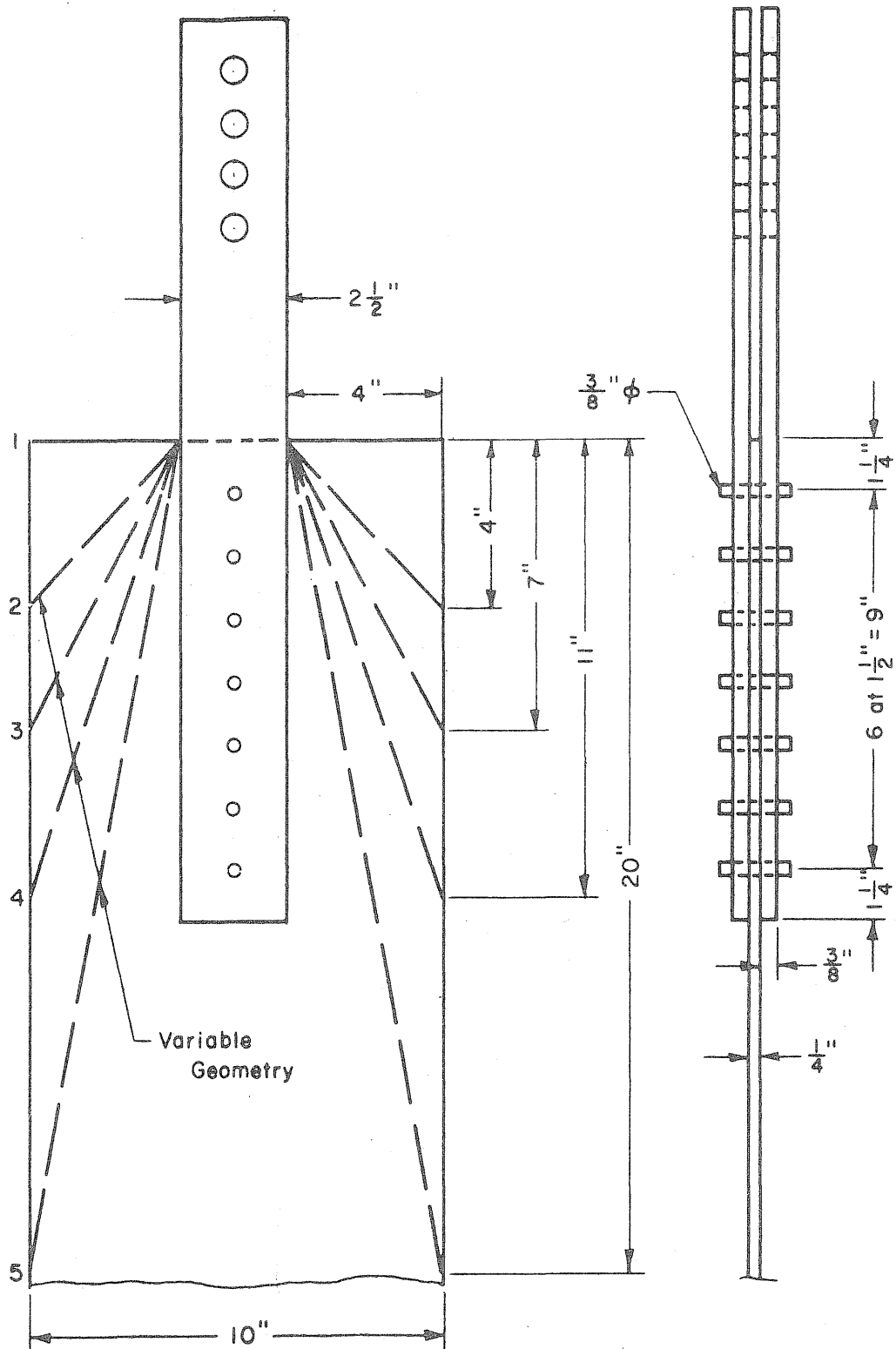


FIG. 4.1 GUSSET PLATE DETAIL.

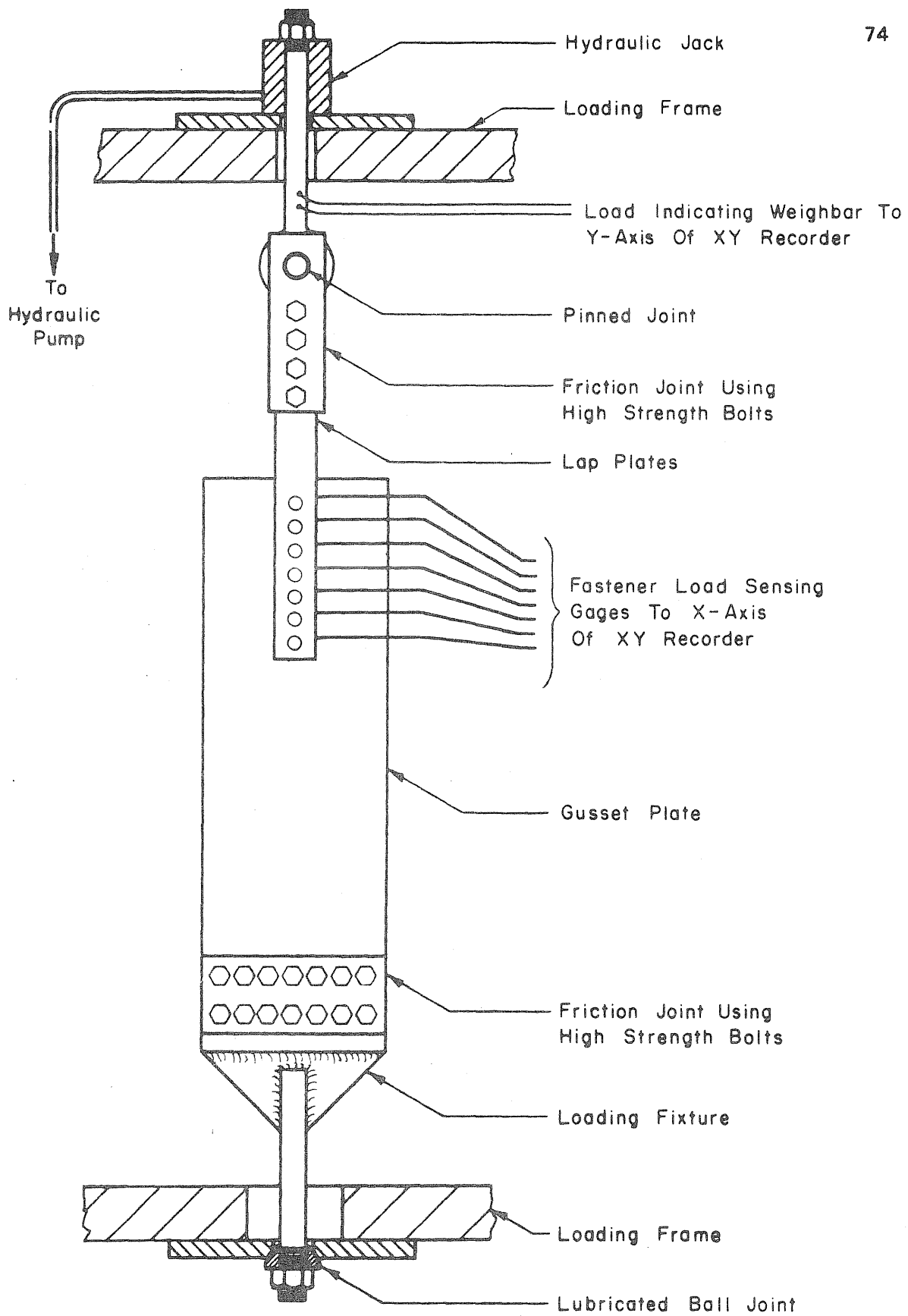


FIG. 4.2 SCHEMATIC DIAGRAM OF EXPERIMENTAL APPARATUS.

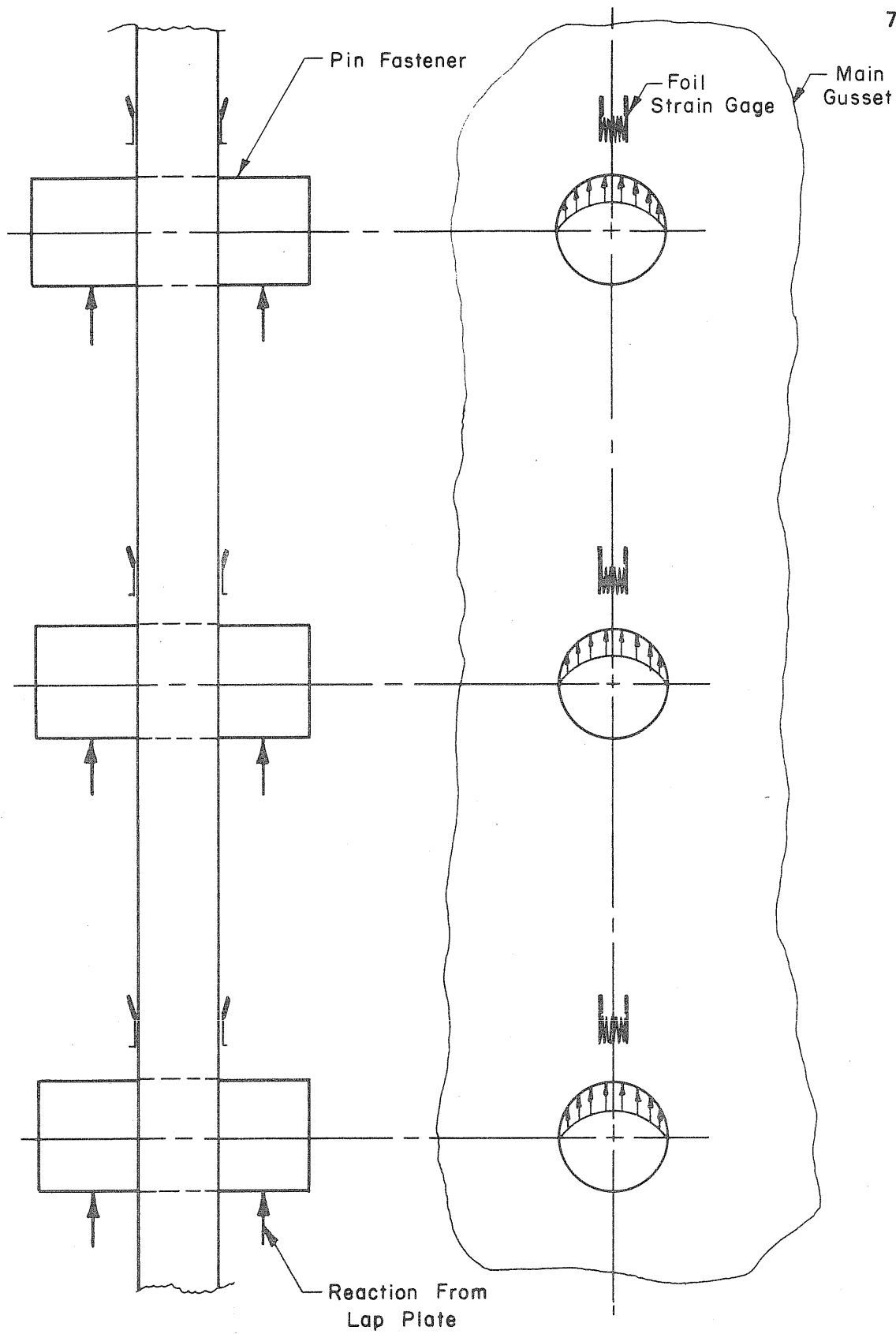


FIG. 4.3 FASTENER LOAD SENSING INSTRUMENTATION

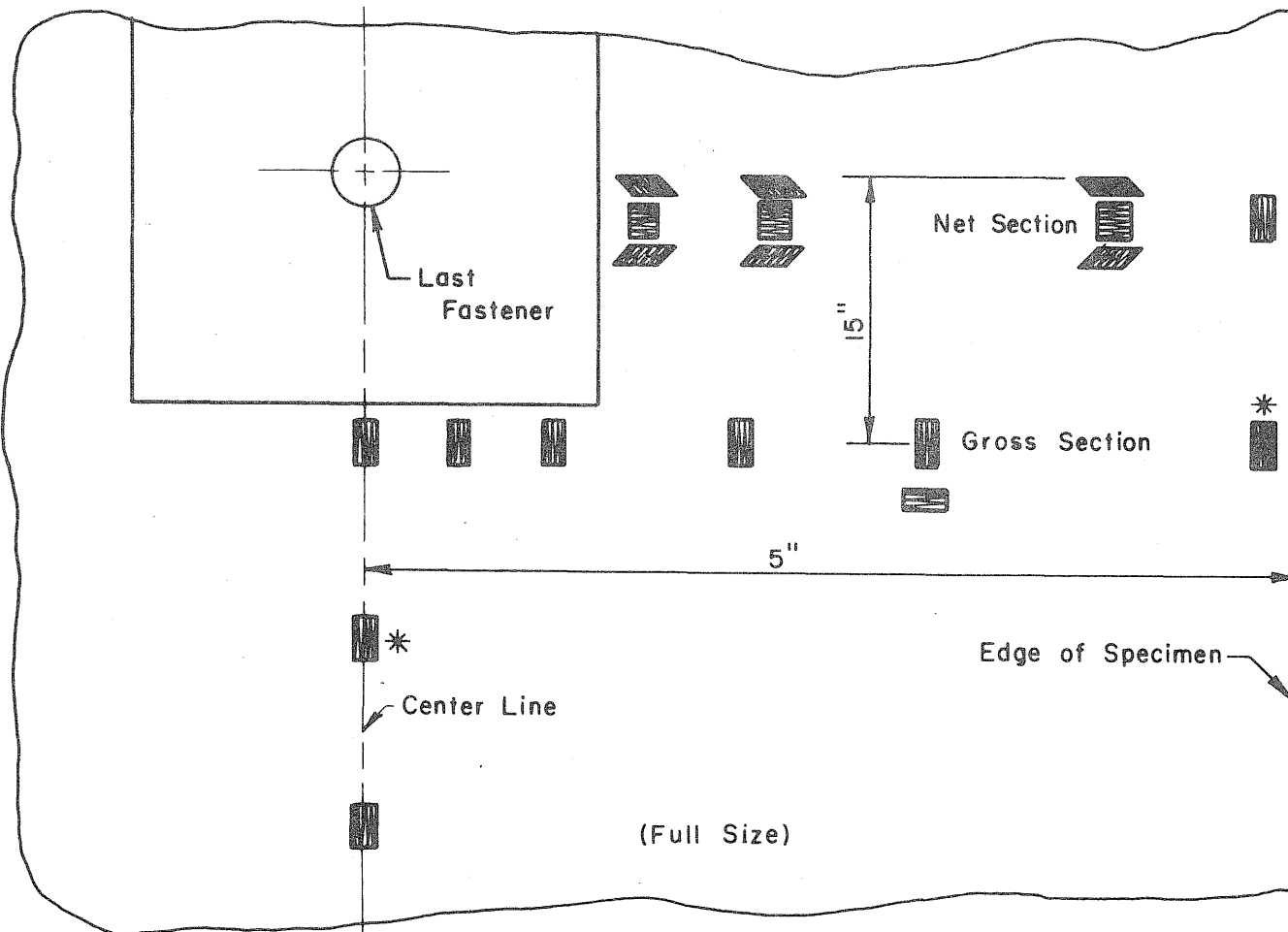


FIG. 4.4 STRAIN GAGE LOCATIONS.

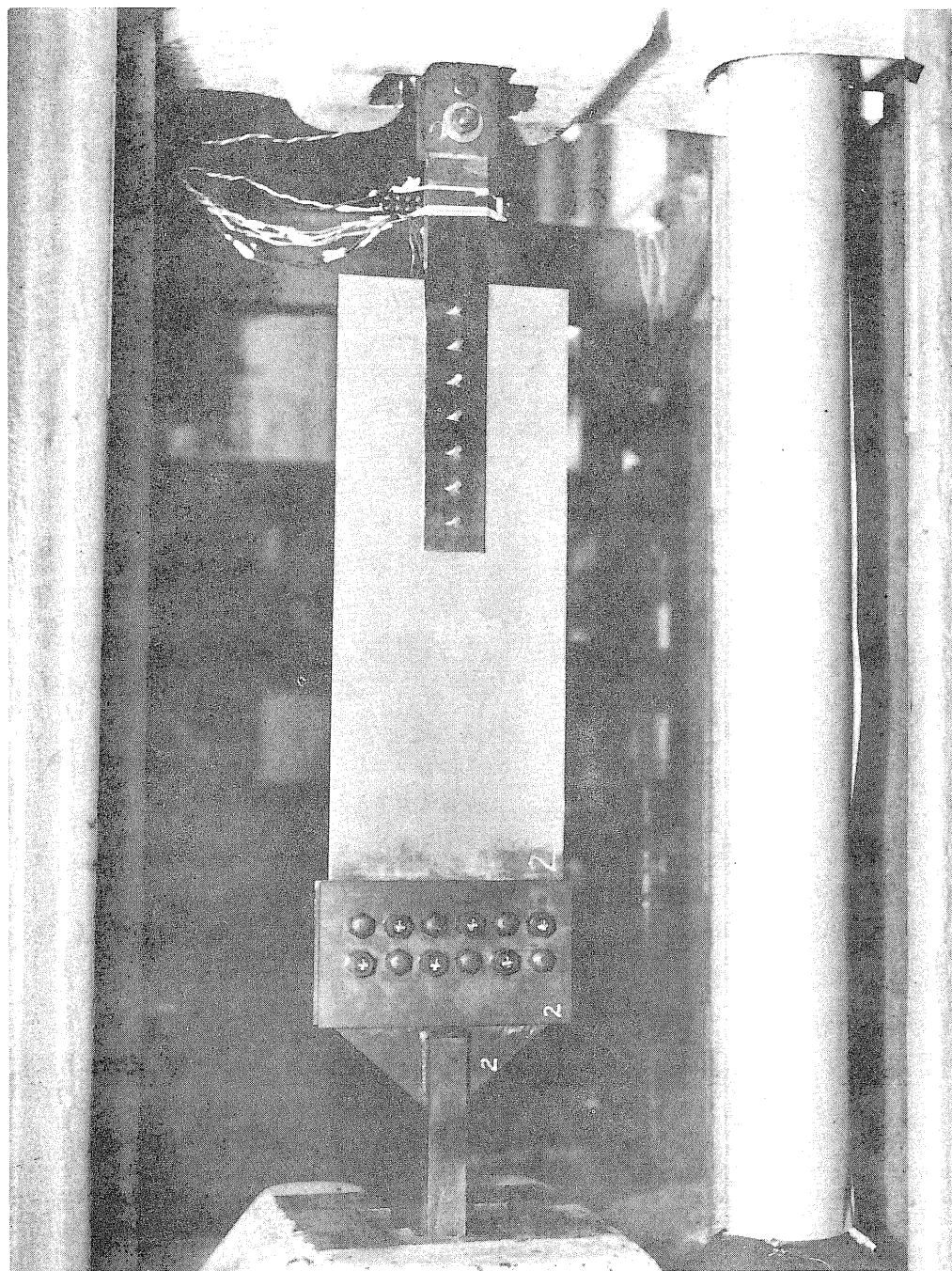


FIG.4.5 GUSSET PLATE AND FIXTURES IN TEST CONFIGURATION

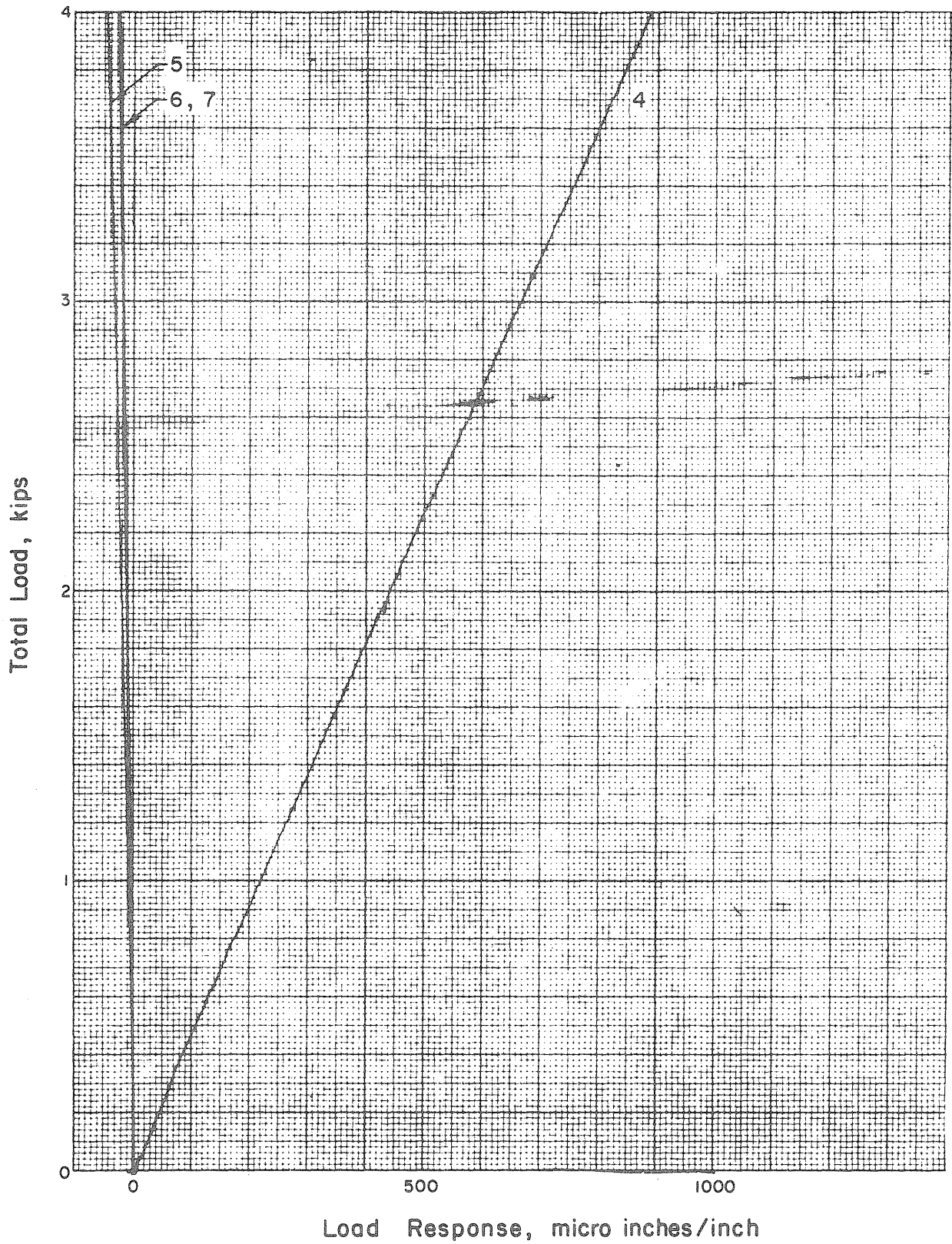


FIG. 4.6 SAMPLE OF FASTENER CALIBRATION DATA .

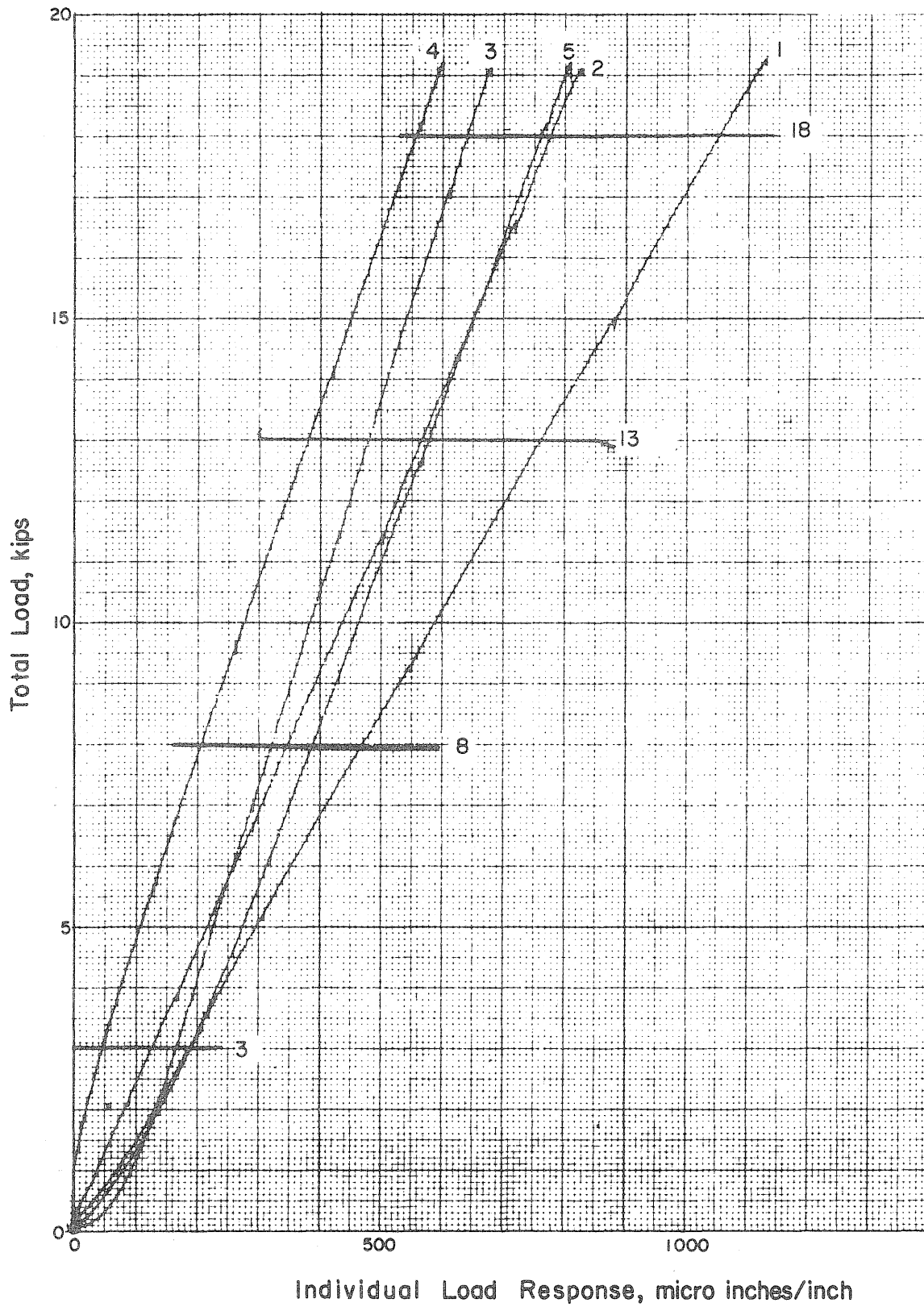
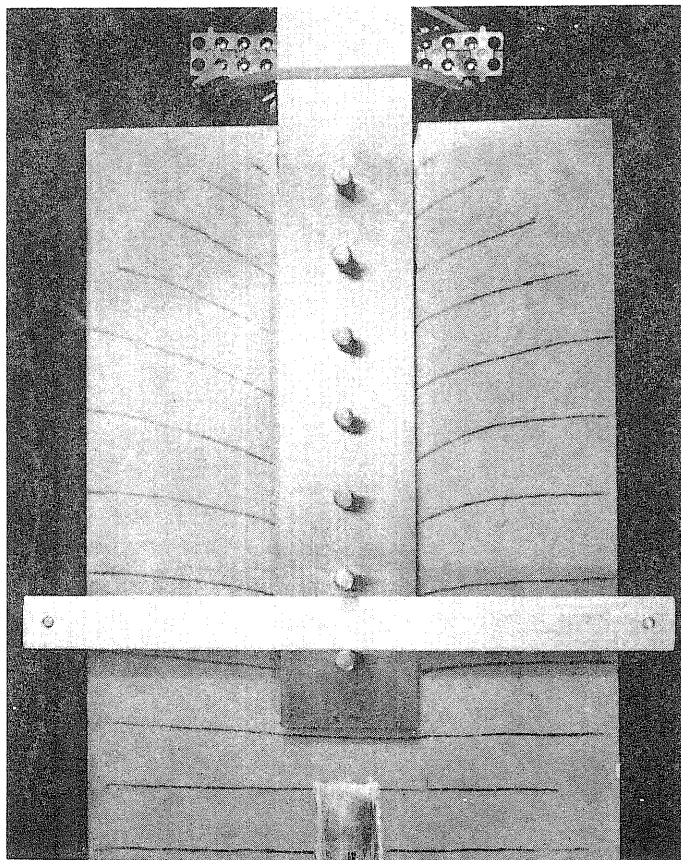
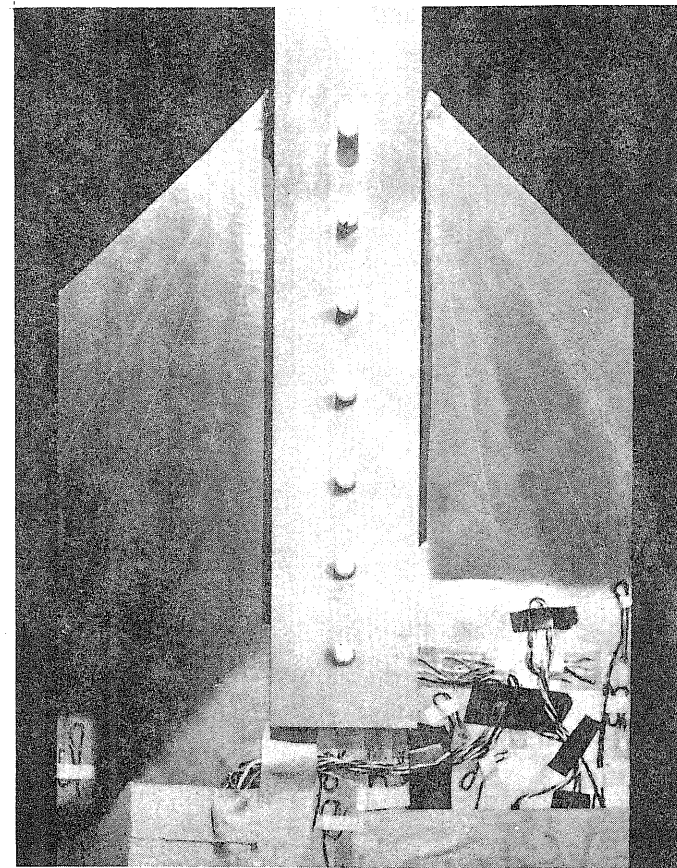


FIG. 4.7 SAMPLE OF FASTENER LOAD DATA .



(a) Brittle Lacquer Side, Geometry No.1



(b) Gaged Side, Geometry No. 2

FIG.4.8 GUSSET PLATE SPECIMEN AT DIFFERENT TEST STAGES

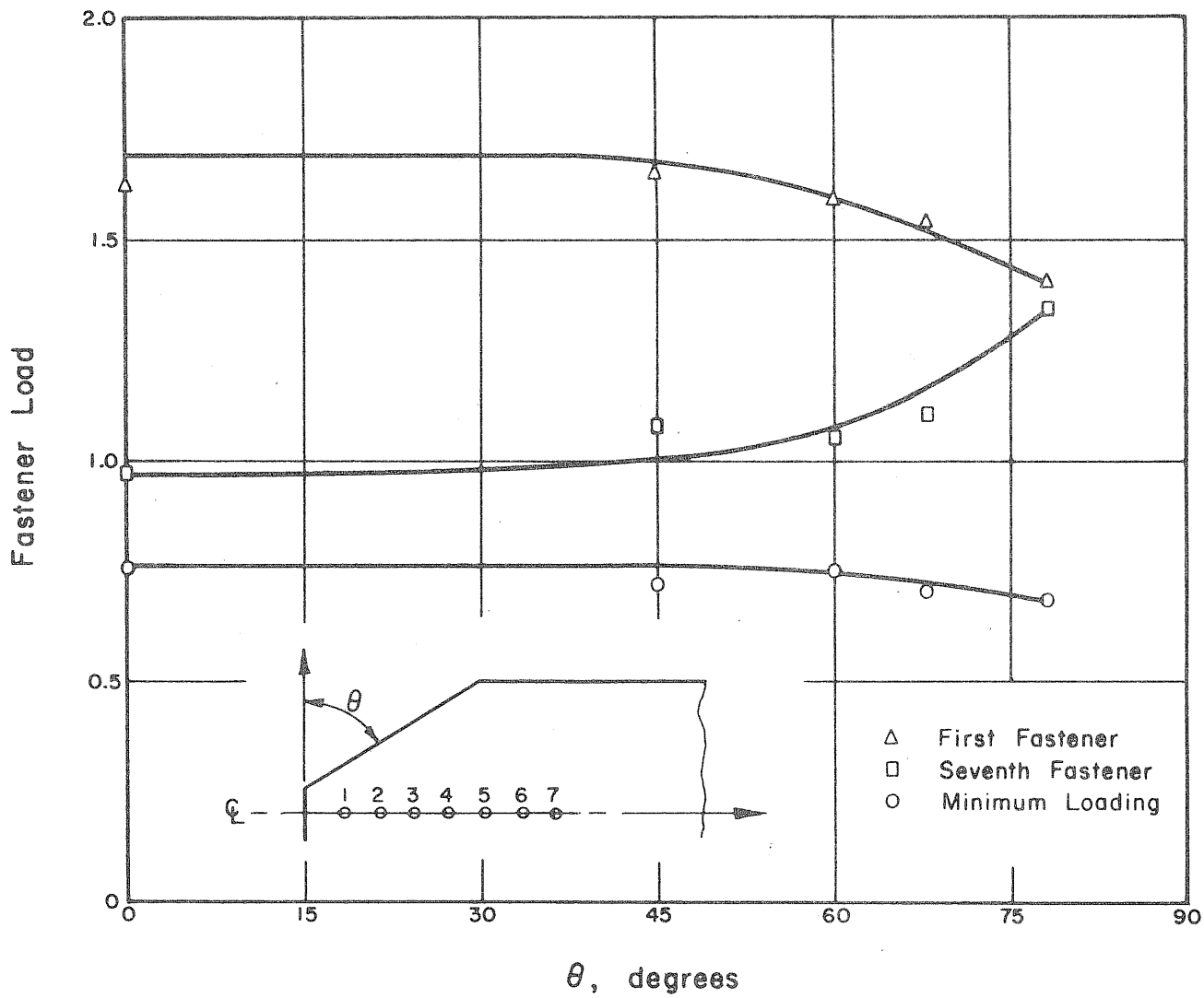


FIG. 4.9 VARIATION OF FASTENER LOAD WITH PLATE GEOMETRY CHANGES.

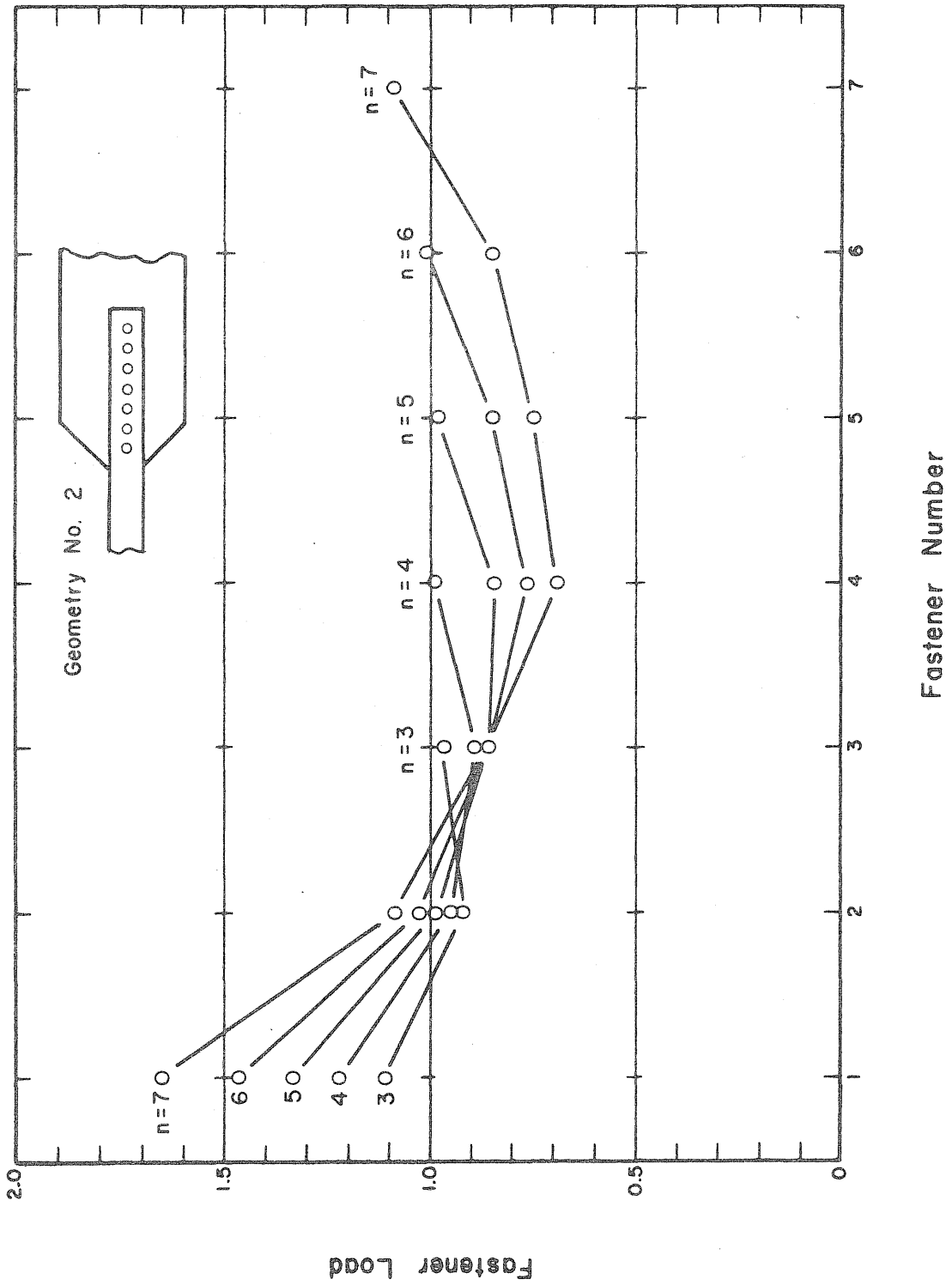


FIG. 4.10 LOAD PARTITION FOR VARIABLE NUMBER OF FASTENERS.

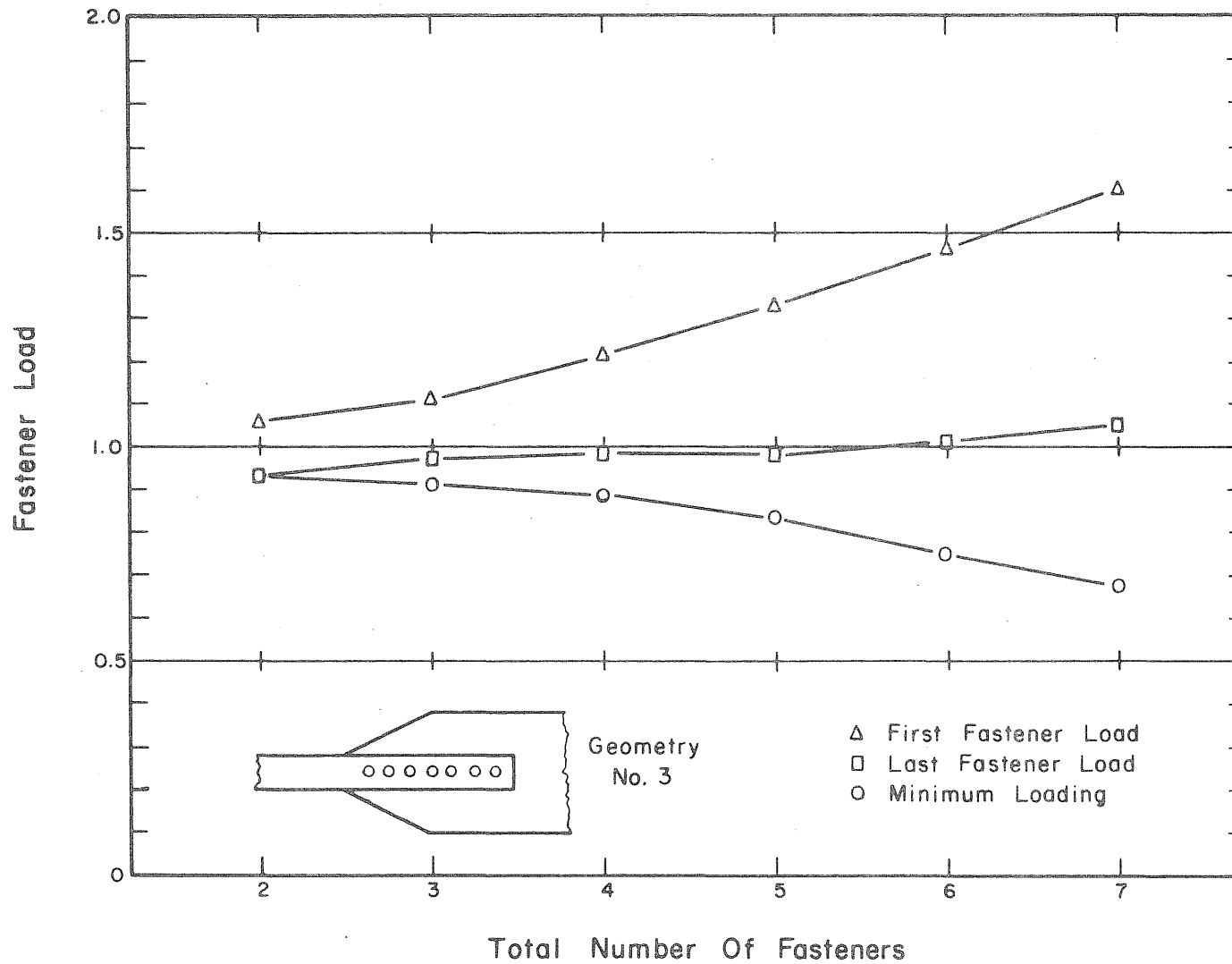


FIG.4.II VARIATION OF FASTENER LOAD WITH TOTAL NUMBER OF FASTENERS.

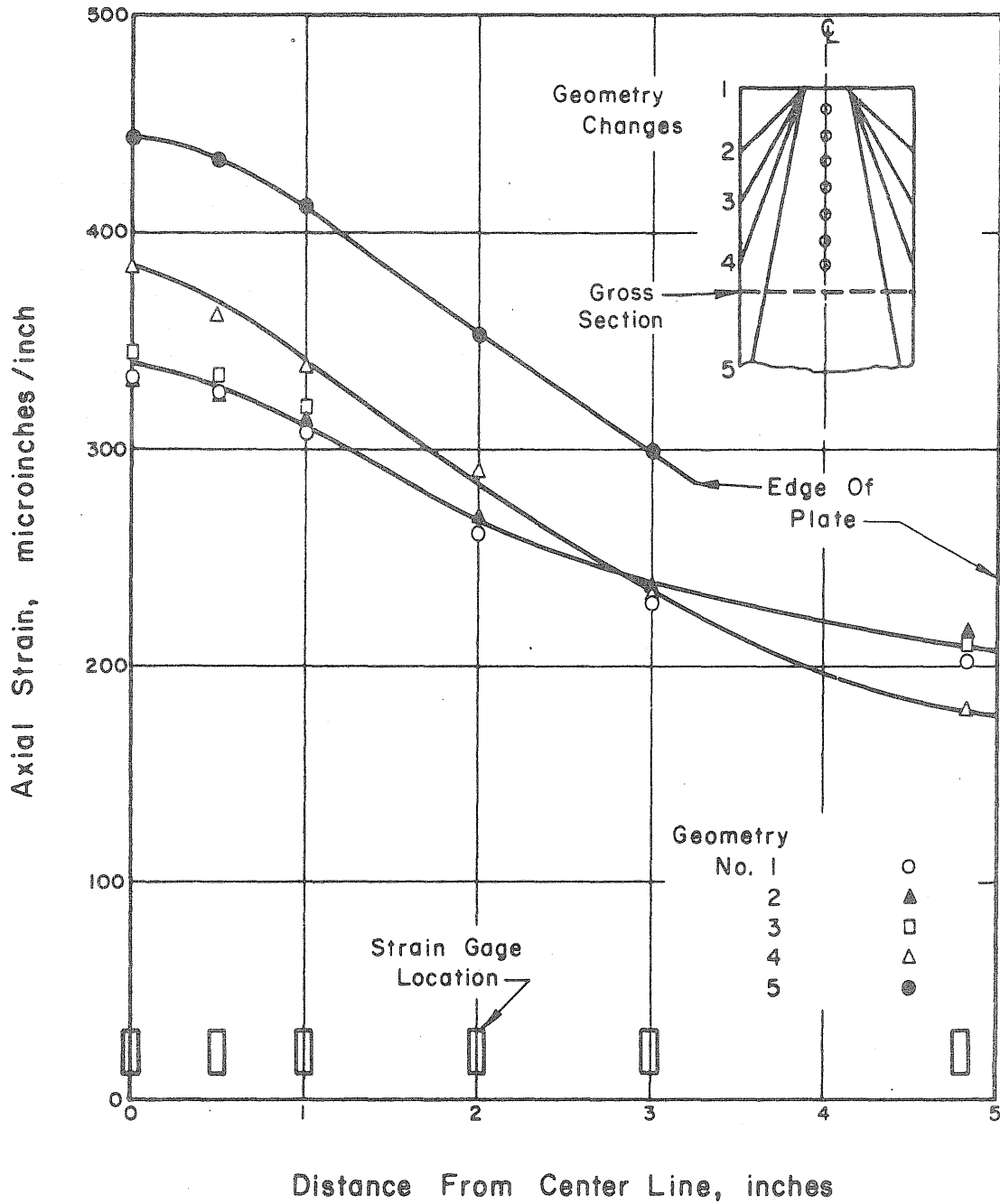


FIG.4.12 AXIAL STRAIN AT GROSS SECTION OF PLATE FOR VARIABLE GEOMETRY (TOTAL LOAD OF 21 KIPS).

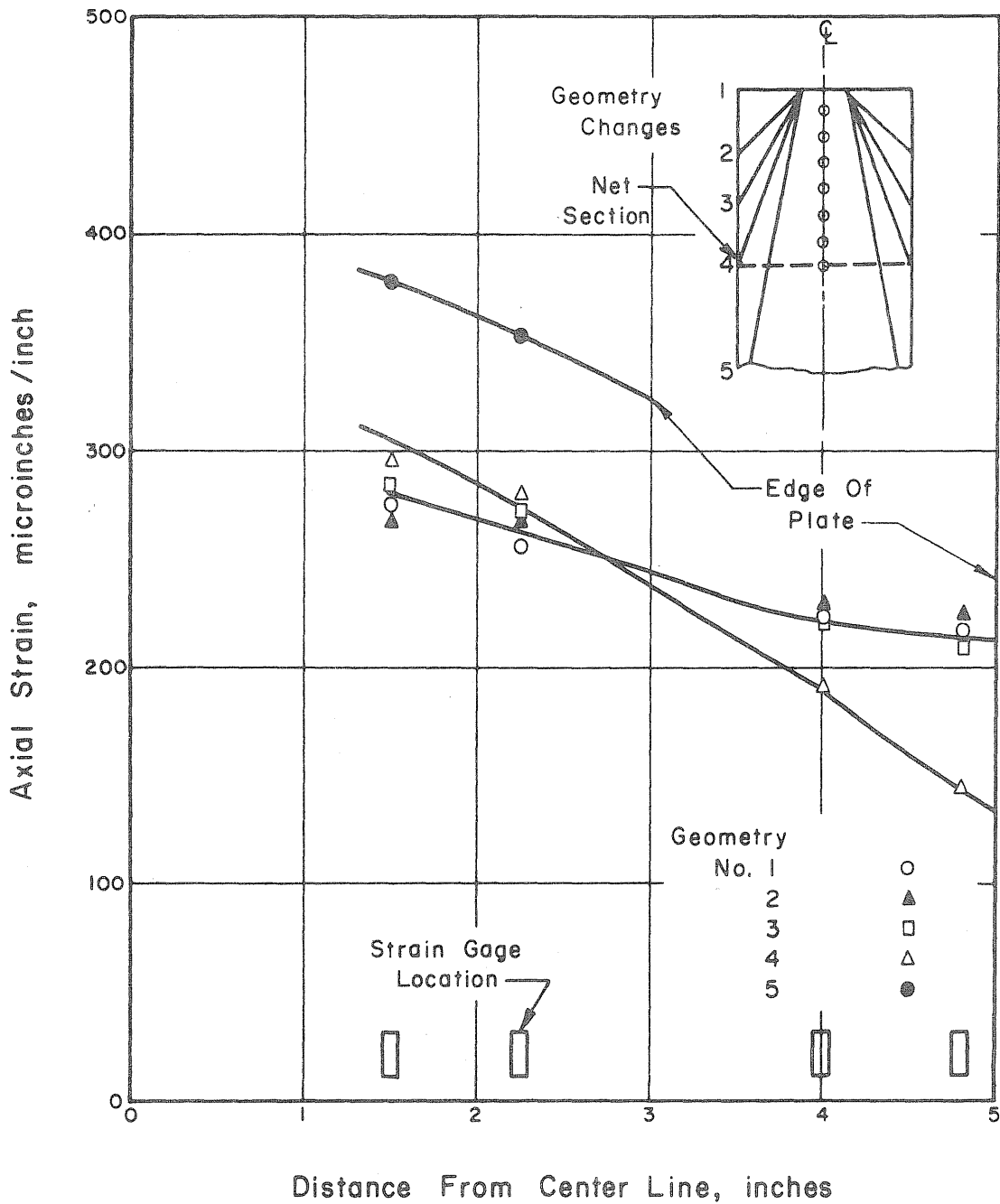


FIG. 4.13 AXIAL STRAIN AT NET SECTION OF PLATE FOR VARIABLE GEOMETRY.

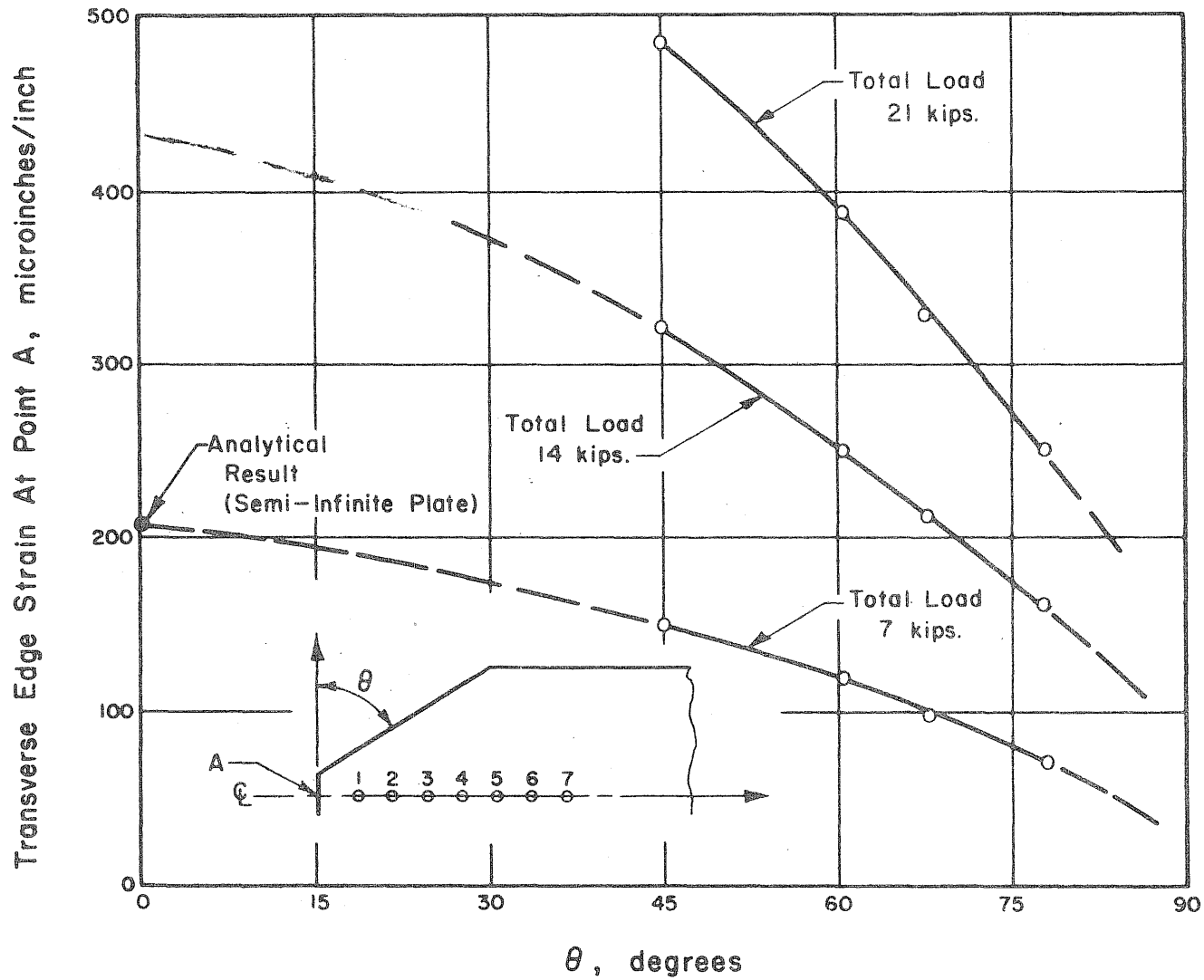
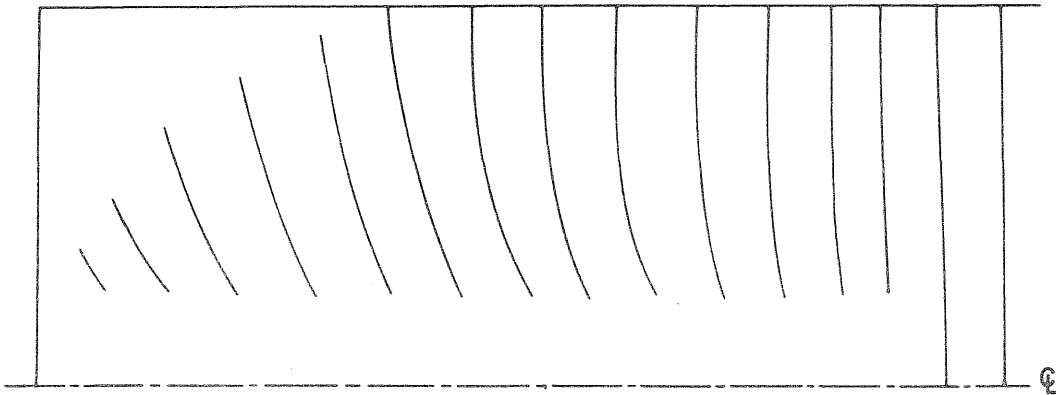
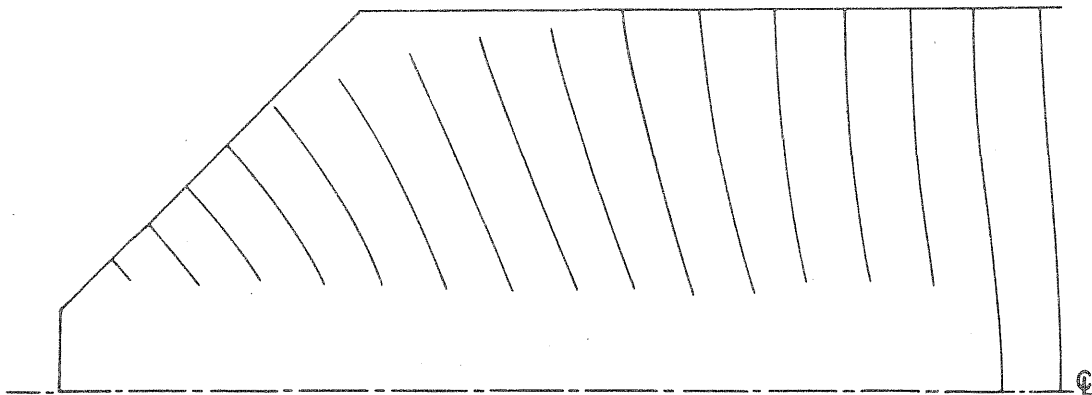


FIG.4.14 TRANSVERSE EDGE STRAIN FOR VARIABLE GEOMETRY AND JOINT LOAD.

GEOMETRY NO. 1



GEOMETRY NO. 2



GEOMETRY NO. 3

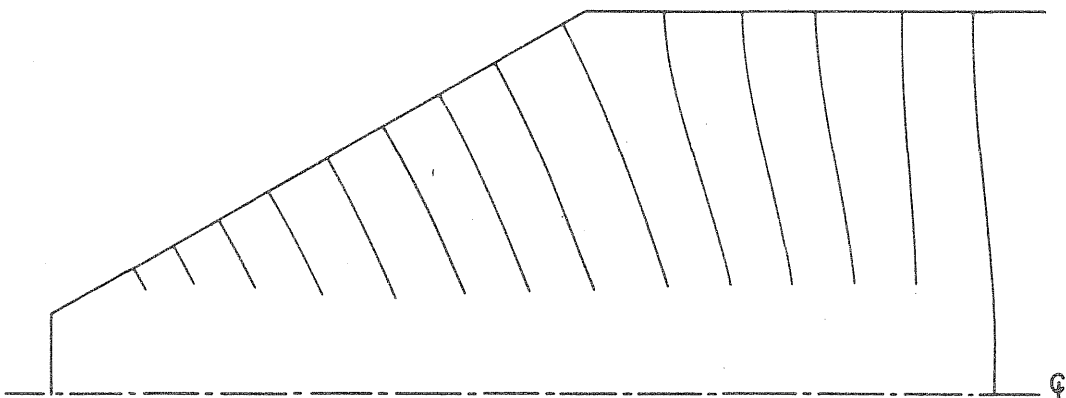


FIG. 4.15 BRITTLE LACQUER STRESS TRAJECTORIES  
FOR VARIABLE PLATE GEOMETRY.

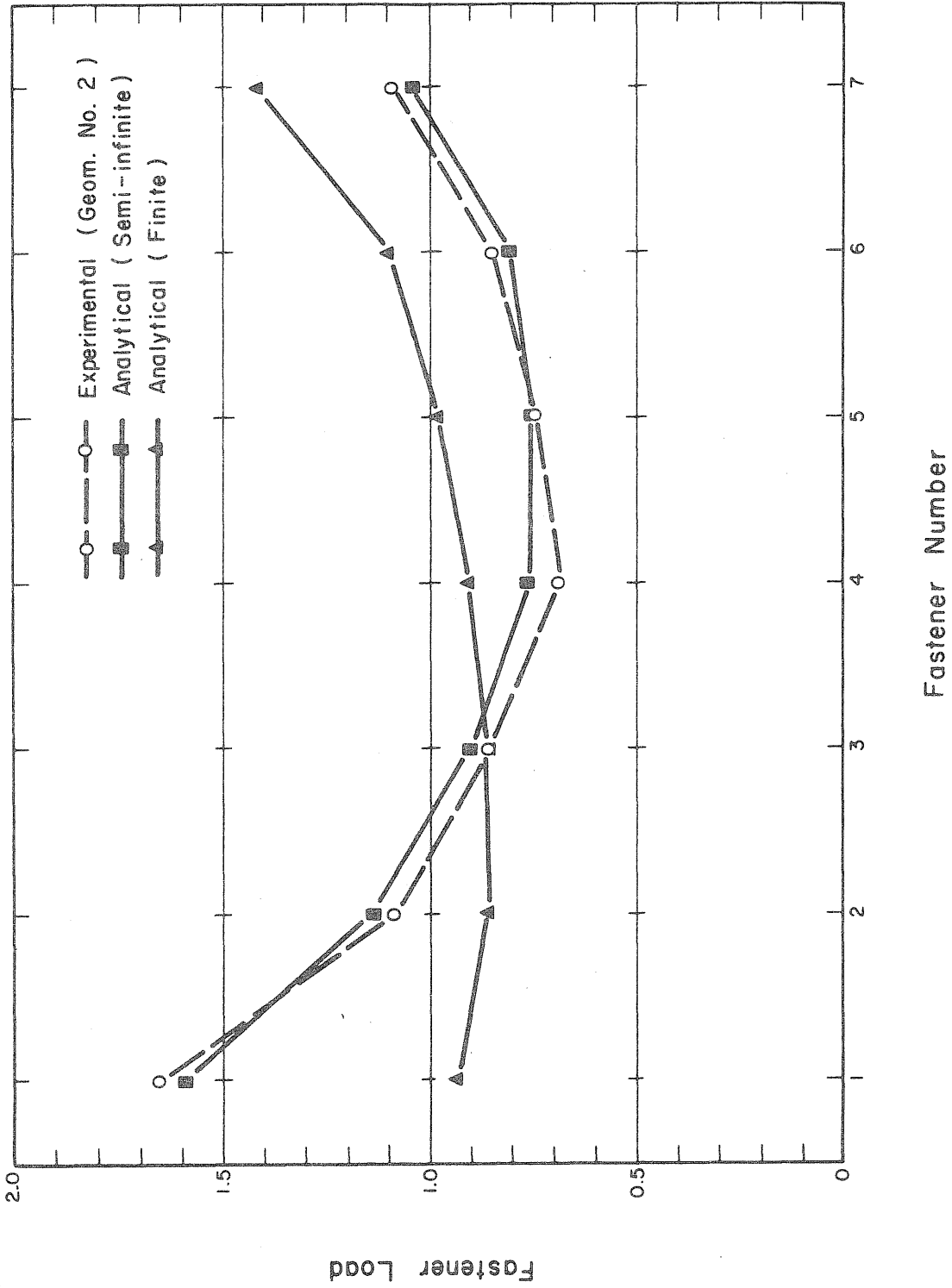


FIG. 5.1 COMPARISON OF ANALYTICAL AND EXPERIMENTAL LOAD PARTITION .

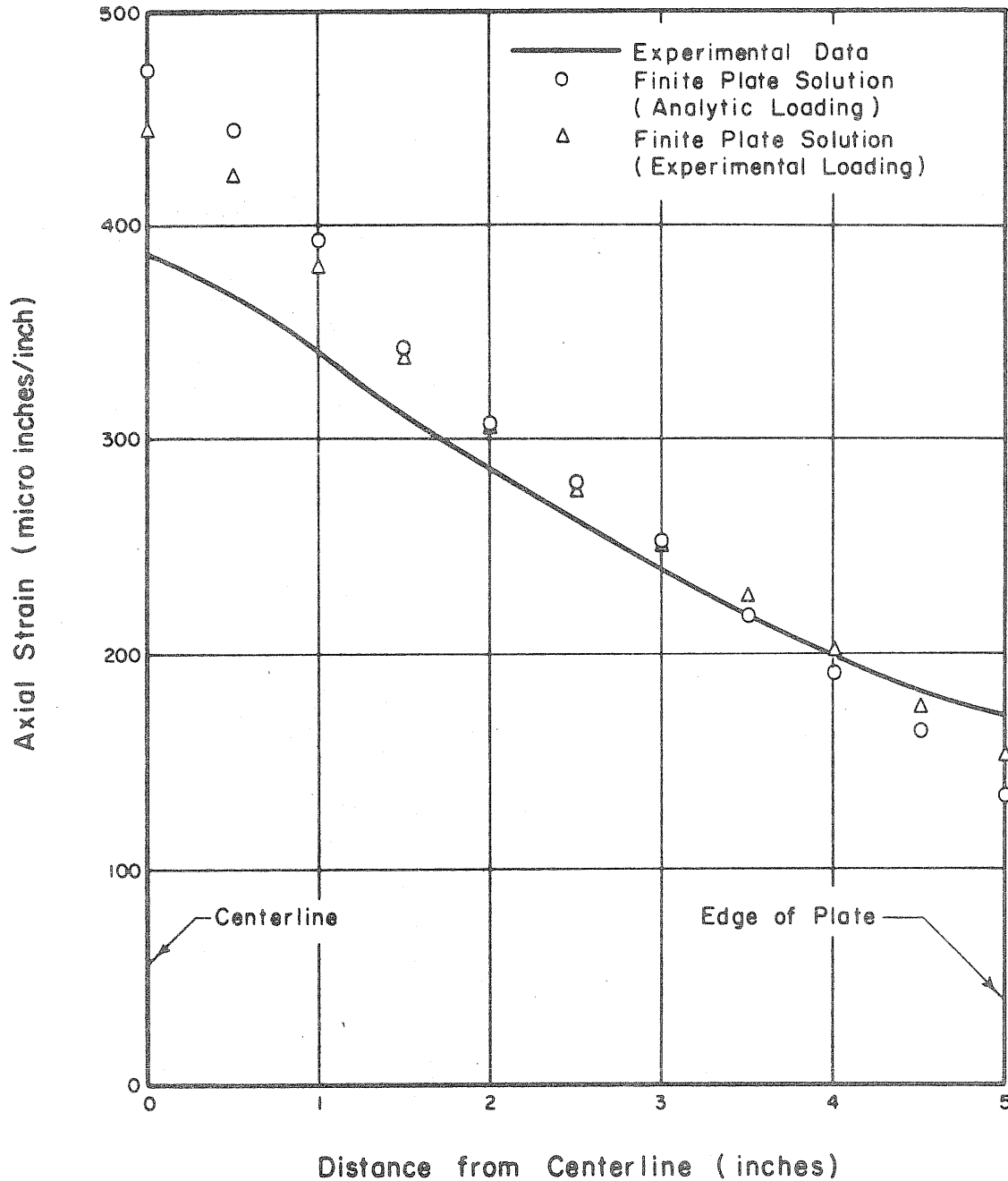


FIG. 5.2 COMPARISON OF ANALYTICAL AND EXPERIMENTAL AXIAL STRAINS. ( GROSS SECTION )

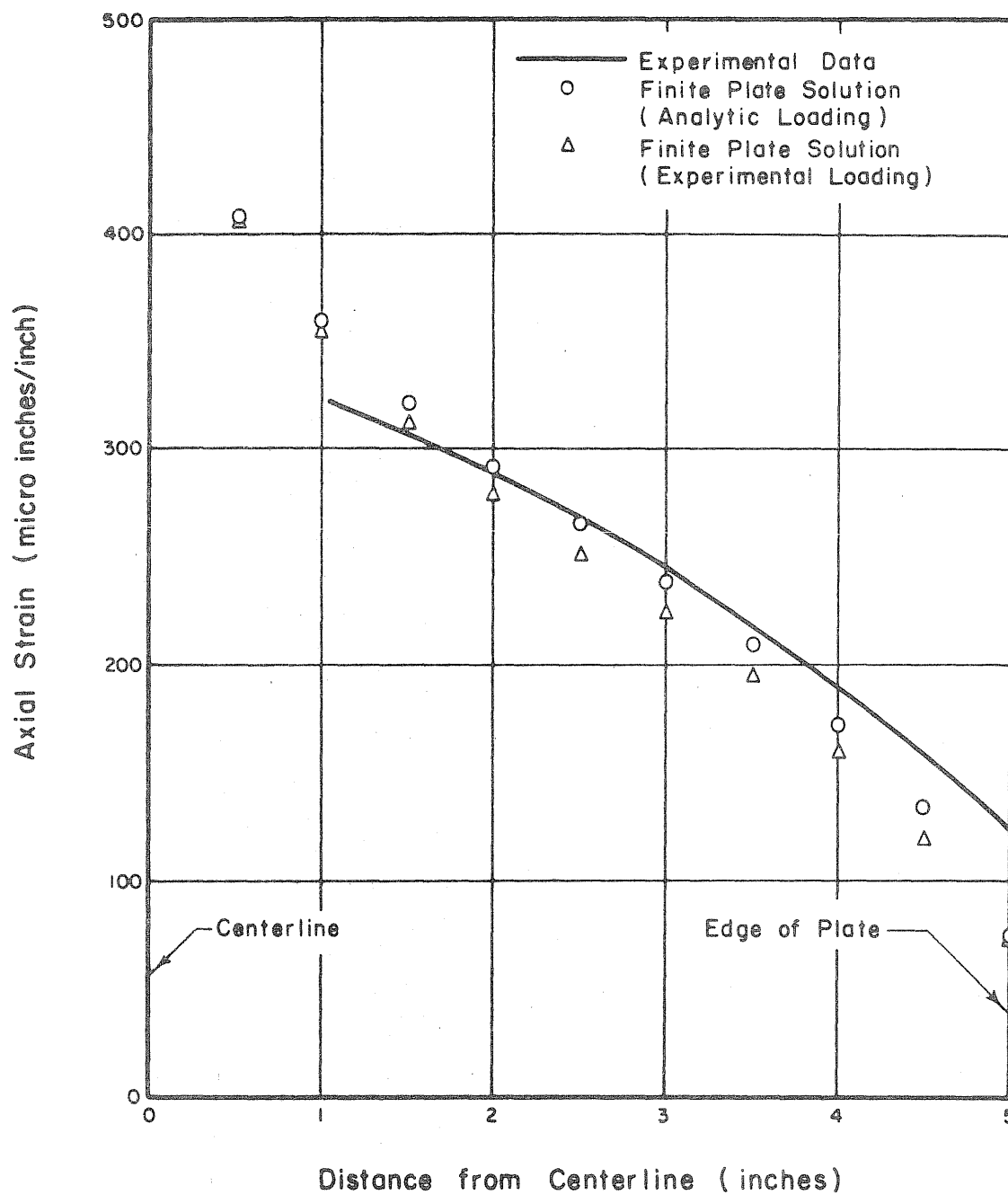


FIG. 5.3 COMPARISON OF ANALYTICAL AND EXPERIMENTAL AXIAL STRAINS. (NET SECTION)

## APPENDIX A

## NOMENCLATURE

A.1 General Nomenclature

$A_s$	area of lap plates, connecting member
$a_n$	$n$ th coefficient of the power series solution for $\phi$ of the residual finite plate problem
$A_f$	shear area of fastener in double shear
$b_n$	$n$ th coefficient of the power series solution for $\psi$ of the residual finite plate problem
$d$	nominal diameter of rigid inclusion or fastener
$E$	modulus of elasticity
$f_i$	total force transmitted by the $i$ th fastener
$G$	shear modulus of elasticity
$h_e$	edge distance of the first fastener
$h_i$	distance from origin to $i$ th fastener
$I$	prefix denoting the imaginary part of a complex function
$I_f$	bending moment of inertia of a fastener
$C_t$	total flexibility accounting for fastener deformation and local lap plate deformation
$n$	number of fasteners
$p$	fastener pitch or spacing in direction of loading
$Q_i$	force transmitted by the lap plates in the $i$ th interval

Re	prefix denoting the real part of a complex function
t	thickness of gusset plate
$t_s$	thickness of lap plate
u	displacement in the x direction
v	displacement in the y direction
$u_{ij}$	u displacement at the <u>i</u> th fastener due to a load of unity at the <u>j</u> th fastener
x,y	rectangular coordinates
z	complex variable equal to $x + iy$ where $i = \sqrt{-1}$
$\Gamma$	constant factor equal to $(1 + \nu)^2 / 8\pi Et$
$\delta_i$	total deformation of the <u>i</u> th fastener including local lap plate deformations
$\Delta_i^G$	deformation of the <u>i</u> th interval of the gusset plate
$\Delta_i^L$	deformation of the <u>i</u> th interval of the lap plates
$\epsilon_{ij}$	deformation of the <u>i</u> th interval due to a load of unity on the <u>j</u> th fastener
$\kappa$	elastic constant equal to $\frac{3-\nu}{1+\nu}$ for plane stress solutions in two dimensional elasticity
$\nu$	Poisson's ratio
$\sigma_x$	normal component of stress parallel to x axis
$\sigma_y$	normal component of stress parallel to y axis
$\tau_{xy}$	shearing stress component in rectangular coordinates
$\phi(z)$	Muskhelishvili displacement potential
$\psi(z)$	Muskhelishvili displacement potential

## APPENDIX B

## LOADED RIGID CIRCULAR INCLUSION IN A SEMI-INFINITE SHEET

The generalized plane stress solution of the stated problem is derived here as the first approximation to a mixed boundary value problem in plane elasticity using the classical solution of a loaded rigid circular inclusion in an infinite sheet or plate. This solution was obtained earlier by J. S. Bloom<sup>(29)</sup> and was included in an appendix to his work with related problems.

The complex Muskhelishvili<sup>(31)</sup> displacement potentials  $\phi(z)$  and  $\psi(z)$  ( $z = x + iy$ ) are related to the stresses and displacements in a plane stress solution in the following manner.

$$\sigma_x + \sigma_y = 4 \operatorname{Re} [\phi']$$

$$\sigma_y - \sigma_x + 2i \tau_{xy} = 2[\bar{z} \phi'' + \psi']$$

$$2G(u + iv) = \kappa\phi - z\bar{\phi}' - \bar{\psi}$$

where  $\kappa = \frac{3 - \nu}{1 + \nu}$  and  $G$  is the shear modulus of elasticity.

For a unit load acting at the origin in the negative  $x$  direction on a rigid inclusion of diameter  $d$  whose center is at the origin (Fig. B.1(a)), the displacement potentials are<sup>(28)</sup>

$$\phi_o = \Gamma \log (z)$$

$$\psi_o = -\Gamma \left[ \kappa \log (z) + \left( \frac{d}{2z} \right)^2 \right]$$

where  $\Gamma = \frac{1}{2\pi(1+\kappa)t}$  and  $t$  is thickness of the plate. Additive constants have been omitted from this solution since they do not affect the resulting stresses. This solution can be modified to provide the more general displacement potentials for a loaded rigid inclusion a distance  $h$  from the origin on the  $x$  axis (Fig. B.1(b)).

$$\phi_o = \Gamma \log (z - h)$$

(B.3)

$$\psi_o = \Gamma \left[ \kappa \log (z - h) + \frac{(d/2)^2}{(z - h)^2} + \frac{h}{(z - h)} \right]$$

Considering the semi-infinite elastic sheet to be the positive side of the  $y$  axis, the stress free edge will be the  $y$  axis ( $x = 0$ ) (Fig. B.1(c)). The stress free boundary condition in terms of  $\phi$  and  $\psi$  is

$$\phi + z \bar{\phi}' + \bar{\psi} = 0 \quad (\text{B.4})$$

This condition represents an integration of the stresses along the boundary<sup>(32)</sup>.

As a first approximation to the solution  $\phi_1$  and  $\psi_1$  were chosen such that  $\phi = \phi_0 + \phi_1$  and  $\psi = \psi_0 + \psi_1$  satisfy the stress free boundary condition. A judicious selection of functions  $\phi_1$  and  $\psi_1$  with singularities exterior to the region in concern, was made.

$$\phi_1 = A_0 \log(z+h) + A_1 \frac{1}{(z+h)} + A_2 \frac{1}{(z+h)^2} \quad (\text{B.5})$$

$$\psi_1 = B_0 \log(z+h) + B_1 \frac{1}{(z+h)} + B_2 \frac{1}{(z+h)^2} + B_3 \frac{1}{(z+h)^3}$$

where  $A_n$  and  $B_n$  are, in general, complex constants. Upon substituting  $\phi$  and  $\psi$  into the expression for the stress free boundary at  $z = iy$ , Eq. (B.4), the following values were obtained for  $A_n$  and  $B_n$ .

$$\begin{aligned} A_0 &= \kappa & B_0 &= -1 \\ A_1 &= -2h & B_1 &= h(2 - \kappa) \\ A_2 &= \left(\frac{d}{2}\right)^2 & B_2 &= -2 \left[ h^2 - \left(\frac{d}{2}\right)^2 \right] \\ & & B_3 &= 2h \left(\frac{d}{2}\right)^2 \end{aligned}$$

This yields the final form of the first approximation to the solution of the semi-infinite plate loaded at a rigid inclusion and having a stress free edge.

$$\begin{aligned}\phi &= \Gamma \left[ \log (z - h) + \kappa \log (z + h) - \frac{2h}{(z + h)} + \frac{\left(\frac{d}{2}\right)^2}{(z + h)^2} \right] \quad (8.6) \\ \psi &= \Gamma \left[ -\kappa \log (z - h) - \frac{\left(\frac{d}{2}\right)^2}{(z - h)^2} - \frac{h}{(z - h)} \right. \\ &\quad \left. - \log (z + h) + \frac{h(2 - \kappa)}{(z + h)} - \frac{2\left(h^2 + \left(\frac{d}{2}\right)^2\right)}{(z + h)^2} + \frac{2h\left(\frac{d}{2}\right)^2}{(z + h)^3} \right]\end{aligned}$$

The displacement potentials  $\phi$  and  $\psi$  satisfy exactly the condition for a stress free edge at  $x = 0$ , however, the assumption of a rigid inclusion at  $z = h$  has been violated.  $\phi_1$  and  $\psi_1$  do not satisfy this condition. By selecting suitable functions  $\phi_2$  and  $\psi_2$  one could correct this deficiency while violating the stress free boundary condition. This is known as the Schwartz Alternating Method . J. S. Bloom went a step further, determining  $\phi_2$  and  $\psi_2$ , and made an error analysis on the difference in displacement and found that for  $h/d = 3$  (edge distance equals three inclusion diameters), the error was less than 5%. (\*)

\* Private communication with the author.

The author feels that, in light of other assumptions, this first approximation is quite adequate for the present study.

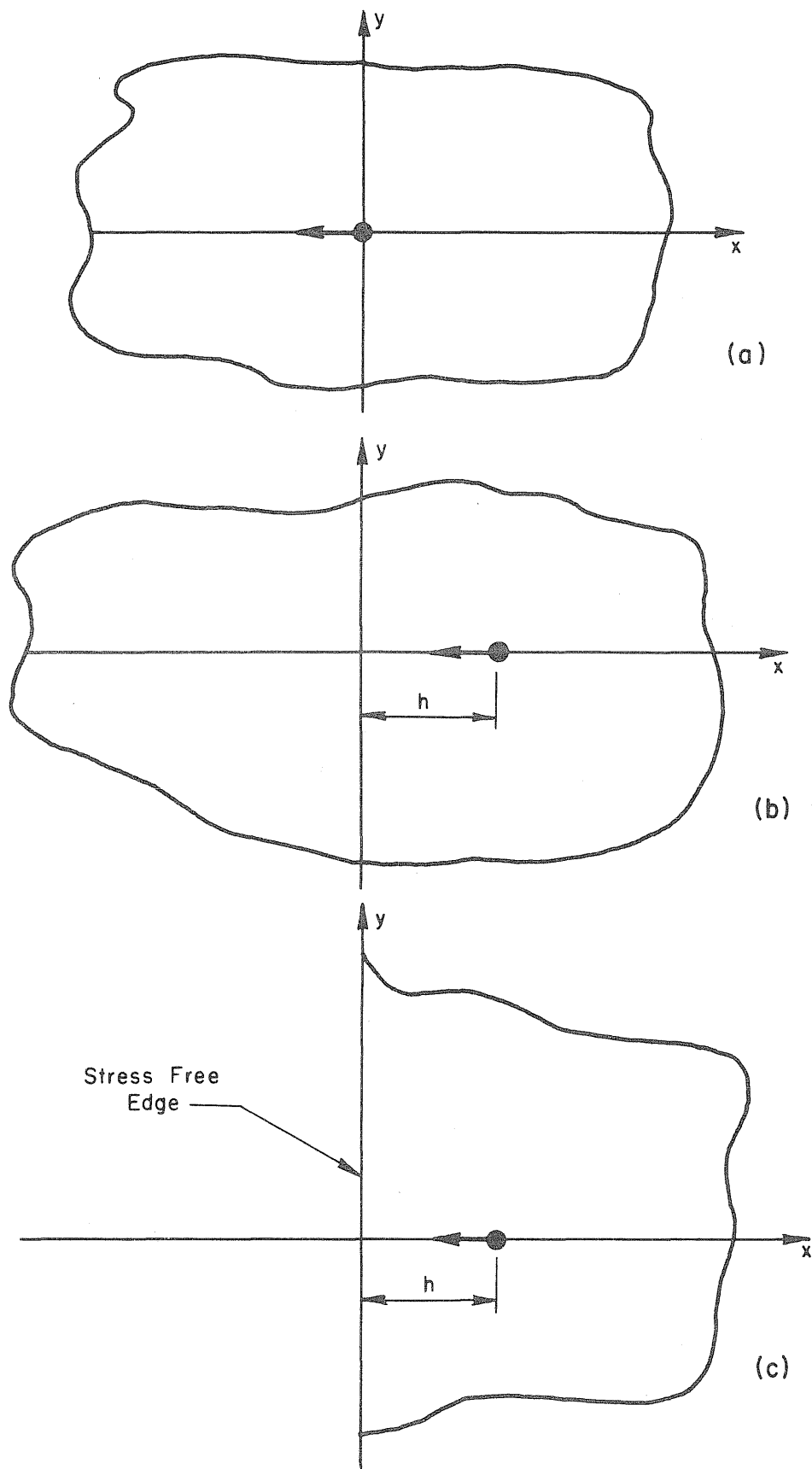


FIG. B.1 SEMI-INFINITE PLATE PROBLEM

## APPENDIX C

## LOADED RIGID CIRCULAR INCLUSION IN A FINITE SHEET

A rigorous presentation of the elasticity solution of the finite plate problem is presented here, as an appendix, for a more complete understanding of this portion of the gusset plate problem. To obtain an approximate solution to this mixed boundary value problem the author has used the point matching technique of Conway<sup>(33)</sup>, a method of increasing popularity for solution of a certain class of boundary value problems. Generally, the point matching procedure involves the adjustment of a truncated series solution of a differential equation at a selected finite set of boundary points of the region. The solution to the problem will parallel the development of the semi-infinite plate solution of Appendix B; a brief discussion of assumptions involved in performing certain operations will follow the derivation of the solution.

It is desired that displacement potentials  $\phi_1$  and  $\psi_1$  be found to modify the infinite plate displacement potentials  $\phi_0$  and  $\psi_0$  and provide an approximate solution for the displacement potentials of the finite plate,  $\phi$  and  $\psi$ , where  $\phi = \phi_0 + \phi_1$  and  $\psi = \psi_0 + \psi_1$ . In the following work the cartesian form of the variable  $z$  is used ( $z = x + iy$ ), the intention being to take advantage of the complex arithmetic operations which are easily programmed and performed on modern digital computers.

The choice of a plate shape and loading configuration has been previously discussed in Section 3.3. The shape to be studied will be of the type found in simple bridge hanger connections, i.e. usually tapered with straight edges and symmetrical about the line of action of the load. The general approach will be to load a rigid inclusion in an infinite plate and satisfy stress boundary conditions on the desired finite plate boundary while maintaining the equilibrium of the plate. To maintain equilibrium of the plate it was found convenient to begin with an equilibrated system as shown in Fig. C.1(a)). With opposing loads at  $x = \pm h$ , any region can be cut from the infinite plate containing both loads, and the resulting tractions at the edge of this region, which maintain the shape of the region, will be in equilibrium independent of the magnitude of interior loads. Another advantage of this system is that the entire boundary for the base problem will have stress free boundary conditions. The equilibrium condition allows the superposition of an identical continuous region loaded by tractions equal and opposite to the tractions of the infinite plate solution. The superposition of the two solutions results in a plate loaded with equal and opposite loads having a stress free edge at the boundary of the chosen finite plate region. The solution of the problem can be further simplified by choosing the finite plate region symmetrical in two directions as shown in Fig. C.1(b); this replaces the inclusion with plate material.

The infinite plate displacement potentials  $\phi_0$  and  $\psi_0$  for the opposed loads are obtained by superimposing solutions of the type given in Eq. B.3.

$$\begin{aligned}\phi_0 &= -\Gamma \log \left[ \frac{z-h}{z+h} \right] \\ \psi_0 &= \underline{\Gamma} \left\{ \kappa \log \left[ \frac{z-h}{z+h} \right] + \left( \frac{d}{2} \right)^2 \left[ \frac{1}{(z-h)^2} - \frac{1}{(z+h)^2} \right] \right. \\ &\quad \left. + h \left[ \frac{1}{z-h} + \frac{1}{z+h} \right] \right\}\end{aligned}\tag{C.1}$$

For solution of the residual problem described by the region of Fig.C.1(b) with tractions resulting from  $\phi_0$  and  $\psi_0$  one can choose the power series representations<sup>(32)</sup>

$$\phi_1(z) = \sum_{n=0}^{\infty} a_n z^n; \quad \psi(z) = \sum_{n=0}^{\infty} b_n z^n\tag{C.2}$$

where  $a_n$  and  $b_n$  are in general, complex constants. An examination of the displacement potentials  $\phi_1$  and  $\psi_1$  for the case of double symmetry allows one to simplify these series expansions. The substitution of  $\phi_1$  into the first of Equations B.1 yields

$$\sigma_x + \sigma_y = 2 \left[ \sum_{n=1}^{\infty} n a_n z^{n-1} - \sum_{n=1}^{\infty} n a_n \bar{z}^{n-1} \right] \quad (C.3)$$

Symmetry of the normal stresses  $\sigma_x$  and  $\sigma_y$  about the  $x$  axis requires that the imaginary parts of the coefficients  $a_n$  must vanish;  $a_n$  must, therefore, be real. A similar examination of Eq. C.3 for symmetry of  $\sigma_x$  and  $\sigma_y$  about the  $y$  axis indicates that  $a_n$  must vanish for even powers of  $n$ ; only odd powers of  $z$  need be considered in the  $\phi_1$  series.

Substitution of  $\phi_1$  and  $\psi_1$  into the second of Equations B.1 yields

$$\sigma_y - \sigma_x + 2i\tau_{xy} = 2 \left\{ \bar{z} \sum_{n=2}^{\infty} n(n-1) a_n z^{n-2} + \sum_{n=1}^{\infty} n b_n z^{n-1} \right\} \quad (C.4)$$

The shearing stresses  $\tau_{xy}$  are necessarily zero on the  $x$  and  $y$  axes since these are axes of symmetry. From examination of the symmetry of  $\sigma_y - \sigma_x$  in Eq. C.4 on the real axis ( $z = x$ ), noting that  $a_n$  is real, one finds that the imaginary parts of  $b_n$  must vanish;  $b_n$  must, therefore, be real. Studying this symmetry about the imaginary axis ( $z = iy$ ) one finds that coefficients  $b_n$  of even powers of  $z$  must vanish and consequently that only odd powers of  $n$  need be considered in the  $\psi_1$  series.

$$\phi_1(z) = a_0 + \sum_{n=1}^{\infty} a_n z^{2n-1}$$

$$\psi_1(z) = b_0 + \sum_{n=1}^{\infty} b_n z^{2n-1}$$
(C.5)

where  $a_n$  and  $b_n$  are real constants, and the constants  $a_0$  and  $b_0$  do not affect the stresses resulting from  $\phi_1$  and  $\psi_1$ .

A unique determination of the functions  $\phi_1$  and  $\psi_1$  results from imposition of the following conditions at the origin. <sup>(32)</sup>

$$\phi_1(0) = 0, \quad \text{I } \phi_1'(0) = 0, \quad \psi_1(0) = 0$$
(C.6)

The first and third conditions require that  $a_0$  and  $b_0$  vanish. The second condition has been satisfied by the fact that  $a_1$  is real.

The integral boundary condition (Eq. B.4), which represents the evaluation of the integral of the tractions along the boundary will now be used in the development of the point matching requirements for a stress free edge on the loaded finite plate. The formulas (Eq. C.1) for  $\phi_0$  and  $\psi_0$  possess the same symmetry as do the formulas (Eq. C.5) for the  $\phi_1$  and  $\psi_1$  series previously discussed. This allows the direct matching of the boundary conditions (Eq. B.4) to provide a stress free edge on the boundary of the finite plate. Upon substitution

of  $\phi = \phi_0 + \phi_1$  and  $\psi = \psi_0 + \psi_1$  into Eq. B.4 the boundary condition becomes

$$\phi_1 + z \bar{\phi}_1 + \bar{\psi}_1 = -\phi_0 - z \bar{\phi}_0 - \bar{\psi}_0 \quad (C.7)$$

on the boundary. Substitution of the infinite series  $\phi_1$  and  $\psi_1$  would yield an infinite number of equations with an infinite number of unknowns  $a_n$  and  $b_n$ . Solution of this system would yield an exact solution of the problem.

Such infinite systems are cumbersome and difficult to handle. The point matching scheme depends basically on the replacement of the exact infinite system with an approximation based on a finite system. Thus, only a finite number,  $N$ , of terms of Eq. C.5 are assumed to adequately represent the solution to the problem; resulting in a simplification of Eq. C.7.

$$\begin{aligned} \sum_{n=1}^N a_n z^{2n-1} + z \sum_{n=1}^N (2n-1) a_n \bar{z}^{2(n-1)} + \sum_{n=1}^N b_n \bar{z}^{2n-1} \\ = -\phi_0 - z \bar{\phi}_0 - \bar{\psi}_0 \end{aligned} \quad (C.8)$$

Equation C.8 is satisfied at arbitrarily specified points on the boundary, each specification resulting in two real equations for the  $2N$  unknowns  $a_n, b_n$ .

Because of the double symmetry of the plate problem being studied, only one quadrant of the plate boundary need be considered. If  $M$  boundary points are to be considered in the solution, generally  $2M$  independent equations will be generated and will require a total of  $2M$  terms from the  $\phi_1$  and  $\psi_1$  series. If one of the chosen points happens to be on the real or imaginary axis only one meaningful equation will be generated since on the real axis the imaginary part of Eq. C.8 is satisfied identically and on the imaginary axis the real part of Eq. C.8 is satisfied identically.

A number of authors have used an extension of the point matching approach while allows a greater number of boundary conditions or points to be considered for a given number of unknown coefficients than is possible with the direct approach previously described. This approach was described and used by Hulbert<sup>(34)</sup> and an explanation follows.

Consider the set of matrix equations  $A_{ij} X_j = B_j$  where the number of unknowns is less than the number of equations. In general these equations will not be satisfied exactly for any solution set  $X_j$ ; the residual error will have the form  $R_i = A_{ij} X_j - B_j$ . From the condition that the sum of the squares of the residuals is a minimum, we may write

$$\frac{\partial (R_i^2)}{\partial x_j} = 0 = A_{ji}^T A_{ij} x_j - A_{ji}^T R_i, \quad (C.9)$$

where T denotes transpose. This set of equations is equivalent to the original boundary equations premultiplied by the transpose of the coefficient matrix  $A_{ij}$ .

$$A_{ji}^T A_{ij} x_j = A_{ji}^T R_i \quad (C.10)$$

This is the method used for the solution of Equations C.8 for  $a_n$  and  $b_n$ .

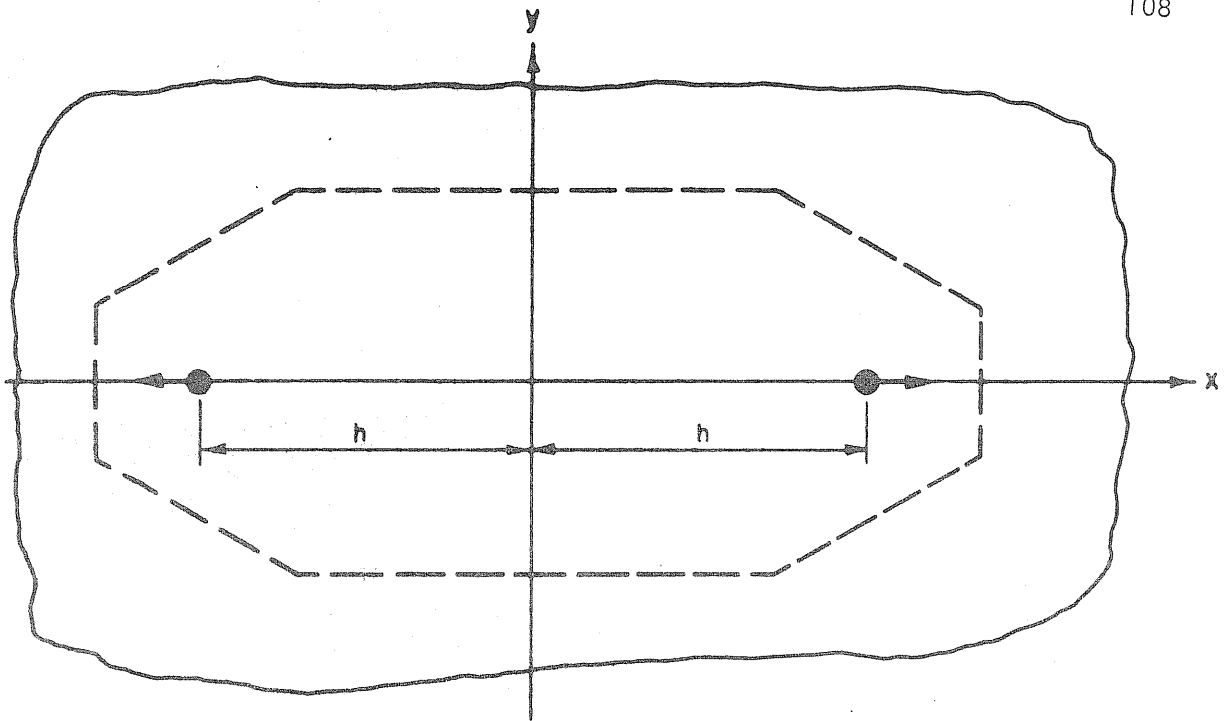
Having determined the coefficients  $a_n$  and  $b_n$  of the chosen  $\phi_1$  and  $\psi_1$  series, one now has an approximate solution for the plate problem of Fig. C.1(b). From this solution the stresses and displacements can be calculated for any point in the plate. The accuracy of such calculations will depend on such factors as:

1. Shape of the plate
2. Position of the load
3. Number points considered on the boundary
4. Number of terms used in each of the series  $\phi_1$  and  $\psi_1$
5. Precision of the computations
6. Point for which stress or displacement is desired

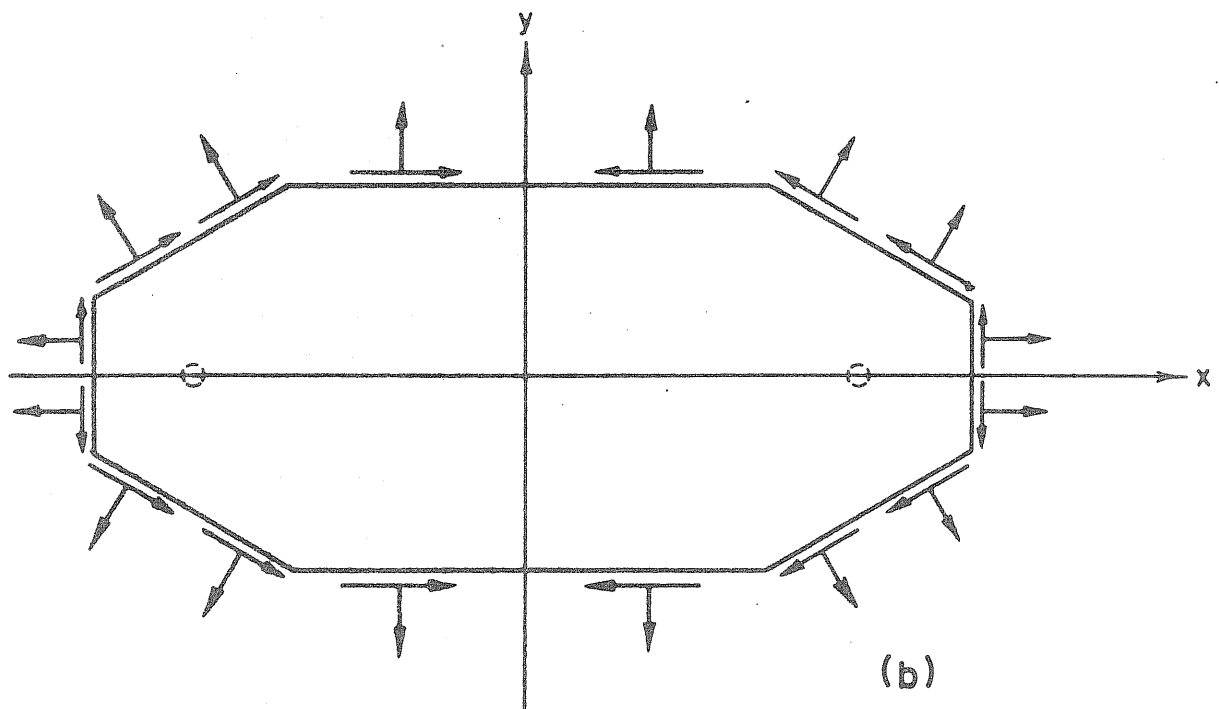
The first five of these factors all affect the satisfaction of the original boundary conditions of the problem.

The original assumption of the boundary condition of a rigid inclusion has been violated in two ways. The assumption involved in the addition or superposition of the functions for rigid inclusions at  $x = +h$  and  $x = -h$  (Eq. C.1), namely, that the inclusions remain rigid, is only reasonable for  $h$  much greater than  $d$  (inclusion diameter). The second violation of the assumption of the rigid inclusion is the release of stresses at the finite plate boundary, without taking into account the shape change of the inclusion. Again as in Appendix B this error was assumed to be small when considering an edge distance greater than  $3d$ .

It is difficult to generalize about the effects of all of the assumptions on a problem of this complexity. The discussion of the results of applying this method to a practical problem is included in the main part of the text.



(a)



(b)

FIG. C.1 FINITE PLATE RESIDUAL PROBLEM

## APPENDIX D

## FASTENER FLEXIBILITY AND LOCAL BEARING DEFORMATION

In describing the deformational characteristics of the components of a gusseted connection, the deformation of the fastener and the plate near the fastener are important. The fastener deformation and local bearing deformation are not prime considerations in this study but an evaluation of their effect is necessary for completeness. Simplifying assumptions allow one to make a reasonable evaluation of the magnitude of these properties. The work presented here is a combination of approximations made by Vogt<sup>(12)</sup> and by Tate and Rosenfeld<sup>(13)</sup>. Calculations are made for deformations caused by the transfer of load by a rivet or pin which fills the hole in the connected parts and causes no friction between the connected parts.

The fastener which is in double shear is considered to deform as a fixed-end beam (Fig. D.1). Fastener deformations due to shear and bending are calculated. Assuming a uniform loading (Fig. D.1), a total load of unity transmitted by the fastener causes a fastener deformation at the center of the gusset due to bending of,

$$\delta(\text{bending}) = \frac{8t_s^3 + 16t_s^2 t + 8t_s t^2 + t^3}{384 E I_f} \quad (\text{D.1})$$

where  $t_s$  is the thickness of a lap plate, and  $I_f$  is the bending moment of inertia of the fastener. The shear contribution to the deformation of the fastener for the same load is,

$$\delta(\text{shear}) = \frac{2t_s + t}{6 GA_f} \quad (\text{D.2})$$

where  $A_f$  is the cross-sectional area of a fastener.

To approximate the deformations in the fasteners and lap plates due to local bearing several simplifying assumptions are made. All deformations use the original center-line axis of the fastener as a reference.

From an elasticity solution of a plate with a fastener in bearing Vogt<sup>(12)</sup> found that a reasonable local plate deflection for a unit load on the fastener to be,

$$\delta(\text{plate bearing}) = \frac{0.9}{Et} \quad (\text{D.3})$$

where  $t$  is the thickness of the loaded plate. For the compression between the surface of the fastener and fastener axis, the average bearing stress for a unit load on a plate of thickness  $t$  would be  $\frac{1}{dt}$  at the surface and, at the axis of the fastener, approximately half of this value. The deformation over a length  $\frac{d}{2}$  is approximated by a simple integration over

this length assuming the stress to change linearly. The resulting bearing deformation in a fastener for a unit load on a plate of thickness  $t$  is approximated as,

$$\delta(\text{fastener bearing}) = \frac{.375}{Et} \approx \frac{0.4}{Et} \quad (\text{D.4})$$

The gusset plate local deformations have been accounted for in the elasticity solution of the plate and will not be included in the calculation of the total fastener flexibility. With this omission the total plate and fastener bearing deformation for a unit load transmitted by the fastener becomes,

$$\delta(\text{fastener and plate bearing}) = \frac{1}{E} \left( \frac{0.4}{t} + \frac{0.65}{t_s} \right) \quad (\text{D.5})$$

where  $t$  is the thickness of the gusset and  $t_s$  is the thickness of a lap plate.

In the relationship,  $\delta_i = C_t f_i$ , where  $\delta_i$  is the total local lap plate and fastener deformation and  $f_i$  is the rivet load, the total flexibility  $C_t$  is equal to the sum of the relationships Eq. D.1, Eq. D.2, and Eq. D.5.

$$C_t = \delta(\text{bending}) + \delta(\text{shear}) + \delta(\text{fastener and plate bearing})$$

(D.6)

$$= \frac{8t_s^3 + 16t_s^2t + 8t_s t^2 + t^3}{384 E I_f} + \frac{2t_s + t}{6 G A_f} + \frac{1}{E} \left( \frac{0.4}{t} + \frac{0.65}{t_s} \right)$$

Using a value of  $E = 30,000$  ksi the total flexibility, as calculated using Eq. D.6, is presented in terms of  $t/t_s$  and  $d/t$  in Fig. D.1.

To find a realistic value for  $C_t$  related to the other base variables used in the parameter study of Section 3.4,  $t/t_s$  was chosen as 0.75; this number is also comensurate with the experimental lap plate dimensions. The value of  $d/t$  equals 1.5. The assumptions made in arriving at  $C_t$  are valid for small deformations only. This explains the upward trend of  $C_t$  for small  $d/t$ . It is suggested that a more realistic continuation of the curve for  $t/t_s = 0.75$  and values of  $d/t < 2.0$  would be as is shown dotted in Fig. D.1. For  $d/t = 1.5$  and  $t/t_s = 0.75$  a reasonable value for  $C_t$  appears to be approximately  $0.25 \times 10^{-3}$  inches/kip. This value is used as one of the base values of comparison in Section 3.4.

Obviously many assumptions have been made which tend to simplify a very complex physical phenomenon; however, it is believed that these approximations are quite adequate with respect to the limited extent which it is used in this study.

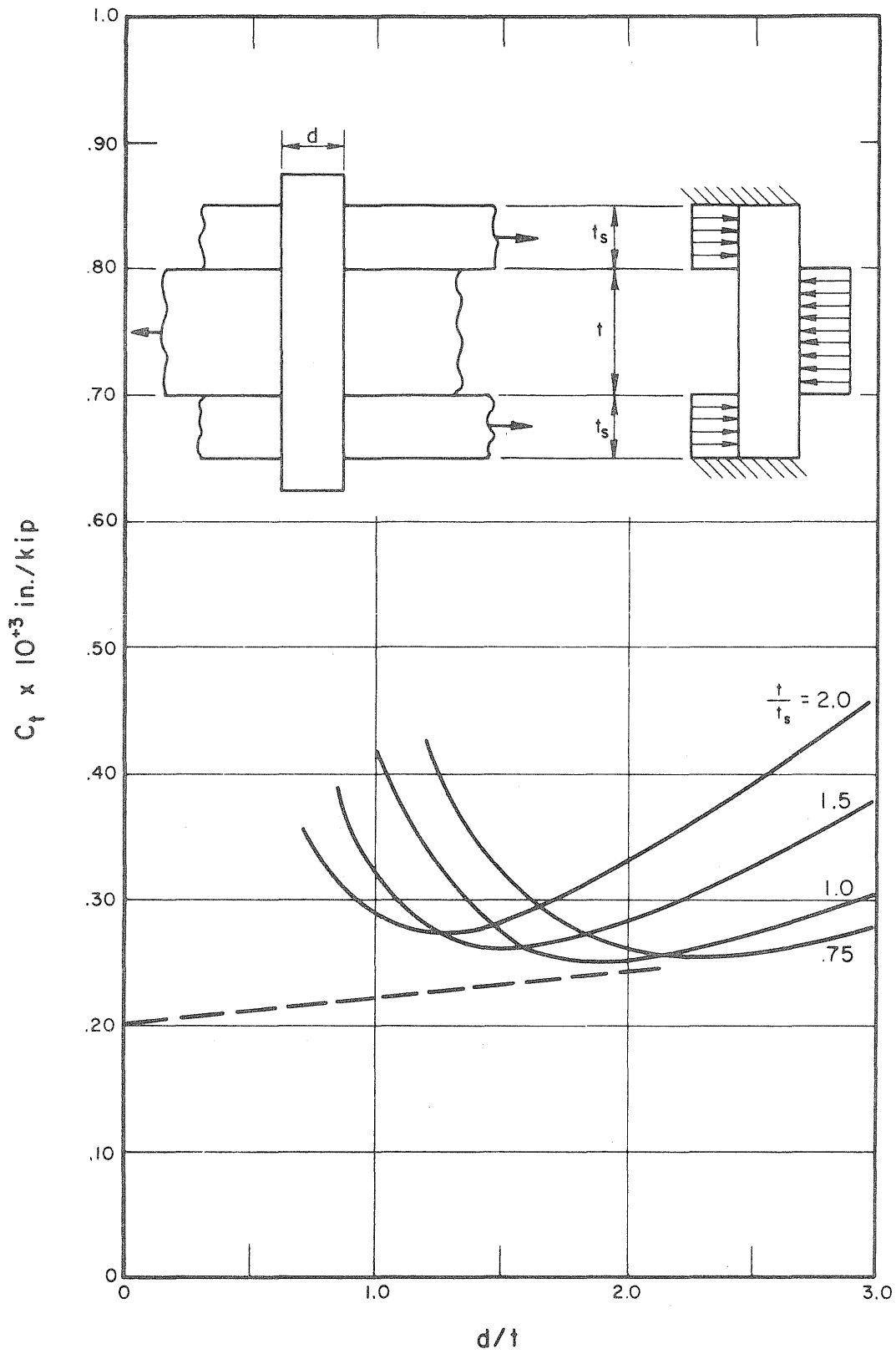


FIG. D.I TOTAL FASTENER FLEXIBILITY